BIRLA CENTRAL LIBRARY
PILANI (Rajasthan)

Class No:- 621.384132

Book No:- B38V

Accession No:- 55814

MODERN RADIO TECHNIQUE

General Editor: J. A. RATCLIFFE

VELOCITY-MODULATED THERMIONIC TUBES

Printed in Great Britain at the University Press, Cambridge
(Brooke Crutchley, University Printer)
and published by the Cambridge University Press
(Cambridge, and Bentley House, London)
Agents for U.S.A., Canada, and India: Macmillan

PREFACE

The plan of this book is to give a general introduction to velocity-modulation tubes and their mode of operation in such a form as to be readily intelligible to anyone with a reasonably adequate knowledge of pre-1939 radio technique. The essential minimum of information on resonant cavities is included, and there is some information on heavy current electron beams. The major part of the work is, however, the general theory of the interchange of energy between field and beam given in Chapter 3, together with the application of this theory to various types of V.M. tube in Chapters 5, 6, 7 and 8.

It was not intended that this book should be a formal text-book with full and critical documentation, but rather that it should give a personal account of a division of research which is still progressing rapidly. The free interchange of information between British and American government and commercial tube laboratories has, however, meant that a large fund of common knowledge has been built up, and it is therefore hoped that the work is in general agreement with the views of other researchers in the same field.

An attempt has been made to build up the theory from simple postulates by successive refinements so that physical facts dominate mathematical considerations, and a realistic picture of the way in which a physical theory is arrived at can be obtained.

Little has been said about the uses to which V.M. valves are put or about measurements on them. These matters are dealt with elsewhere and space did not permit their inclusion. The manuscript was completed in April 1946, before the Radiolocation Conference of the I.E.E., but references to most of the work published since that date have been included, in addition to an appendix on the travelling wave tube. Where an author's name is given without a reference, unpublished work is implied. I have tried to make as little use of such work as possible, but where it has been unavoidable, I have included the author's name as some acknowledgement.

It is a great pleasure to be able to testify to the spirit of co-operation which existed between all the laboratories engaged on this work. In particular, visits to the groups at E.M.I. led by Dr L. F. Broadway, and at the Clarendon Laboratory led by Dr J. H. E. Griffiths, were always stimulating. My thanks are due to Dr L. C. Jackson of Bristol University for many discussions. I am indebted to many of my colleagues in A.S.E., in particular Mr R. W. Sutton was always ready to give advice and assistance, and British radar owes much to his far-sightedness. Finally, Mr J. H. Burrow was always willing to try to make any tube that could be thought of, and his mastery of glass-working techniques contributed much to the work of the group. I am indebted to *M. Warnecke for the gift of many papers by himself and his co-workers. The assistance of my wife, in typing the manuscript and reading the proof, has been invaluable.*

I wish to thank the Director of Scientific Research, Admiralty, for permission to publish this work.

A. H. B.

LONDON
July 1947

CONTENTS

PAGE

HISTORICAL INTRODUCTION 1

Chapter 1. THE ELEMENTARY PRINCIPLES OF VELOCITY-MODULATION TUBES

1·1 Introduction 4
1·2 The klystron as amplifier 5
  1·2·1 The action of a velocity-modulation gap 8
1·3 The klystron self-oscillator 13
1·4 The reflex klystron oscillator 14
1·5 The Heil tube 17
1·6 The inductive output tube and the Hahn-Metcalf velocity-modulation tubes 19
1·7 Conclusion 21

Chapter 2. CAVITY RESONATORS

2·1 Introduction 22
2·2 Acoustic resonators 22
2·3 Electromagnetic waves 24
2·4 Resonant frequencies of a rectangular box 27
2·5 A circular cylinder with a central post 29
2·6 The rectangular section toroid with capacitance loading 31
2·7 The coaxial line resonator 33
2·8 Loss calculations 35
2·9 Equivalent circuits 36
2·10 Tuning methods 37
2·11 Approximation methods for the calculation of resonant frequencies 38
2·12 Conclusion 40

Chapter 3. THE THEORY OF VELOCITY MODULATION

3·1 The fundamentals of electron dynamics 42
3·2 First-order theory of gap action 45
3·3 The Webster approximation to the conversion efficiency of a klystron 46

PAGE
3·4 Small signal theory of the output efficiency of a klystron oscillator 50
3·5 The velocity-modulation action of a gap. Second-order approximation 55
3·6 The general expression for power interchange at a gap 58
3·7 The calculation of β and γ 62
3·8 Non-sinusoidal bunching 68

Chapter 4. HEAVY CURRENT ELECTRON BEAMS

4·1 Electrostatic focusing in a cylindrical tunnel 73
4·2 Electrostatic focusing in rectangular and annular apertures 75
4·3 Magnetic focusing in circular tunnels 76
4·4 Magnetic focusing in rectangular tunnels 78
4·5 Conclusion 79

Chapter 5. VELOCITY-MODULATION AMPLIFIERS AND FREQUENCY MULTIPLIERS

5·1 Velocity-modulation power amplifiers 81
5·2 Webster's debunching theory 83
5·3 Other calculations of debunching 86
5·4 Multiresonator klystron amplifiers 88
5·5 Signal-to-noise ratio in klystron amplifiers 92
5·6 Klystron frequency multipliers 95

Chapter 6. KLYSTRON OSCILLATORS

6·1 Equivalent circuit of a klystron oscillator 97
6·2 The conversion efficiency 100
6·3 Maximum amplitude conditions 103
6·4 The output efficiency of a klystron oscillator 104
6·5 The output efficiency of single gap-double transit tubes 111
6·6 Design considerations 112

Chapter 7. REFLEX KLYSTRON OSCILLATORS

7·1 The Webster approximation for the reflex klystron 116
7·2 General reflexion field 118
7·3 Maximum power output and efficiency using the general field 120
7·4 Discussion of design requirements 122

PAGE

7·5 Frequency control by reflector voltage changes 123
7·6 Frequency stability and long-line effects 126
7·7 Conclusion 127

Chapter 8. MISCELLANEOUS TYPES OF VELOCITY-MODULATION TUBE

8·1 The velocity-modulation mixer 128
8·2 Velocity discrimination 129
8·3 Frequency conversion by bunching 132
8·4 The monotron 133
8·5 Velocity-modulated reactance valves 135
8·6 The multireflexion tube 136
8·7 Conclusion 137

Chapter 9. LIMITATIONS AND DEFECTS IN VELOCITY-MODULATION TUBES

9·1 Maximum frequency of klystron operation 139
9·2 Hysteresis 141
9·3 Modulation problems 143

Chapter 10. THE DESIGN REQUIREMENTS, AND MANUFACTURE OF VELOCITY-MODULATION TUBE COMPONENTS

10·1 Cathodes 146
    10·1·1 Oxide-coated cathodes 146
    10·1·2 Bombarded cathodes 149
10·2 Heaters 150
10·3 Gun electrodes 151
10·4 Gap grids 154
10·5 Resonators and resonator seals 156
10·6 Reflectors 159
10·7 Collectors 160
    10·7·1 Radiation cooling 160
    10·7·2 Air blast and water cooling 161
10·8 Tuning means 163
    10·8·1 Deformation from outside the vacuum 163
    10·8·2 Thermal tuning 163
10·9 Coupling in totally enclosed tubes 164
10·10 Conclusion 165

PAGE

APPENDIX 1. Example of the design of a high-powered C.W. klystron 166

APPENDIX 2. The travelling wave tube 169

TABLES 174

LIST OF SYMBOLS 176

BIBLIOGRAPHY 177

INDEX 179

HISTORICAL INTRODUCTION

In the thirties the main problem of radio-technology was the production of more power at shorter wave-lengths. This problem was posed originally by the necessity of providing television and frequency-modulated transmitters with their necessarily large band widths. As the international situation deteriorated, it became clear that the decimetre waves were destined to play a large part in warfare because general considerations showed that, for a given transmitter beam angle, the dimensions of the aerial system are directly proportional to the wave-length, and that to realize the full potentialities of radio-reflexion methods, the beam must be swung like the beam of a searchlight.

The classic researches of Llewellyn on transit-time effects had provided a good theory of the operation of triodes at high frequencies and had shown that the only advances which could be made in their design were to decrease electrode dimensions and spacings or to raise the operating voltages. In fact this analysis has stood the test of time, and although great advances have been made in triode design, especially constructional improvements which allow the h.f. power to reach the region in which it can do work on the electron beam, the problems remain essentially the same. In 1939 the acorn represented about the highest point of receiver-tube achievement, but it would not oscillate much below 50 cm. wave-length.

Of course, the triode was not the only possibility. Much work had been done on magnetrons, particularly by Megaw at the G.E.C. and by Kilgore and Linder of R.C.A., while Rice of G.E. had obtained 1 cm. oscillations. However, these magnetrons were inefficient as well as being difficult to tune and modulate. Clavier had produced Barkhausen-Kurz tubes which were reliable enough to use on a 16 cm. cross-channel link, but the efficiencies were even worse than those of magnetrons, and the allowable power input was very low because of the difficulty of leading heat away from the positive grid which takes the used electrons out of the system.

In this situation the almost simultaneous publication of information on the 'klystron' of the Varian brothers, the velocity-modulated tubes of Hahn and Metcalf, and the inductive output amplifier of

Haeff aroused the greatest interest. In the first two devices the principle of operation which has become universally known as velocity modulation (V.M.) was fully realized, but only partially so in the third. At this point it should be said that V.M. had been described some years earlier by Heil in Germany, but the paper had not attracted much attention. The question, who invented the V.M. tube, will probably not be decided without extensive litigation, but the Stanford University Group certainly deserve the credit for first utilizing cavity resonators in conjunction with V.M. to produce the prototype of modern tubes.

The klystron was at first looked on as a source of high-powered oscillations, and work was started with this end in view in many British and American laboratories. In England this work was chiefly carried on at H.M. Signal School, Portsmouth, and at Birmingham University, later continued by the B.T.H. Co. By the middle of 1940 demountable klystrons had given several hundred watts on wave-lengths between 10 and 15 cm., using about 12 kV. acceleration. However, by this time Randall and Boot, working at Birmingham, had produced resonator magnetrons which soon proved to be much more efficient than the klystron, and superseded it as a transmitter.

Meanwhile, Sutton, then in charge of Admiralty Signal Establishment, Bristol, had seen the need for a local oscillator for use in superheterodyne receivers and had appreciated the special advantages of the reflex klystron for this purpose. Intensive work was carried out on the project at A.S.E. Bristol, and at the Clarendon Laboratory, Oxford, with the result that by the end of 1940 a production design had been agreed on with the valve companies. This valve, the NR89, was the first V.M. tube in the world to be put into large-scale manufacture, and although it was soon superseded by an improved tube designed in the E.M.I. laboratories, it played a very important role in establishing microwave technique.

By the middle of 1941 McNally of the Bell Laboratories had produced a low-voltage (300 V.) reflex klystron to overcome the difficulties inherent in the British valves which required 1·2–2·0 kV., and this became the prototype of a long series of tubes.

It is impossible to give any real picture in a few words of the rapidity with which development has taken place since those early days, and still more impossible to give due credit to everyone who made a contribution to the work, particularly so because we are not yet fully informed of what was done in Russian, French and German laboratories.* Much of the work would not have been considered reliable in peacetime, but the accumulation of experience is sufficient to allow me to present a fairly complete and trustworthy account of the theory and practice of V.M. tubes, and to hazard some opinions as to their potentialities.

Quite apart from the technical importance of V.M. tubes themselves, the theoretical study of the processes involved has clarified many difficulties in the theory of triodes working under transit-time conditions and of magnetron operation. This is because the various functions are separated out in the V.M. tube so that we can study the effects of variation of a single parameter. V.M. theory is therefore a very good introduction to a careful study of the more complicated devices. As we shall see, it is quite natural to consider the interaction of h.f. fields with electron beams without worrying about how the fields are produced. The field-producing means then appear in their correct perspective as extensions of the external circuits through the vacuum retaining walls.

---

* Since this was written, Griffiths has described the British work in greater detail. *J. Instn Elect. Engrs*, 93, pt. III A, no. 1 (1946), 173.

Chapter 1

THE ELEMENTARY PRINCIPLES OF VELOCITY-MODULATION TUBES

1·1. In this chapter we seek to present an accurate physical picture of the operation of V.M. tubes in order that the later mathematical development shall have a firm basis in empirical fact.

A thermionic generator or amplifier is usually conceived as an evacuated or gas-filled enclosure with a number of terminals, two or four of which have significance in the performance of the system considered as an active network. Although the electrodes inside the envelope are simply continuations of the external circuits, attention is concentrated on the enclosure as a whole. The electrode potentials are assumed to be known, and the usual characteristics μ, g_m, r_p are calculated from them by the device of equivalent potential. For instance, the parameters of a triode are determined to a first approximation by functions of the algebraic sum $(e_g + e_p/\mu)$. This viewpoint serves very well at low frequencies, when the number of electrons reaching the anode changes at exactly the same instant as the grid potential changes. However, as the frequency increases and the transit time of the electrons in the cathode-grid space increases above about one-twelfth of one period of the applied frequency, the input impedance considered as a parallel circuit changes from a pure reactance to a resistive reactance. As the frequency increases still further, the value of the resistive component diminishes until it vanishes entirely. To give an adequate explanation of these phenomena we have to drop the older potential viewpoint entirely and discuss the motion of electrons in the interelectrode spaces in very much more general terms. That is to say, the electric and magnetic fields inside the envelope must be determined as solutions of Maxwell's equations, and the forces acting on an electron can then be calculated from the Lorentz force law. In other words, we now concentrate our attention on the interaction between electrons and fields, and all our physical pictures are based on this interaction. We make no effort, however, to describe the mechanism of the interaction itself in detail, for that is the province of quantum theory; we simply observe that the principle of conservation of energy demands that if an electron in passing through an electromagnetic field gains or loses energy, the field loses or gains an equal amount of energy. The same deduction can be made from Maxwell's equations, but this is clearly a less direct approach than the simple energetic view.

The division of the thermionic tube into fields plus electron stream has been studied in general terms by Llewellyn in his excellent monograph and in a later paper. In a sense we shall be dealing with applications of his method to certain classes of tube, but, as is usually the case, general methods are not the most suitable for simple applications, although they give the clearest picture, and we shall therefore at first use the more direct ballistic methods which are historically associated with V.M. tubes. It is probably true to say that these general ideas have only gained universal acceptance because of the technical importance of V.M. tubes and magnetrons, which can only be fully understood by a thoroughgoing adoption of the newer picture. The only exception we shall make is to discuss the static or d.c. characteristics of the tubes in terms of the applied potentials because of the simplifications introduced thereby. In practice this means that beam-forming and producing devices are described in the conventional language of electron optics.

1·2. The klystron as amplifier

We shall first describe the operation of the two-resonator klystron as an amplifier and oscillator before going on to describe some slightly more complicated embodiments of the V.M. principle, although this tube is by no means commonly used at present.

The arrangement is shown in fig. 1·1. The tube consists of an electron gun with a unipotential cathode usually indirectly heated but sometimes of the bombarded tantalum type in high-voltage tubes, or even a directly heated tungsten spiral in less highly developed types. The electrons are accelerated by a d.c. voltage applied to the cavity resonators which are almost invariably held at the same potential, and the focusing action of the gun is designed to produce the desired current through the 'tunnel', as the cylinder through which the electrons flow is called. The electron beam is often shown as a parallel-sided cylinder, even in the absence of a magnetic focusing field. This is completely incorrect because space-charge forces between the electrons render it impossible to produce such a beam. The point is of some importance because the space-charge spreading of the beam limits the current which can be focused through a tunnel of given dimensions. As we shall see, this maximum current is directly proportional to the square of the ratio of tunnel diameter to tunnel length. If the tube has been designed to work with this maximum current, the beam converges to the centre and then diverges as indicated by the dotted lines in fig. 1·1. The apertures in the cavity resonators may or may not have grids stretched across them. We shall consider this question in detail later, but for the moment we assume that the tube has grids and that the grids are ideal. That is, we assume that the grid meshes are so small that an electromagnetic field inside the resonator cannot leak through them to an extent which is greater than a few per cent of the spacing between the grids in the resonator. This naturally implies that the length of flight in the h.f. field is equal to the spacing between the grids.

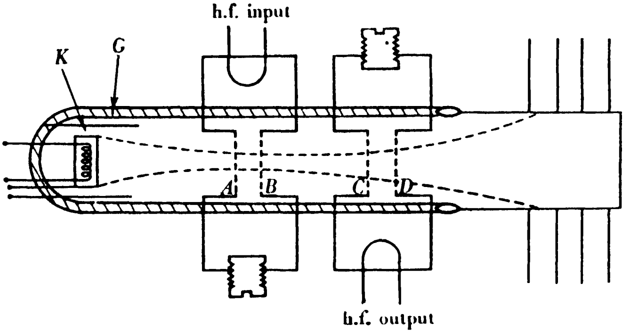

Fig. 1·1. The schematic diagram of a klystron amplifier.

The properties of the resonant cavities are dealt with in the next chapter. All we need say here is that they behave like parallel resonant circuits which are completely screened and therefore cannot radiate or be influenced by external fields. Coupling into the cavities is usually carried out by means of a concentric line terminated in a loop which is so arranged that it induces a magnetic field in the desired direction. In the cavities shown in fig. 1·1 the electric field is in the axial direction, and the magnetic field lines run in concentric circles round the axis. A loop in the plane indicated in the figure will clearly couple to such a magnetic field. The tightness of the coupling is controlled by adjusting the size of the loop or by tilting it with respect to the axis of the tube, or by including a transformer section in the concentric line. Means of tuning the cavities to the input frequency must be provided, and these are indicated by the screws projecting into the toroidal portion. These screws may be thought of as altering the inductance of the circuit.

The electrons proceed from the gun through two pairs of grids and thence to a collector which, as its name implies, removes the electrons from the system. The main function of the collector is to dissipate the required amount of energy which may be done by any of the usual methods, i.e. radiation cooling or air-blast cooling or water cooling. A secondary requirement is that it should not allow any secondary electrons which may be produced to return down the tunnel. This is done by using a cylindrical tube long in comparison with the diameter. We shall have more to say about the design of the tube elements later on, so at this point we confine ourselves to stating the function of each part.

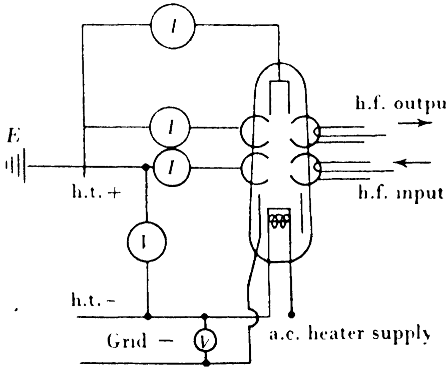

Fig. 1·2. Electrical connexions to a klystron.

The external electrical connexions are simple in the extreme. They are shown in fig. 1·2. Since it is usually desirable to operate the resonators at earth potential, for safety in handling, the h.t. positive lead is earthed as in cathode-ray oscilloscope practice. Current meters are included wherever necessary to ensure that power ratings are not exceeded and to check the operation of the tube. The focusing electrode may be either positive or negative, but it is clearly better to design it to be held negative because it then takes no current from the beam. Klystrons are designed to work at an approximately fixed voltage, so the sequence of operations is to apply the rated voltage, adjust the focusing control for maximum collector current subject to the condition that none of the current-taking electrodes are overloaded, and then to readjust the voltage. It is worth while recalling that if all the voltages are scaled up or down by a given factor, the current to any given electrode is scaled up or down by the same factor raised to the $\frac{3}{2}$ power, and the d.c. power dissipated on the electrode is scaled according to the $\frac{5}{2}$ power. Adjustments and static tests can therefore be made at voltages lower than the operating figure with no risk of burning out grids.

1·2·1. *The action of a velocity-modulation gap*

We now consider that the tube has been correctly set up and that a source of h.f. power has been connected to the input loop. The input cavity is then tuned to resonance with the h.f. generator. Resonance may be detected in several ways, for instance, by lightly coupling a crystal detector to the input resonator, or by using a similar detector to observe absorption of power from the generator. When this has been done we know that an electric field exists between the input resonator grids. This field consists only of an axial component in the resonators shown, and the sense of the field changes from left to right to right to left at the commencement of each half-cycle of the h.f. wave.

Electrons enter the space between the grids at a constant rate with a velocity which depends on the accelerating voltage applied to the tube. If an electron has fallen through a potential drop of V_0 V., it must have gained kinetic energy equal to the loss in potential energy. Therefore

$$\tfrac{1}{2}mu_0^2 = eV_0$$

or

$$u_0 = (2e/m)^{\frac{1}{2}}\, V_0^{\frac{1}{2}}$$

$$= 5{\cdot}95 \times 10^5 V_0^{\frac{1}{2}} \text{ m./sec.,} \qquad (1)$$

where e = electronic charge

$= 1{\cdot}59 \times 10^{-19}$ coulomb,

m = electronic mass

$= 9{\cdot}01 \times 10^{-31}$ kg.

Since $V_0^{\frac{1}{2}}$ is of the order of 10 it is clear that the distance travelled by an electron in one cycle of oscillation is comparable with the dimensions of ordinary apparatus for frequencies of the order of 60 Mc./sec.

The electrons entering the h.f. field acting between *AB* in fig. 1·1 are accelerated or decelerated according to whether they enter when the field acts from *A* to *B* or vice versa. The magnitude of the acceleration depends on the precise instant at which an electron enters. This is made clear by reference to fig. 1·3. For the moment we shall suppose that the time taken by any electron to cross the space *AB* is infinitesimally smaller than one-half of the cycle, but we shall soon eliminate this assumption. The electrons therefore emerge from grid *B* at a constant rate, but the velocities vary between $u_0 \pm u_1$, where u_1 is the velocity gained by an electron passing *A* at the instant t_1 when the h.f. field gives a maximum acceleration. We now consider the motion of two electrons which enter the gap at t_0 and t_2, neither of which experiences any change of velocity in the gap, and so can be used as reference electrons. Electrons which passed through the gap at times earlier than t_0 were slowed down and therefore appear to an observer on the reference electron to be moving towards him. Conversely, electrons which passed through after t_0 gain velocity and therefore appear to be overtaking the observer. This means that as the reference electron moves along the field-free tunnel between the cavities, the concentration of electrons in the immediate vicinity of the reference is increasing. Similar considerations applied to the t_2 reference show that the concentration is there decreasing.

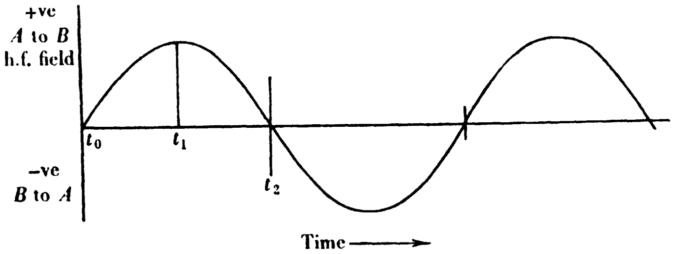

Fig. 1·3. The h.f. field in the modulating gap.

The concentration round the t_0 reference increases to a maximum for a certain value of the distance along the field-free part of the tunnel. This is known as the drift tube, because the velocities with which the electrons concentrate are considered to be much smaller than the initial velocity u_0, although this is not necessarily true. That there is a maximum concentration is clear from the fact that the electrons which have been speeded up can drift forward through the plane occupied by the reference. The maximum concentration will occur when an electron which passed between AB at some instant between t_1 and t_2 has overtaken the electrons which passed at t_0, but we cannot determine the precise instant without a quantitative discussion. We observe that one bunch is formed for every complete cycle of h.f. input. The variation in concentration of the beam is termed 'bunching' and the input resonator is called the buncher. By passing a beam of electrons through a V.M. gap and allowing time for the drift action to take place we have achieved something very like ordinary conduction-current modulation, although the expression relating the number of electrons passing any given plane to the time is no longer directly proportional to $\sin \omega t$.

The process of concentration may be made somewhat more graphic by constructing a diagram which seems to have been first used by Applegate in America. In this diagram the motion of electrons is exhibited by using distance from the centre of the buncher gap as ordinate and the time as abscissa. The electron motions are represented by straight lines on this diagram, the slope of the line being equal to the velocity. If we plot the motion of electrons which enter the buncher at 15° intervals, we obtain the diagram of fig. 1·4.

The concentration of electrons between the planes A and B is obvious.

We now consider what happens when the beam enters the space CD. However short the spacing between B and C there must be some bunching so that the beam passing between CD has a maximum once per cycle at the input frequency. Now if an isolated electron packet were to cross the gap CD, the positive charge distribution induced on the grid C (assumed ideal) would retard the bunch. The positive charge cannot move from C–D quickly because of the inductance of the path between, so the bunch leaves the field before the latter changes direction. The field across CD therefore opposes the motion of the electron packet which is slowed down

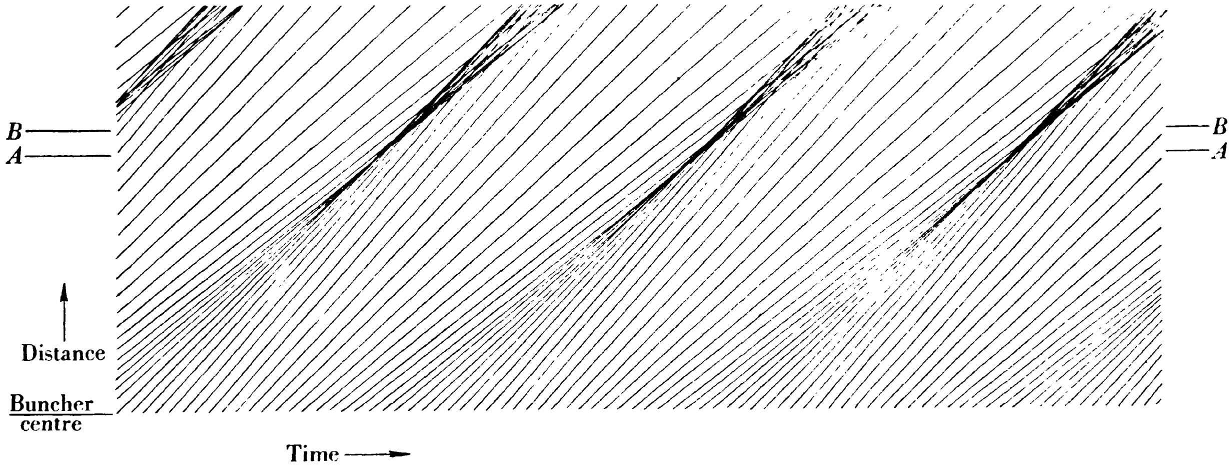

Fig. 1·4. Applegate diagram, showing electron position as a function of distance and time.

thereby, and gives up some of its kinetic energy to the field. The process is indicated diagrammatically in fig. 1·5. Since the cavity is a low-loss resonant circuit, oscillations will persist for some time after the exciting electron packet has left the plane *D*. If an unmodulated electron beam is passed through the gap, energy will be extracted from the beam during one half-cycle of the cavity oscillation, but an equal amount will be given back during the half-cycle when the field acts from *C* to *D*.*

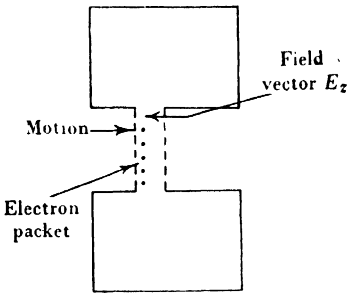

Fig. 1·5. Induction of field in a resonator by an electron packet.

The klystron beam exhibits, however, variations in current density, and the energy taken from the beam when the bunch crosses the gap is greater than that lost when the rarefied part of the beam passes through in the positive half-cycle. Thus there is a net loss of energy from the beam when the process is averaged over one cycle. This energy is gained by the field, and therefore continuous undamped oscillations are set up in the output cavity, which is often called the catcher. The catcher phase is such that the catcher field goes through the negative maximum at the instant the reference electron which is at the centre of the bunch reaches the centre of the gap, because the energy extracted from the beam is then a maximum. This also follows from a study of the induction process.

The load has to be correctly matched to the parallel combination of the resonator impedance and the active-beam impedance. This is naturally carried out by varying the coupling between the resonator and the output line. It is often incorrectly stated that the load must be matched to the resonator impedance, whereas in fact the active-beam impedance is much lower than the resonator impedance in a good design. We shall see that the beam impedance is one of the most important parameters in klystron design.

* This last remark is only true in the present approximation; in more general cases in which the gap field is non-uniform and the transit-time across the gap is comparable with a half-cycle, there will be a net interchange of energy averaged over one cycle.

We have now seen qualitatively how a two-resonator klystron can act as an amplifier; we next proceed to consider the operation of the tube as a self-oscillator.

1·3. The klystron self-oscillator

The conditions that any tube amplifier must obey, if it is to be made into an oscillator, are that the amplification shall be greater than unity and that the total phase change round the circuit shall be $2n\pi$, where n is an integer. We cannot say anything about the gain without a quantitative discussion, but we can deduce the phase conditions easily enough. This is worth doing because of the increased physical insight we gain in spite of the fact that the phase condition comes directly out of the mathematical analysis.

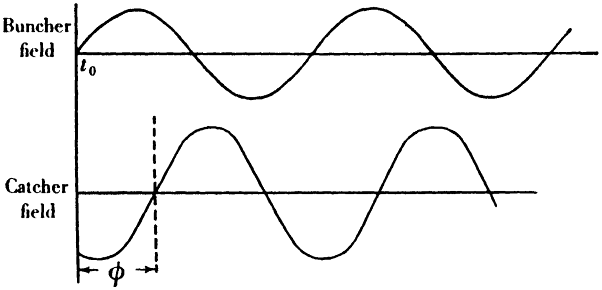

Fig. 1·6. Buncher and catcher fields in time.

The klystron is made to oscillate by coupling a part of the power in the catcher back into the buncher. This may be done by a short length of concentric line connected to loops in each resonator, or if the resonators have a common wall, coupling is arranged by cutting a hole in it. We assume that the electrical length of the coupling device is such that there is a phase difference of ϕ radians between buncher and catcher. We have already deduced that if the beam is to deliver full power to the catcher, the reference electron which passed through the buncher at time t_0 must arrive at the centre of the catcher gap at a time when the catcher field is at its negative maximum. Reference to fig. 1·6 shows that these instants occur at the angles

$$\phi+(4n-1)\tfrac{1}{2}\pi \quad (n=0,1,2, \text{etc.}).$$

The transit angle of the reference electron in the drift tube must therefore be equal to this. If the drift tube is s m. long the time spent in it is approximately s/u_0 sec. and the transit angle is $2\pi s/u_0\tau$, where τ is the period of the oscillation. But

$$\frac{2\pi s}{u_0\tau}=\frac{\omega s}{u_0},$$

therefore $$\frac{\omega s}{u_0}=\phi+(4n-1)\tfrac{1}{2}\pi \quad (n=0,1,2,\text{ etc.}). \tag{2}$$

This expression for the phase condition shows that for a fixed s and ω oscillations will be obtained only at certain discrete voltages. This type of condition is common to all transit-time devices and differentiates them sharply from low-frequency oscillators. Eqn. (2) is always exactly obeyed, and if the voltage is slightly altered the frequency will alter in such a way as to maintain the phase condition. Oscillation will be possible as long as the power gain exceeds unity. The frequency difference between the points at which oscillation stops primarily depends on the loaded Q of the cavities. The frequency stability of klystron oscillators is inherently high compared with triode self-oscillators, but does not approach the stability of crystal-controlled systems. Naturally voltage stabilizers are used whenever optimum frequency stability is important.

1·4. The reflex klystron oscillator

The reflex klystron is by far the most common type of V.M. tube and is used as the local oscillator in almost all centimetric receivers. It has achieved this position because of the simplicity and ease of tuning gained by using only one resonator and because some degree of frequency control is obtained by adjusting a negative voltage. This feature is important in A.F.C. systems. The tube is sketched in fig. 1·7. Electrons are sent from a gun through a velocity modulating gap and into a retarding d.c. field in which they come to rest and then reverse their direction, making a second transit through the h.f. field on the return journey. When the electrons arrive back in the cathode-resonator space the d.c. field deflects them on to the body of the resonator which therefore has to dissipate the anode loss of the tube. Because it is difficult to arrange good cooling of the resonator the reflex is much less suitable as a high-powered c.w. oscillator than the straightforward klystron.

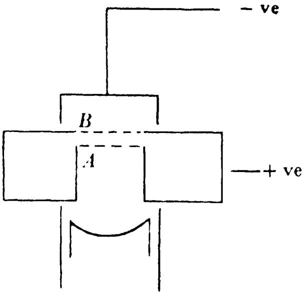

Fig. 1·7. Schematic diagram of a reflex klystron.

To understand the action of the tube we assume that due to random fluctuations in the beam a small voltage at the resonator frequency exists across the resonator grids. This voltage velocity modulates the beam in the manner we have previously described. Consider the motion of an electron in a retarding field which, for the time being, is assumed to vary linearly with distance from the exit grid. If the field strength is A V./m. and the electron has an initial velocity u_0 m./sec., the time taken to return to the starting-point is

$$T = \frac{2u_0 m}{eA}, \tag{3}$$

from which it is obvious that the accelerated electrons spend a longer time in the reflecting field than the reference electrons, whose velocities are unchanged by passing through the field. The bunch therefore tends to form on the reference electron which passes through the gap when the h.f. field passes through zero while changing from positive to negative. The electrons are reversed by the reflexion field, so the condition that they shall lose energy to the field, thereby causing the amplitude of the oscillations to increase, implies that they must make the second transit through the gap when the field is directed from A to B (fig. 1·7). A glance at fig. 1·8 shows the phase condition to be

$$\omega T = (n + \tfrac{3}{4})\, 2\pi \quad (n = 0, 1, 2, 3, \text{ etc.}), \tag{4}$$

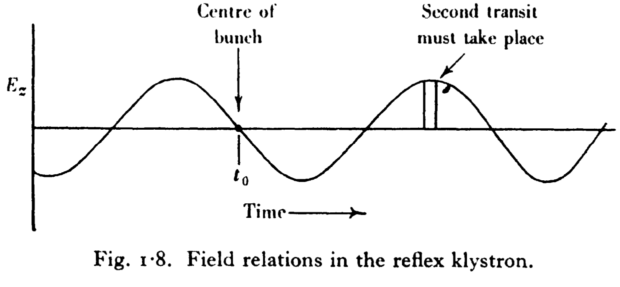

Fig. 1·8. Field relations in the reflex klystron.

where ω = angular frequency and T = mean transit time in the reflector field. This condition is the same as the one we derived for the klystron in the particular case when the two resonators are oscillating in phase with one another, because both the phase of the reference electron and the phase of the h.f. field have been altered by 180° from the klystron values.

Eqns. (3) and (4) show that the oscillations appear only for discrete resonator and reflector voltages, for with the assumptions made,

$$A = \frac{V_0 - V_r}{d}, \tag{5}$$

$$u_0 = 5{\cdot}95 \times 10^5 V_0^{\frac{1}{2}}, \tag{6}$$

where V_0 = resonator voltage, V_r = reflector voltage (usually negative) and d = reflector spacing, therefore

$$T = \frac{V_0^{\frac{1}{2}}}{V_0 - V_r} \frac{4d}{5{\cdot}95 \times 10^5}. \tag{7}$$

It is most useful to consider the operation at a fixed anode voltage, and in this case the tube oscillates for the series of reflector voltages which, when substituted in (3), cause T to satisfy (4). Although (7) is not correct for any real tube geometry it is sometimes useful when it is required to determine the n value of a particular oscillation. In England it is usual to define the mode of oscillation by giving the number of quarter periods spent by the reference electron in the reflector field. For instance, a reflex tube operating with $n = 1$ is referred to as oscillating in mode 7. This usage has the advantage of being unambiguous and is applicable to both reflex and two-resonator klystrons, whereas notations based on the value of n require further specification.

A rather interesting variant of the reflex klystron has sometimes been used. The physical appearance of the tube is unaltered, but the reflector is replaced by an electrode which is able to emit a copious secondary emission. Since the surfaces usually used as secondary emitters are destroyed in a few hours by the relatively heavy currents required in V.M. tubes, aluminium is often chosen for the purpose. The secondary anode is maintained at a potential which ensures that its secondary emission coefficient is greater than unity. Most of the secondaries (about 90 %) are emitted with energies ranging up to 20 e.V., and the emission of a secondary is simultaneous with the arrival of a primary. The anode is bombarded with a bunched beam which returns to the resonator still bunched, because the secondaries have only a random velocity distribution, and increased in magnitude by a factor equal to the average secondary emission coefficient of the surface. The advantages of this scheme are, in fact, somewhat illusory, because correct design of the reflector field in a reflex klystron will give nearly the same results, and the provision of a special power supply for the anode, necessitated by the unusual current characteristics, is a nuisance.

1·5. The Heil tube

As we have already said, the Heil tube was the first V.M. tube to be invented, and it has been very extensively studied by the workers in the Standard Telephone and Cable Laboratories. The arrangement described in Heil's original paper is shown in fig. 1·9.

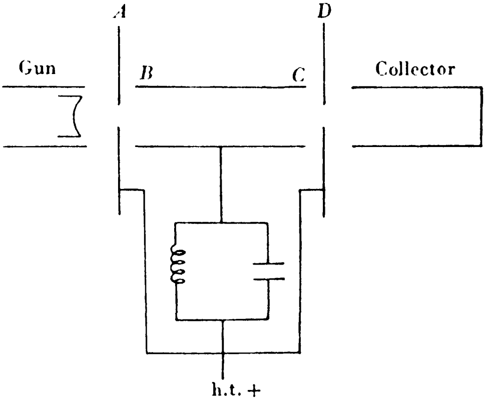

Fig. 1·9. The original Heil tube (schematic).

Electrons are accelerated from the gun by the anode A. They pass through a hole in A and traverse an h.f. field in the gap AB, passing out of the field into a metal tube running from B to C. The tubular electrode BC is connected to one side of a parallel resonant circuit, A and D being returned to the other side.

If we consider that the tube is in a state of steady oscillation we see that the beam is velocity modulated in the field between A and B in exactly the same way as happens in the case of the klystron. The only difference made by the absence of grids is that the h.f.

field extends slightly into *BC*. The high-tension voltage is adjusted so that the transit time of the reference electron from *B* to *C* is $(n+\frac{3}{4})$ periods of the oscillation. The beam is then slowed down by the h.f. field from *D* to *C* and gives up energy to it. The oscillations will therefore be maintained and a load can be coupled to the resonant circuit. When the h.f. field is directed from *A* to *B* it is also directed from *D* to *C*. The fields in the gaps *AB* and *DC* are therefore in antiphase. If we put $\phi = \pi$ in eqn. (2) we obtain

$$\frac{\omega s}{u_0} = (4n+1)\tfrac{1}{2}\pi \quad (n = 0, 1, 2, \text{etc.}), \tag{8}$$

as the condition for correct phasing. The Heil tube is therefore exactly the same as a klystron in which the resonators are oscillating 180° out of phase with one another and in which the coupling between the resonators has been adjusted so that the same voltage appears across each. The modern embodiment of the Heil tube differs from the arrangement described by using a concentric line resonator in place of the lumped constant circuit. A wedge-shaped beam is passed through the resonator as shown in fig. 1·10*a*, *b*. The coaxial line is usually effectively $\frac{1}{2}\lambda$ long and is tuned by a sliding short circuit. The beam breadth is considerably less than $\frac{1}{2}\lambda$ because the radial field varies approximately sinusoidally along the resonator (fig. 1·10*c*), and if the beam extends too far, the power lost in the resonator due to the beam loading will increase more rapidly than the power gain due to the increase in bunched current.

A slight modification of the Heil tube due to Samuel of the Bell Telephone Laboratories is obtained by removing the common wall between the resonators of an ordinary klystron, leaving only a radial wire to act as a d.c. connexion. The resonators are thus unity coupled and constrained to oscillate in phase with one another. The phase condition now reads

$$\frac{\omega s}{u_0} = (4n-1)\tfrac{1}{2}\pi \quad (n = 1, 2, 3, \text{etc.}). \tag{9}$$

The Samuel tube will therefore oscillate in modes 3, 7, 11, etc., while the Heil tube only gives modes 1, 5, 9, etc.

The reflex klystron has one great advantage over the Heil tube, the Samuel tube and the two-resonator klystron, when extended tuning ranges are required. In the reflex the phase condition can be satisfied for a fixed resonator potential and mode number by varying the reflector voltage. The input power therefore remains constant. In the other tubes ω/u_0 has to remain constant and $u_0 \propto V_0^{\frac{1}{2}}$, so for a 2 : 1 change in frequency V_0 changes 4 : 1 which in turn causes the power input to change 32 : 1. If a screen electrode is used the current may be kept constant, but at best a 4 : 1 variation in input has to be tolerated.

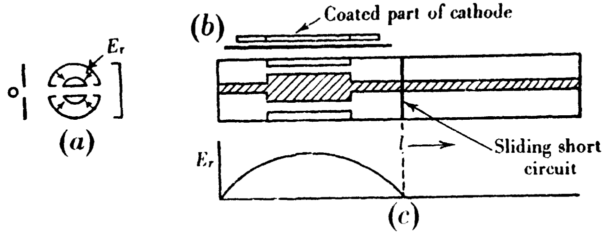

Fig. 1·10. Schematic diagram of modern coaxial line tube.

1·6. The inductive output tube and the Hahn-Metcalf velocity-modulation tubes

These types are obsolete, but a brief description is included for the sake of completeness. In the inductive output amplifier the input voltage is applied between the cathode and a conventional grid. The current concentration therefore varies in just the same way as in an ordinary triode. The beam is next accelerated and traverses a gap which takes up some of the energy from the beam. The output resonator was clamped to the outside of the glass envelope in the examples described by Haeff in his papers. The best designation of the tube is to call it a triode with a resonator output.

The Hahn-Metcalf[*] tube was a thoroughgoing application of the V.M. principle but did not use tuned resonators as integral parts of the tube. The input voltage was applied to one or more modulators of the form shown in fig. 1·11 by means of a concentric line. The dimensions of the modulator were small enough to make it act as a lumped capacitance. The transit-time through the field-free drift tunnel could be so adjusted that energy was absorbed from the h.f. field both at entrance and exit. The depth of modulation was increased by using a number of modulators along the beam. A similar modulator was arranged so as to abstract the energy and feed it to the load.

[*] Hahn and Metcalf, *Proc. Inst. Radio Engrs, N.Y.*, 27 (1939), 106.

The chief merit of Hahn and Metcalf's original paper was that it gave a very clear physical picture of the velocity-modulation process and also enumerated the methods by which velocity modulation could be converted into conduction-current modulation. We have already described the most important of these in detail, i.e. the action of a drift tube. The remaining methods are the following.

(1) To pass the velocity-modulated beam through a magnetostatic or electrostatic deflecting field. The high-velocity electrons are deflected less than the slower electrons, and can be separated from them by suitable means such as an aperture in a shield. A pulse of electrons thus occurs once per cycle of the driving frequency.

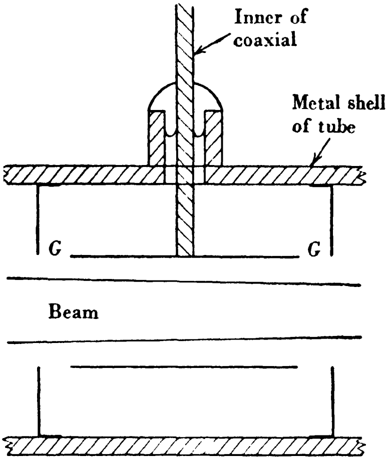

Fig. 1·11. Modulator used by Hahn and Metcalf.

(2) The action of a retarding field. There are two modifications of this method. First, to use the retarding field as a drift space as has been described in the section on the reflex klystron, and secondly, another method in which the reflector is held near cathode potential. In this condition faster electrons reach the reflector while the slower ones are turned back. The reflector can be biased to the steepest part of its current voltage characteristic.

Although many schemes have been suggested to make use of deflexion conversion none has passed out of the laboratory stage. The main difficulty lies in making use of a sufficient proportion of the beam current to compete in efficiency with drift-tube conversion. Retarding field sorting has been used in an attempt to make V.M. mixer tubes. Hahn and Metcalf* described one way of doing this which is shown in fig. 1·12. The signal voltage is applied to one modulator and the local oscillation voltage to the other, the reflector being biased to the point of maximum slope. The collector current will then contain a component at the difference frequency, which is fed to an i.f. amplifier in the standard way. In some cases the mixer was made to produce its own oscillation by adjusting the angle of the reflector so that electrons were passed back through the second modulator but not through the first. V.M. mixers have proved unsuccessful up to the present because of the existence of a large noise source whose nature is not yet understood, but it is likely that their advantages over crystals will encourage further studies to be made.

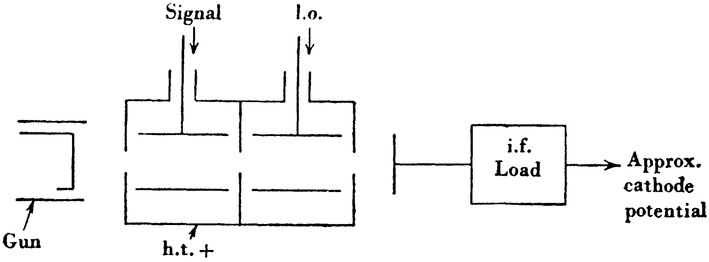

Fig. 1·12. V.M. mixer of Hahn and Metcalf.

1·7. Conclusion

We have now completed the description of the V.M. tube art as it stood at the beginning of the war. After an account of the properties of cavity resonators we shall reformulate the physics in mathematical terms, first in a form only suitable for small signal studies, and then in a more refined form. The general theory will then be applied to the several types of V.M. tubes. The ballistic approach to magnetron and Barkhausen-Kurz tubes, as well as V.M. tubes, has been described by Samuel† in an interesting general survey.

---

* Hahn and Metcalf, *Proc. Inst. Radio Engrs, N.Y.*, 27 (1939), 106.

† Samuel, A. L., *Bell Syst. Tech. J.* 24 (1945), 322.

Chapter 2

CAVITY RESONATORS

2·1. In this chapter we shall give a résumé of the theory of cavity resonators leading up to the approximation methods which have proved useful in tube design; for, as will soon be apparent, exact solutions are only possible for a relatively small variety of shapes. The resonator shapes which are forced on one by manufacturing conditions are usually far from simple, and the best one can hope for from a theoretical standpoint is an approximate value for the lowest resonant frequency. However, even this knowledge saves a great deal of experimental work.

Cavity resonators can be approached from two points of view. The engineer with a knowledge of h.f. transmission lines prefers to think of them as generalized lines, while the physicist usually finds it more useful to start from the vibration modes of oscillating mechanical systems. This viewpoint is more fundamental and gives more insight into the processes involved, and will therefore be adopted here. We shall apply this method to lines so as to form a bridge for the engineer.

2·2. Acoustic resonators

Before we study any cases of electrical oscillation it will be valuable to review some cases in the theory of sound. This allows us to consider only one set of modes instead of the double set necessary in the electromagnetic case. We know, for instance, that if a wire is tightly stretched between two massive retaining members and subjected to an arbitrary displacement subsequently being allowed to move freely, the resulting sound consists of the fundamental frequency of the wire with a number of superposed harmonics. The choice of the observed harmonics from the infinite series which is theoretically possible and the values of their amplitudes depends on the displacing force. The important physical fact is that the boundary conditions, in this case the length of the wire and rigidity of the supports, determine all the possible frequencies. The displacement function selects from among them and fixes the amplitudes. This is true of all resonant systems, whether electrical or mechanical.

If, instead of applying an impulsive force, we drive the wires with a periodic function, the results are rather different. If the losses of the vibrating system are low, i.e. in the case of the wire the supports are rigid, air damping reduced and the Young's modulus of the material high, the response consists of a transient at the natural frequency of the system plus a steady component at the driving frequency. If the losses are high the duration of the transient may be short enough to disguise its existence. If the driving frequency is adjusted to the natural frequency the phenomenon of resonance is observed.

We now consider the mathematical formulation of these ideas. If the tension in the wire is T kg./m. and the specific mass of the wire m kg./m., the equation of motion is

$$\frac{\partial^2 y}{\partial x^2} - \frac{m}{T}\frac{\partial^2 y}{\partial t^2} = 0, \tag{1}$$

where y is the ordinate and x the abscissa.

This partial differential equation can be solved by the method of separation. We put

$$y = X(x)\,T(t).$$

Then
$$\frac{X''(x)}{X(x)} - \frac{m}{T}\frac{T''(t)}{T(t)} = 0,$$

or if $k^2 =$ the separation constant

$$X''(x) - k^2 X(x) = 0, \quad T''(t) - k^2 \frac{T}{m} T(t) = 0.$$

Then
$$X(x) = e^{jkx}, \tag{2}$$

$$T(t) = e^{jk(T/m)^{\frac{1}{2}}t}. \tag{3}$$

Clearly
$$k\left(\frac{T}{m}\right)^{\frac{1}{2}} = \omega, \quad \text{the pulsatance,}$$

therefore
$$k = \omega\left(\frac{m}{T}\right)^{\frac{1}{2}}.$$

Since the equation is linear and homogeneous we can write

$$y = \sum_n e^{j\omega_n t}(A_n \sin k_n x + B_n \cos k_n x).$$

Now consider the boundary conditions. Since the wire is held at both ends $y = 0$ when $x = 0$ and when $x = L$. From these we see that $B = 0$. Furthermore, $\sin kL = 0$ or $k = n\pi/L$,

$$y_n = A_n e^{j\omega_n t} \sin \frac{n\pi x}{L}, \tag{4}$$

$$\omega_n = \frac{n\pi}{L}\left(\frac{T}{m}\right)^{\frac{1}{2}}. \tag{5}$$

Eqn. (5) shows that the boundary conditions for the problem are only fulfilled for certain specific frequencies.

If the same problem were worked out for the case of a rectangular sheet, the frequencies would be found to depend on two separation constants such that the pulsatance is given by

$$\omega_{n_1 n_2} = \left(\frac{T}{m}\right)^{\frac{1}{2}} \left\{\left(\frac{n_1 \pi}{a}\right)^2 + \left(\frac{n_2 \pi}{b}\right)^2\right\}^{\frac{1}{2}}, \tag{6}$$

where n_1 and n_2 are integers and a and b are the sides of the rectangle. Naturally a similar formula will hold for the case of a three-dimensional bar.

Thus we see that the natural frequencies of vibration of solid bodies are functions of integral multiples of the reciprocals of the linear dimensions.

2·3. Electromagnetic waves

A cavity resonator consists of a metal box in which a system of standing electromagnetic waves can be excited. As we shall see, the frequencies at which the cavity resonates depend on the dimensions in the same sort of way as in the sonic cases which we have already studied. One of the boundary conditions which we shall use for electrical problems is strictly true only for bounding walls of zero resistivity, but gives results which are accurate enough for any metallic surface. This is that an electric field cannot exist tangential to a metal wall. A second condition is that the magnetic field at a wall is tangential to the wall and its value is equal to the surface-current density. A further requirement is obvious, that no functions shall be chosen which go to infinity at any point in the volume of integration. This requirement enables us to eliminate whole classes of functions in some of the more common problems.

It should be remembered that the number of co-ordinate systems in which the wave equations which we require to solve are separable, is limited to eleven. These co-ordinates all give rise to simple geometrical shapes which are unlikely to arise in practical designs. We have to renounce the idea of obtaining analytic solutions to most of our problems, but the study of the simple cases provides a general understanding of the phenomena likely to be encountered.

Maxwell's equations in free space and in the absence of free charges read

$$\left.\begin{aligned} &(a)\ \nabla\times\mathbf{H} = \epsilon_0\frac{\partial\mathbf{E}}{\partial t}, && (c)\ \nabla.\mathbf{E} = 0,\\ &(b)\ \nabla\times\mathbf{E} = -\mu_0\frac{\partial\mathbf{H}}{\partial t}, && (d)\ \nabla.\mathbf{H} = 0.\end{aligned}\right\} \tag{7}$$

The units are m.k.s. in which

$$\mu_0 = 4\pi\times 10^{-7}\text{ henry/m.},\quad \epsilon_0 = \frac{1}{36\pi}\times 10^{-9}\text{ farad/m.}$$

All the fields considered have the time dependence $e^{j\omega t}$.

We consider a system of generalized orthogonal co-ordinates in which the line element is

$$ds^2 = e_1^2dx_1^2+e_2^2dx_2^2+e_3^2dx_3^2.$$

Furthermore, we introduce the wave number k. (7a) and (7b) can now be written

$$\left.\begin{aligned} je_2e_3k\left(\frac{\epsilon_0}{\mu_0}\right)^{\frac{1}{2}}E_1 &= \frac{\partial}{\partial x_2}e_3H_3-\frac{\partial}{\partial x_3}e_2H_2,\\ je_3e_1k\left(\frac{\epsilon_0}{\mu_0}\right)^{\frac{1}{2}}E_2 &= \frac{\partial}{\partial x_3}e_1H_1-\frac{\partial}{\partial x_1}e_3H_3,\\ je_1e_2k\left(\frac{\epsilon_0}{\mu_0}\right)^{\frac{1}{2}}E_3 &= \frac{\partial}{\partial x_1}e_2H_2-\frac{\partial}{\partial x_2}e_1H_1,\end{aligned}\right\} \tag{8a}$$

$$\left.\begin{aligned} -je_2e_3k\left(\frac{\mu_0}{\epsilon_0}\right)^{\frac{1}{2}}H_1 &= \frac{\partial}{\partial x_2}e_3E_3-\frac{\partial}{\partial x_3}e_2E_2,\\ -je_3e_1k\left(\frac{\mu_0}{\epsilon_0}\right)^{\frac{1}{2}}H_2 &= \frac{\partial}{\partial x_3}e_1E_1-\frac{\partial}{\partial x_1}e_3E_3,\\ -je_1e_2k\left(\frac{\mu_0}{\epsilon_0}\right)^{\frac{1}{2}}H_3 &= \frac{\partial}{\partial x_1}e_2E_2-\frac{\partial}{\partial x_2}e_1E_1.\end{aligned}\right\} \tag{8b}$$

In applying these equations we shall assume that metallic boundaries are of infinite conductivity when calculating resonances. The fields thus obtained can then be used to calculate the resistive losses in the walls when these are required. This approximation is good enough for all metals.

Following the technique of Borgnis* we limit ourselves to the cases in which $e_1 = 1$ and e_2/e_3 is independent of x_1. These cases include those of practical importance.

Furthermore, we can distinguish two general types of field which are particularly important in the case of running waves but also serve as a basis for a systematic nomenclature for all cavity modes. These are the transverse electric (TE) field type, in which there is no electric field along the direction of propagation ($E_1 = 0$), and the transverse magnetic type (TM) in which $H_1 = 0$. These fields are sometimes referred to as H-waves and E-waves respectively, but this usage is dying out in favour of the more precise titles.

When all these substitutions are made it is found that solutions of the equation

$$\frac{\partial^2 U}{\partial x_1^2}+\frac{1}{e_2 e_3}\left[\frac{\partial}{\partial x_2}\frac{e_3}{e_2}\frac{\partial U}{\partial x_2}+\frac{\partial}{\partial x_3}\frac{e_2}{e_3}\frac{\partial U}{\partial x_3}\right]+k^2 U = 0 \qquad (9)$$

are solutions of Maxwell's equations.

Here U is a function defined by the following equations:

TE modes:

$$\left.\begin{aligned} E_1 &= 0, & H_1 &= -k^2 U - \frac{\partial^2 U}{\partial x_1^2}, \\ E_2 &= j\frac{k}{e_3}\left(\frac{\mu_0}{\epsilon_0}\right)^{\frac{1}{2}}\frac{\partial U}{\partial x_3}, & H_2 &= -\frac{1}{e_2}\frac{\partial^2 U}{\partial x_1\,\partial x_2}, \\ E_3 &= -j\frac{k}{e_2}\left(\frac{\mu_0}{\epsilon_0}\right)^{\frac{1}{2}}\frac{\partial U}{\partial x_2}, & H_3 &= -\frac{1}{e_3}\frac{\partial^2 U}{\partial x_1\,\partial x_3}. \end{aligned}\right\} \qquad (10)$$

TM modes:

$$\left.\begin{aligned} H_1 &= 0, & E_1 &= k^2 U + \frac{\partial^2 U}{\partial x_1^2}, \\ H_2 &= j\frac{k}{e_3}\left(\frac{\epsilon_0}{\mu_0}\right)^{\frac{1}{2}}\frac{\partial U}{\partial x_3}, & E_2 &= \frac{1}{e_2}\frac{\partial^2 U}{\partial x_1\,\partial x_2}, \\ H_3 &= -j\frac{k}{e_2}\left(\frac{\epsilon_0}{\mu_0}\right)^{\frac{1}{2}}\frac{\partial U}{\partial x_2}, & E_3 &= \frac{1}{e_3}\frac{\partial^2 U}{\partial x_1\,\partial x_3}. \end{aligned}\right\} \qquad (11)$$

We shall now consider some applications of this analysis.

---

* Borgnis, *Ann. Phys., Lpz.*, 35 (1939), 359.

2·4. Resonant frequencies of a rectangular box

Let the box have sides of length a, b and c. Then

$$x_1 = x, \quad x_2 = y, \quad x_3 = z, \qquad e_1 = e_2 = e_3 = 1.$$

Eqn. (9) now reads
$$\frac{\partial^2 U}{\partial x^2}+\frac{\partial^2 U}{\partial y^2}+\frac{\partial^2 U}{\partial z^2} = 0. \tag{12}$$

The solution of this equation now is

$$U = e^{\pm jk_1x \pm jk_2y \pm jk_3z},$$

where
$$k^2 = k_1^2+k_2^2+k_3^2.$$

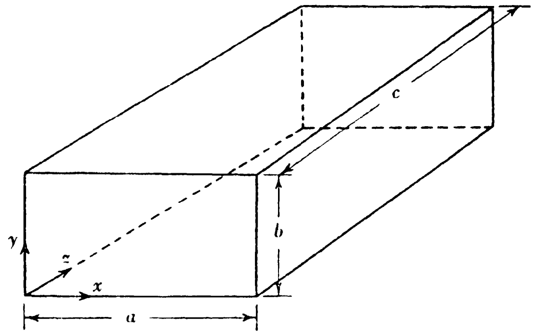

Fig. 2·1. System of Cartesian co-ordinates in a rectangular box.

The boundary conditions are that at

$$\begin{aligned} x &= 0 \text{ and } x = a, & E_y &= E_z = 0,\\ y &= 0 \text{ and } y = b, & E_z &= E_x = 0,\\ z &= 0 \text{ and } z = c, & E_x &= E_y = 0.\end{aligned}$$

TE modes:

The solution which is symmetrical about the centre of the box is

$$U = \cos k_1 x \cos k_2 y \sin k_3 z. \tag{13}$$

The boundary conditions further show that

$$k_1 = \frac{l\pi}{a}, \quad k_2 = \frac{n\pi}{b}, \quad k_3 = \frac{m\pi}{c},$$

where l, m and n are integers. Then

$$k^2 = \pi^2\left[\frac{l^2}{a^2}+\frac{m^2}{b^2}+\frac{n^2}{c^2}\right] = \frac{4\pi^2}{\lambda^2}, \tag{14}$$

or

$$\lambda^2 = \frac{2}{\left(\frac{l^2}{a^2}+\frac{m^2}{b^2}+\frac{n^2}{c^2}\right)^{\frac{1}{2}}}. \tag{15}$$

The component field can, of course, be found by substituting the value of U given by eqn. (13) back into (10). When this is done we obtain the following expressions:

$$\left.\begin{aligned} E_z &= 0,\\ E_x &= -jkk_2\left(\frac{\mu_0}{\epsilon_0}\right)^{\frac{1}{2}} \cos k_1x \sin k_2y \sin k_3z,\\ E_y &= jkk_1\left(\frac{\mu_0}{\epsilon_0}\right)^{\frac{1}{2}} \sin k_1x \cos k_2y \sin k_3z,\\ H_z &= (k^2-k_3^2) \cos k_1x \cos k_2y \sin k_3z,\\ H_x &= -k_3k_1 \sin k_1x \cos k_2y \cos k_3z,\\ H_y &= -k_3k_2 \cos k_1x \sin k_2y \cos k_3z. \end{aligned}\right\} \tag{16}$$

TM modes:

In this case $U = \sin k_1x \sin k_2y \cos k_3z.$ (17)

The eigenvalues are again given by eqn. (15). The field components are

$$\left.\begin{aligned} H_z &= 0,\\ H_x &= jkk_3\left(\frac{\epsilon_0}{\mu_0}\right)^{\frac{1}{2}} \sin k_1x \cos k_2y \cos k_3z,\\ H_y &= -jkk_1\left(\frac{\epsilon_0}{\mu_0}\right)^{\frac{1}{2}} \cos k_1x \sin k_2y \cos k_3z,\\ E_z &= (k^2-k_3^2) \sin k_1x \sin k_2y \cos k_3z,\\ E_x &= -k_3k_1 \cos k_1x \sin k_2y \sin k_3z,\\ E_y &= -k_3k_2 \sin k_1x \cos k_2y \sin k_3z. \end{aligned}\right\} \tag{18}$$

Any particular mode can now be described by giving the values of (l, m, n) and the wave type. For instance, one speaks of a TM (1, 0, 1) mode or a TE (1, 1, 0) mode, and so on.

The lowest modes are the TE (1, 0, 1), TE (0, 1, 1), as can be seen by inspecting eqns. (14) and (15).

2·5. A circular cylinder with a central post

In this case we use cylindrical polar co-ordinates

$$x_1 = z, \quad x_2 = r, \quad x_3 = \phi, \qquad e_1 = e_2 = 1, \quad e_3 = r.$$

The wave equation for U now reads

$$\frac{\partial^2 U}{\partial z^2} + \frac{\partial^2 U}{\partial r^2} + \frac{1}{r}\frac{\partial U}{\partial r} - \frac{1}{r^2}\frac{\partial^2 U}{\partial \phi^2} + k^2 U = 0.$$

We can solve this equation by separation, writing

$$U = Z(z)\, R(r)\, \Phi(\phi).$$

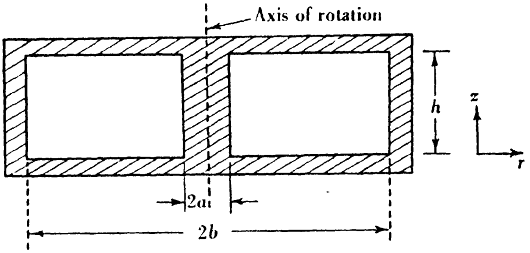

Fig. 2·2. Cross-section of toroidal resonator.

The solution is well known and is of the form

$$U = [AJ_m(k'r) + BY_m(k'r)]\, e^{\pm jm\phi \pm jk_z z}, \tag{19}$$

where $k' = (k^2 - k_z^2)^{\frac{1}{2}}$ and J_m and Y_m are Bessel functions of order m of the first and second kinds. It is worth noting that if the centre post were removed we need not include Y_m because these functions go to minus infinity at $(k'r) = 0$. Also m must be an integer because the circumferential field must join up correctly.

The solutions are given by the following equations:

TE type:

$$\left.\begin{aligned} E_z &= 0, \\ E_r &= j\frac{km}{r}\left(\frac{\mu_0}{\epsilon_0}\right)^{\frac{1}{2}} [AJ_m(k'r) + BY_m(k'r)] \sin m\phi \sin k_z z, \\ E_\phi &= jkk'\left(\frac{\mu_0}{\epsilon_0}\right)^{\frac{1}{2}} [AJ'_m(k'r) + BY'_m(k'r)] \cos m\phi \sin k_z z, \\ H_z &= k'^2 [AJ_m(k'r) + BY_m(k'r)] \cos m\phi \sin k_z z, \\ H_r &= k_z k' [AJ'_m(k'r) + BY'_m(k'r)] \cos m\phi \cos k_z z, \\ H_\phi &= \frac{k_z m}{r} [AJ_m(k'r) + BY_m(k'r)] \sin m\phi \cos k_z z. \end{aligned}\right\} \tag{20}$$

TM type:

$$\left.\begin{aligned}
E_z &= k'^2\,[AJ_m(k'r)+BY_m(k'r)]\cos m\phi\cos k_z z,\\
E_r &= -k'k_z[AJ'_m(k'r)+BY'_m(k'r)]\cos m\phi\sin k_z z,\\
E_\phi &= \frac{k_z m}{r}\,[AJ_m(k'r)+BY_m(k'r)]\sin m\phi\sin k_z z,\\
H_z &= 0,\\
H_r &= -j\frac{km}{r}\left(\frac{\epsilon_0}{\mu_0}\right)^{\frac{1}{2}}[AJ'_m(k'r)+BY'_m(k'r)]\sin m\phi\cos k_z z,\\
H_\phi &= -jkk'\left(\frac{\epsilon_0}{\mu_0}\right)^{\frac{1}{2}}[AJ_m(k'r)+BY_m(k'r)]\cos m\phi\cos k_z z.
\end{aligned}\right\} \quad (21)$$

The boundary conditions are that

$$E_\phi = E_r = 0 \quad \text{at } z = 0 \text{ and at } z = h.$$

Therefore $$k_z = \frac{n\pi}{h}, \qquad (22)$$

and $E_z = E_\phi = 0$ when $r = a$ and $r = b$. In the TM cases this leads to

$$AJ_m(k'a)+BY_m(k'a) = 0, \quad AJ_m(k'b)+BY_m(k'b) = 0,$$

or $$J_m(k'a)\,Y_m(k'b) = J_m(k'b)\,Y_m(k'a), \qquad (23)$$

if $A \neq B \neq 0$. The roots of this equation are best determined graphically. For given a and b they give the permitted values of k' which together with k_z determine k and therefore the resonant frequencies. In the TE case we get

$$AJ'_m(k'a)+BY'_m(k'a) = 0, \quad AJ'_m(k'b)+BY'_m(k'b) = 0,$$

or $$J'_m(k'a)\,Y'_m(k'b) = J'_m(k'b)\,Y'_m(k'a). \qquad (24)$$

We should remark that in this particular case there is a simpler solution than any of these. It is the transverse electromagnetic case in which both E_z and $H_z = 0$ and the fields reduce to radial electric lines with concentric circles of magnetic field. This is the case normally met in the study of coaxial lines. A coaxial line can, of course, be made to resonate in the TE mode by adjusting the length to an integral number of quarter wave-lengths, and it thus forms a link between transmission lines and cavity resonators. We shall return to this topic later.

The numbers defining the mode (n, m, l) now refer to the z direction, the circumferential direction and the root of eqns. (23) or (24) which is used. The TM (001) mode is particularly important; for this case the only fields are

$$E_z = k^2[AJ_0(kr)+BY_0(kr)], \tag{25}$$

$$H_\phi = -jk^2\left(\frac{e_0}{\mu_0}\right)^{\frac{1}{2}}[AJ_1(kr)+BY_1(kr)], \tag{26}$$

and A and B are known from the boundary condition.

These fields allow us to treat with a fair degree of accuracy a case of considerable practical importance.

2·6. The rectangular section toroid with capacitance loading

We treat this shape by a combination of lumped circuit analysis and field theory, looking at the system as being made up of lumped capacitance in parallel with distributed inductance.

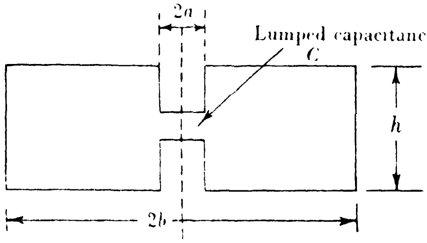

Fig. 2·3. Capacity loaded toroid.

The first boundary condition is that $E_r = 0$ at $r = b$, therefore

$$\frac{A}{B} = -\frac{Y_0(kb)}{J_0(kb)}.$$

We now treat the radial transmission line starting at $r = a$. The sending end-voltage

$$\begin{aligned} V_s &= E_z^a h \\ &= hk^2[AJ_0(ka)+BY_0(ka)]. \end{aligned} \tag{27}$$

The sending end-current

$$\begin{aligned} I_s &= 2\pi aH_\phi^a \\ &= -j^{2\pi}k^2a\left(\frac{\epsilon_0}{\mu_0}\right)^{\frac{1}{2}}[AJ_1(ka)+BY_1(ka)]. \end{aligned} \tag{28}$$

Then the resonances of the system are given by the condition that the total admittance should be zero, therefore

$$\frac{I_s}{V_s}+j\omega C = 0,$$

therefore

$$\omega C - \frac{2\pi a}{h}\left(\frac{\epsilon_0}{\mu_0}\right)^{\frac{1}{2}}\left[\frac{Y_0(kb)J_1(ka)-J_0(kb)\,Y_1(ka)}{J_0(ka)Y_0(kb)-Y_0(ka)J_0(kb)}\right],$$

or

$$fC\frac{h}{a}\left(\frac{\mu_0}{\epsilon_0}\right)^{\frac{1}{2}} = \left[\frac{Y_0(kb)J_1(ka)-J_0(kb)\,Y_1(ka)}{J_0(ka)\,Y_0(kb)-Y_0(ka)J_0(kb)}\right]. \qquad (29)$$

But $(\mu_0/\epsilon_0)^{\frac{1}{2}}$ is a quantity which Schelkunoff has called the impedance of free space; it has the value 377 ohms. We can finally write the expression as

$$377fC\frac{h}{a} = \left[\frac{Y_0(kb)J_1(ka)-J_0(kb)\,Y_1(ka)}{J_0(ka)\,Y_0(kb)-Y_0(ka)J_0(kb)}\right]. \qquad (30)$$

Eqn. (30) is simple enough to solve if a and b are given and C or h are to be found.

If either a or b is not known one has to obtain a graphical solution, as the required accuracy is not very great. It is convenient to start with $C = 0$ because we know that $b-a \doteqdot \frac{1}{2}\lambda$ in this case.

The practical importance of this formula lies in the fact that it gives useful results even when the shape of the posts departs considerably from that assumed. For instance, truncated cones can be used if $2a$ is put equal to the mean diameter. Moreover, the presence of a thin dielectric cylinder does not influence the resonant frequencies very much, although it may increase the losses by a large factor. In V.M. tubes the gap forming the lumped capacitance C may be well defined by grids or ill defined as in the case of simple apertures. In the latter case the capacitance is approximately equal to that between two solid disks equal in diameter to the posts and spaced by 1·4 times the actual edge spacing. This approximation only holds good when the circular wave guides formed by the hollow posts are being excited well below their cut-off frequency. The capacitance between electrodes of more complicated shape can be determined in the electrolytic trough in the usual way. It is worth mentioning that fringing effects are large, and that to obtain minimum gap length for a given C the gap should be located in the range $\frac{1}{3}h < z < \frac{2}{3}h$.

2·7. The coaxial line resonator

From the point of view of field theory the coaxial line is a resonator oscillating in a TEM mode with its length adjusted to $n\lambda/4$. The fields are readily deduced from the fact that both E_z and $H_z = 0$.

We first investigate the oscillations of this type propagated along the air-filled line according to the propagation factor $e^{j(\omega t-\gamma z)}$.

Eqns. (8*a*) and (8*b*) then show that if all the fields are not to be zero

$$\gamma^2+k^2 = 0,$$

or

$$\gamma = \pm j\omega(\mu_0\epsilon_0)^{\frac{1}{2}}. \tag{31}$$

It should be remembered that this result is perfectly general, as no assumption has been made about the conductivity of the boundary. A purely transverse wave cannot therefore exist in a real medium because the losses must introduce a real part into the expression for γ. However, the fields calculated using eqn. (31) are accurate enough to allow us to make a loss calculation. The field components then turn out to be

$$\left.\begin{aligned} E_r &= \left(\frac{\mu_0}{\epsilon_0}\right)^{\frac{1}{2}} H_\phi, \qquad E_\phi = E_z = H_r = H_z = 0 \\ &= \left(\frac{\mu_0}{\epsilon_0}\right)^{\frac{1}{2}} \frac{1}{r} e^{j(\omega t-\gamma z)}. \end{aligned}\right\} \tag{32}$$

Owing to the fact that E_r and $H_\phi \to \infty$ as $r \to 0$, the TEM wave is not a possible solution to any wave-guide problem.

We can now deduce the voltages and currents. If the current in the inner conductor $= I_0$ we have $I_0 = 2\pi a H_\phi^a$, therefore

$$H_\phi = \frac{I_0}{2\pi r} e^{j(\omega t-\gamma z)},$$

$$V_0 = \int_a^b E_r dr = \left(\frac{\mu_0}{\epsilon_0}\right)^{\frac{1}{2}} \int_a^b \frac{I_0}{2\pi r} dr \tag{33}$$

$$= \left(\frac{\mu_0}{\epsilon_0}\right)^{\frac{1}{2}} \frac{I_0}{2\pi} \log\frac{b}{a}. \tag{34}$$

The characteristic impedance of the line

$$Z_0 = \frac{V_0}{I_0} = \frac{377}{2\pi} \log\frac{b}{a} = 60 \log\frac{b}{a}. \tag{35}$$

But eqn. (35) is exactly the result deduced from the ordinary (Heaviside) theory of transmission lines.

We now consider that the coaxial line is short-circuited by a metallic disk of infinite conductivity at some point z, l m. distant from the origin. If a wave impinges on this short circuit from the left it is totally reflected. The current at any given point is then

$$\begin{aligned} I_z &= Ae^{j\omega t}(e^{-\gamma z}+e^{\gamma z}) \\ &= 2Ae^{j\omega t}\cosh \gamma z. \end{aligned}$$

But eqn. (31) shows that γ is a pure imaginary

$$I_z = 2Ae^{j\omega t}\cos \Gamma z, \tag{36}$$

$$\begin{aligned} V_z &= AZ_0 e^{j\omega t}(e^{-\gamma z}-e^{\gamma z}) \\ &= -2jZ_0 e^{j\omega t}\sin \Gamma z. \end{aligned} \tag{37}$$

Eqns. (36) and (37) show that standing waves have been set up on the line. If we now consider that there is a small real component in γ, i.e. that the line has some slight losses, we can write

$$\gamma = \alpha + j\beta,$$

where α is the attenuation constant, and $\beta = \omega/c = 2\pi/\lambda$ is the wave-length constant.

The input impedance

$$\begin{aligned} Z_i &= Z_0 \tanh(\alpha + j\beta)l \\ &= R + jX. \end{aligned}$$

Here
$$R = Z_0 \frac{\sinh \alpha l \cosh \alpha l}{\cosh^2 \alpha l \cos^2 \beta l + \sinh^2 \alpha l \sin^2 \beta l}, \tag{38}$$

$$X = Z_0 \frac{\sin \beta l \cos \beta l}{\cosh^2 \alpha l \cos^2 \beta l + \sinh^2 \alpha l \sin^2 \beta l}. \tag{39}$$

We have assumed that α is small, so that for short lines eqns. (38) and (39) become

$$R_0 = Z_0 \frac{\alpha l}{\cos^2 \beta l + \alpha^2 l^2 \sin^2 \beta l} = Z_0 \frac{\alpha l}{\alpha^2 l^2 + \cos^2 \beta l(1-\alpha^2 l^2)},$$

$$X = Z_0 \frac{\sin \beta l \cos \beta l}{\cos^2 \beta l + \alpha^2 l^2 \sin^2 \beta l}.$$

Clearly $X = 0$ when $\beta l = n\pi/2$ and R_0 is a minimum when βl is an even integer times $\frac{1}{2}\pi$ and a maximum when βl is an odd integer times $\frac{1}{2}\pi$. Thus the circuit is resonant when $n = 0, 2, 4, 6$, etc., and anti-resonant when $n = 1, 3, 5, 7$, etc. The first impedance maximum occurs when

$$\beta l = \frac{2\pi l}{\lambda} = \tfrac{1}{2}\pi \quad \text{or} \quad l = \tfrac{1}{4}\lambda.$$

Further development of the form of the impedance function near parallel resonance (Slater) shows that the circuit behaves like a normal lumped constant circuit.

2·8. Loss calculations

As we have already said loss calculations are made by assuming that the fields calculated assuming no loss can be used to give the surface currents. The surface resistivity can be calculated using the ordinary skin effect formula

$$R_s = \left(\frac{\pi f \mu}{\sigma}\right)^{\frac{1}{2}} \text{ ohms,} \tag{40}$$

where $f =$ frequency, $\mu =$ permeability and $\sigma =$ conductivity. Table 1 gives numerical values for R_s. The power loss in the surface is then

$$P_s = \frac{R_s}{2}\iint I^2\,ds. \tag{41}$$

Table 1

Material	Conductivity mhos/m. × 10^{-7}	Skin depth × $f^{\frac{1}{2}}$	$R_s \times 10^7/f^{\frac{1}{2}}$
Ag	6·17	0·0642	2·52
Cu	5·80	0·0660	2·61
Au	4·10	0·0785	3·11
Al	3·72	0·0826	3·26
Rh	2·13	0·109	4·31
W	1·83	0·118	4·63
Mo	1·75	0·120	4·76
Brass	1·57	0·127	5·01
Ta	0·645	0·1980	7·83

The energy stored in a cavity is equally divided between the electric and magnetic fields

$$W_E = W_H = \frac{\epsilon_1}{2}\iiint E^2\,d\tau = \frac{\mu_1}{2}\iiint H^2\,d\tau. \tag{42}$$

Here μ_1, ϵ_1 are the permittivity and permeability of the dielectric filling the cavity.

These quantities are important because the most fundamental definition of Q, one which leads to correct results in all cases, is

$$Q = \frac{\text{Energy stored per cycle}}{\text{Energy lost per cycle}}, \tag{43}$$

which is readily calculated from eqns. (41) and (42).

Unfortunately, this method can rarely be applied to the cavity resonators used in V.M. tubes, although it is useful in the design of filter cavities, wave-meters and so on. This is because the losses of tube cavities are usually made up by contributions from several sources of which skin loss is often the least important. For instance, most of the loss in the type of cavity which is sealed through the glass is dielectric loss in the glass, while in tubes like the 723AB the grids introduce contact resistances. Coupling devices usually introduce a large proportion of the total losses. It should also be remembered that in all valves the resonators are well above room temperature, and in some types may be up to 300–400° C. For these reasons it is usually necessary to determine the Q of a tube resonator experimentally even if the shape is sufficiently simple to allow a good approximation to the actual fields to be found.

2·9. Equivalent circuits

We have already said that a coaxial line resonator near a resonance behaves like an ordinary lumped constant circuit. This remark is equally true of any cavity resonator, though since a cavity has an infinite number of resonant frequencies, its behaviour away from any specified resonance may be completely different. We can therefore set up conventional analogies to resonators if we remember that they are of limited validity. The lumped constant parallel resonant circuit is usually described by the three parameters L, C, R. It can equally well be described by three other parameters

$$\omega_0 = \frac{1}{(LC)^{\frac{1}{2}}}, \quad Q_0 = \omega_0 CR, \quad Z_0 = \frac{L}{CR}.$$

From the point of view of microwave technique the second set is very much more useful, since these parameters are observables and the first set are not. We shall therefore make no attempt to evaluate equivalent inductances and capacitances unless, as in the case of pairs of grids, the concepts have intuitive physical significance.

The most accurate methods of measuring ω_0 and Q_0 depend on the use of the standing-wave detector. Standing-wave detector measurements of Z are more involved, particularly if a fixed output coupling is used. A method employing V.M. technique will be described later on.

In this book we shall speak of cavity resonators as though they were parallel resonant circuits with external loads coupled to them by either inductive (magnetic) or capacitative (electrostatic) means.

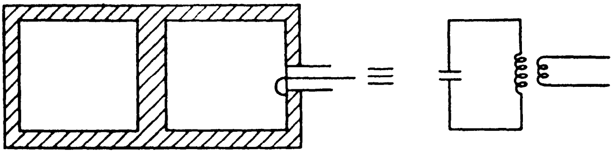

Fig. 2·4. Equivalence between cavity and lumped constant circuit.

For example, consider the equivalent circuit of the resonator shown above. The two circuits behave identically; for instance, as the coupling is increased the loaded Q decreases according to the law

$$\frac{1}{Q_L} = \frac{1}{Q_0} + \frac{1}{Q_{\text{ext.}}},$$

where $Q_{\text{ext.}}$ is the Q of the load and coupling loop. However, further consideration of equivalents belongs more properly to the field of circuit theory and we shall not take the discussion any further.

2·10. Tuning methods

We have already described the method of tuning in which screws of as large a diameter as possible are introduced into the resonator, thereby lowering the wave-length. The tuning range obtained by this method is small, for instance, in the CV35 type of reflex tube four ⅜ in. diameter screws give a range of ±4 %. In any case it is very undesirable to have to adjust several separate screws. Another method which has had a very wide application is to seal a flexible diaphragm into the vacuum container so that it becomes possible to alter the gap spacing. This is equivalent to changing the lumped capacitance of the circuit, and is capable of giving a rather larger tuning range than tuning screws, ±6% being possible. Most of the disadvantages of the scheme can be overcome by careful mechanical design, but the fact that the gap increases as the frequency increases is a fundamental limitation.

Tuning over a wide range has to be accomplished through changing the dimensions of the resonator by a considerable amount. In practice it is impossible to vary more than one dimension, and so one is forced to use concentric lines and wave guides in such a way that the length determines the resonant frequency. Sliding contacts are extremely objectionable because of their erratic behaviour, and it has become accepted in practice to use non-contact sliders which are provided with filter circuits in order to prevent power leaking out of the resonator. The design of appropriate band-stop filters is one of the main obstacles in the path of progress in this direction.

2·11. Approximation methods for the calculation of resonant frequencies

We shall conclude this chapter by giving a very brief description of some of the approximation methods which have been used in cavity calculations. One of these used by Hansen is the Rayleigh-Ritz minimum-energy method which is fairly well known. In brief, one guesses a set of functions which satisfy the boundary conditions and chooses the constants to minimize the energy stored. The defects of the method are that it is complicated and very sensitive to the choice of functions. There is no way of determining the probable error of the frequency, although one knows that it is invariably too high. Stevenson's method allows one to calculate a lower bound to the frequency, but there is still no systematic way of improving the assumed functions.

Bethe has applied the quantum mechanical perturbation theory to the problem of calculating the effect of small alterations on a cavity of simple shape, i.e. one in which the fields can be derived analytically. The objection to this method is just that it deals only with small perturbations and not with major departures from an assumed shape. However, it is not difficult to apply and serves very well for the consideration of the effect of slots or regions of different permittivity on the wave-length.

The technique which has developed most rapidly and shown most promise is an application of the relaxation method of Southwell. The application of this method to cavities is due to Motz* and his collaborators at Oxford.

A section is cut through the resonator in such a way that the resonator can be generated either by translation or by rotation of the section, so as to reduce the problem to one in two dimensions. Suppose the wave equation to be solved is

$$\frac{\partial^2 U}{\partial x^2} + \frac{\partial^2 U}{\partial y^2} + k^2 U = 0. \tag{44}$$

We replace the differential equation by a finite-difference equation by superimposing a rectangular mesh on the resonator section. Then we select a mesh point for which $U = U_0$ and expand in a Taylor series,

$$U = U_0 + \left(\frac{\partial U}{\partial x}\right)_0 \Delta x + \left(\frac{\partial U}{\partial y}\right)_0 \Delta y + \frac{1}{2}\left(\frac{\partial^2 U}{\partial x^2}\right)_0 \Delta_x^2 + \frac{1}{2}\left(\frac{\partial^2 U}{\partial y^2}\right)_0 \Delta_y^2$$
$$+ 2\left(\frac{\partial^2 U}{\partial x\, \partial y}\right)_0 \Delta x \Delta y + O(\Delta)^3. \tag{45}$$

If $\Delta x = a$, $\Delta y = b$ and numbering the mesh points as shown in fig. 2·5,

$$U_1 = U_0 - a\left(\frac{\partial U}{\partial x}\right)_0 + \tfrac{1}{2}a^2\left(\frac{\partial^2 U}{\partial x^2}\right)_0, \quad U_2 = U_0 + a\left(\frac{\partial U}{\partial x}\right)_0 + \tfrac{1}{2}a^2\left(\frac{\partial^2 U}{\partial x^2}\right)_0,$$

$$U_3 = U_0 - b\left(\frac{\partial U}{\partial y}\right)_0 + \tfrac{1}{2}b^2\left(\frac{\partial^2 U}{\partial y^2}\right)_0, \quad U_4 = U_0 + b\left(\frac{\partial U}{\partial y}\right)_0 + \tfrac{1}{2}b^2\left(\frac{\partial^2 U}{\partial y^2}\right)_0.$$

Then $$U_1 + U_2 + \frac{a^2}{b^2}(U_3 + U_4) + \left(k^2 a^2 - 2 - 2\frac{a^2}{b^2}\right) U_0 = 0,$$

or if the mesh is square

$$U_1 + U_2 + U_3 + U_4 + (k^2 a^2 - 4)\, U_0 \lambda = 0. \tag{46}$$

A trial set of values of U obeying the boundary conditions is then guessed. These values will not obey eqn. (46); instead we have

$$\sum_{n=1}^{4} U_n + (a^2 k^2 - 4)\, U_0 = \delta, \tag{47}$$

where δ is called the residual. We now have to adjust the U values so that the δ's vanish at all the mesh points. Southwell's technique for accomplishing this is to choose the mesh point for which the residual is largest and there replace U_0 by $U_0 + \frac{1}{4}\delta$. The new residuals are then calculated and the process applied to the point with the biggest residual again. Now if k^2 had been correctly known at the beginning, the repeated application of this 'relaxation' process would result in a system of U values obeying eqn. (46). However, k^2 is not known, and so we have to make an estimate to begin with and improve it as we go along. This is done as follows. Let there be r mesh points; form the r quantities

---

* Motz *et al.*, *Philos. Trans.* A, 239 (1945), 489.

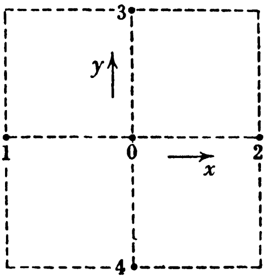

Fig. 2·5. Diagram showing numbering of mesh points.

$$\sum_{n=1}^{4} U_{nm} - 4U_{0m} = \Delta U_m, \tag{48}$$

and the sums $\sum_{m=1}^{r} U_{0m}\Delta U_m$ and $\sum_{m=1}^{r} U_{0m}^2$.

Then the trial k is given by

$$a^2k^2 = \frac{\sum_{m=1}^{r} U_{0m}\Delta U_m}{\sum_{m=1}^{r} U_{0m}^2}. \tag{49}$$

This estimate can be proved to be too high and has to be recalculated from time to time as the relaxation proceeds.

The relaxation method is very laborious if the trial values are badly guessed, but, on the other hand, the work is readily mechanized. It is capable of application to fairly complicated shapes, particularly if the original shape can be simplified by a conformal transformation. One of the important advantages of the method is that it gives a good idea of the field as well as the lowest resonant frequency, which permits one to make an estimate of the ohmic losses.*

2·12. Conclusion

Our knowledge of the theory of resonant cavities has increased enormously during the war, and it is not too much to hope that simpler and more general approximation methods will be developed. The calculation of losses is unfortunately on another footing, because even if one could determine the fields in any given resonator and evaluate the surface integrals in eqn. (41), the calculated loss would bear little relation to the measured loss. In all tube resonators the major part of the loss occurs in bad joints, in coupling devices where abrupt changes of field take place, and particularly as the frequency rises above 30,000 mc. in surface oxidation and roughnesses. This is perhaps not so in the case of echo boxes and high Q wave-meters, but the tube designer lives in an imperfect world and is well advised to check his calculations by experiment.

---

* Since this was written, Southwell has given details of the application of this technique to two-dimensional problems in his *Relaxation Methods in Theoretical Physics*, Oxford University Press, 1946.

Chapter 3

THE THEORY OF VELOCITY MODULATION

3·1. The fundamentals of electron dynamics*

Before making a start on the main theoretical work of this chapter we present a brief survey of electron dynamics.

In the presence of free charge *in vacuo*, Maxwell's equations read:

$$\left.\begin{aligned} &(a)\ \nabla\times\mathbf{E} = -\mu_0\frac{\partial\mathbf{H}}{\partial t}, && (c)\ \nabla.\mathbf{E} = \frac{\rho}{\epsilon_0}, \\ &(b)\ \mathbf{I} = \nabla\times\mathbf{H} = \rho\mathbf{u}+\epsilon_0\frac{\partial\mathbf{E}}{\partial t}, && (d)\ \nabla.\mathbf{H} = 0, \end{aligned}\right\} \qquad (1)$$

where ρ = charge density, $\mathbf{u}$ = charge velocity. The conduction current density at any point is given by

$$\mathbf{j} = \rho\mathbf{u}. \qquad (2)$$

The motion of the charges is determined by the Lorentz equation

$$F = e(\mathbf{E}+\mathbf{u}\times\mu_0\mathbf{H}). \qquad (3)$$

A reference to the field equations given in Chapter 2 shows that the electric field is of the order $(\mu_0/\epsilon_0)^{\frac{1}{2}} = 377$ times as large as the magnetic. $\mu_0\mathbf{H}$ is then only of the order $\mathbf{E}/c$. We are therefore justified in neglecting the magnetic term in the study of resonator beam interaction over the range of velocities which interests us. Eqn. (3) therefore reduces to

$$F = e\mathbf{E} = -e.\nabla\mathbf{V} \qquad (4)$$

in those cases where the potential $\mathbf{V}$ exists.

We now derive an important relation due to Llewellyn. Consider a system of parallel planes and put eqn. (1 *c*) into (1 *b*). The result is

$$\mathbf{I} = \epsilon_0\left(\frac{\partial\mathbf{E}}{\partial x}\mathbf{u}+\frac{\partial E}{\partial t}\right). \qquad (5)$$

---

* Fuller accounts are given in Llewellyn's *Electron-Inertia Effects* and in the excellent first chapter on classical electrodynamics in *The Quantum Theory of Radiation* by W. Heitler.

But E can be written as $f(x, t)$ and therefore

$$\frac{d\mathbf{E}}{dt} = \frac{\partial E}{\partial x}\frac{\partial x}{dt} + \frac{\partial E}{\partial t},$$

therefore
$$\mathbf{I} = \epsilon_0 \frac{d\mathbf{E}}{dt}. \tag{6}$$

This is to be taken as meaning that we consider the variations of field experienced by a given electron as t changes. Now according to eqn. (1 *d*) $\nabla . \mathbf{I} = 0$, so $\mathbf{I}$ is only a function of t and furthermore

$$e\mathbf{E} = ma, \tag{7}$$

where a is the acceleration. Putting eqn. (7) into (6) we have

$$\begin{aligned} \mathbf{I} &= \frac{m\epsilon_0}{e}\dot{a} \\ &= \psi'''(t), \end{aligned} \tag{8}$$

therefore
$$\epsilon_0 \frac{d\mathbf{E}}{dt} = \psi'''(t).$$

Integrating once and putting in initial conditions at the first plane

$$\psi''(t) - \epsilon_0 \mathbf{E} = \psi''(t_0) - \epsilon_0 \mathbf{E}_0. \tag{9}$$

We now take the partial derivative of eqn. (9) which means studying the time variation at a fixed point,

$$\psi'''(t) - \epsilon_0 \frac{\partial \mathbf{E}}{\partial t} = \left[\psi'''(t_0) - \epsilon_0 \frac{\partial \mathbf{E}}{\partial t}\right] \frac{\partial t_0}{\partial t}\bigg|_Z, \tag{10}$$

where the derivative $\partial t_0/\partial t$ is taken at the plane Z of the fixed point. Eqn. (10) can be rewritten using eqn. (8) to become

$$I(t) - \epsilon_0 \frac{\partial \mathbf{E}}{\partial t} = \left[I(t_0) - \epsilon_0 \frac{\partial \mathbf{E}_0}{\partial t_0}\right] \frac{\partial t_0}{\partial t_1}\bigg|_Z. \tag{11}$$

But from the definition of I, (11) reduces to

$$(i_c)_{(Z,t)} = (i_c)_{(0,t_0)} \frac{\partial t_0}{\partial t}\bigg|_Z, \tag{12}$$

where i_c is the conduction current and t_0 the time at the Z plane. Eqn. (12) may be looked upon as a continuity equation, similar to that found in hydrodynamics, but kinematically derived. This equation enables us to calculate the current at any point in a V.M.

device if we know the current at some other point and can obtain a relation giving the time of arrival at the first point in terms of the time of arrival at the second. We shall frequently make use of this expression, because once the h.f. current is known it is possible to calculate the h.f. power gain or loss.

A second method of calculating the power interchange between an electron beam and a field is to determine an expression for the change in kinetic energy of the electrons. This is then averaged over all the electrons and over one cycle of oscillation to give the mean power exchange. This method is the basis of the graphical method of calculating V.M. tube operation. The paths of a series of electrons entering the buncher gap at different phases are calculated step by step through the drift tube and catcher gap. A curve of energy gain or loss as a function of phase is then plotted and a graphical integration gives the overall efficiency of the tube for the assumed conditions of buncher and catcher voltage. These methods naturally can only be applied to the analysis of a given structure, and even this is extremely laborious. More details are given by Harrison[*] and the method has apparently been much used in Germany, but we shall only consider analytical methods in this book.

Jen,[†] Gabor[‡] and Warnecke[§] have given direct derivations from Maxwell's equations which may be used to perform the required calculations, but once the interaction between field and beam has been studied for the general case, it is better to rely on more direct methods for specific purposes.

We now seek to derive a theory of the V.M. process which will be capable of predicting the output power and efficiency obtainable from any given tube. We first calculate approximate results applicable to conditions in which the h.f. voltages at the gaps are much smaller than the accelerating voltage (small-signal theory) and then extend our study to large-signal conditions. Several assumptions are made throughout the whole of this work; these are:

(1) Relativistic effects are negligible; this is true for velocities below about 15 kV.

---

[*] Harrison, *Proc. Inst. Radio Engrs, N.Y.*, 33 (1945), 20.

[†] Jen, *Proc. Inst. Radio Engrs, N.Y.*, 29 (1941), 345, 464.

[‡] Gabor, *J. Instn Elect. Engrs*, 91, pt. III (1945), 128.

[§] Warnecke, *Bull. Soc. fr. élect.* 2 (1942), 238.

(2) Electrons travel in straight lines parallel to the axis unless they have been deflected by an h.f. field.

(3) Secondary emission plays no part in the operation.

Other assumptions will be explained when they are made and discarded as the development proceeds.

3·2. First-order theory of gap action

We consider that a uniform beam of electrons enters an h.f. field confined between two perfect grids. The field varies sinusoidally with time according to the law $V_1/d \sin \omega t$, where d is the spacing between the grids in metres.

The equation of motion is

$$m\ddot{Z} = \frac{eV_1}{d}\sin \omega t; \tag{13}$$

integrating $$\dot{Z} = -\frac{eV_1}{md\omega}\cos \omega t + c$$

$$= u_0 + \frac{eV_1}{md\omega}[\cos \omega t_0 - \cos \omega t], \tag{14}$$

when we put the initial conditions that $\dot{Z} = u_0$ at entry to the field at time t_0. We require the velocity at exit from the h.f. field. If we assume that $V_1/V_0 \ll 1$, i.e. that depth of modulation is small, we can write

$$t_1 = t_0 + \frac{d}{u_0}. \tag{15}$$

The velocity at exit u_1 then becomes

$$u_1 = u_0 + \frac{eV_1}{mu_0}\frac{\sin \frac{1}{2}\phi}{\frac{1}{2}\phi}\sin(\omega t_0 + \tfrac{1}{2}\phi), \tag{16}$$

where $\phi = \omega d/u_0$, the transit angle across the gap. In Chapter 1 we assumed that u_0 was very high so that $\phi \to 0$ and $(\sin \frac{1}{2}\phi/\frac{1}{2}\phi) \to 1$. We see now that the velocity gained in the real case is somewhat less, but that the modulation still varies sinusoidally with the phase at input. The symbol β is usually written in place of $\sin \frac{1}{2}\phi/\frac{1}{2}\phi$, which quantity is called the gap modulation coefficient. Putting in this notation and shifting the time origin to the centre of the gap we have

$$u_1 = u_0 + \frac{e\beta V_1}{mu_0}\sin \omega t_0'. \tag{17}$$

The work done by the field on the beam can be calculated by forming the expression for the average kinetic energy before and after the gap. This leads to a small loading of the resonator by the beam, but the present approximation does not expose the real cause of beam loading, which lies in the fact that those electrons whose velocity is increased spend a shorter time in the field than the others. Their effective β is therefore larger and they take up more energy from the field than is returned to it by the electrons which are slowed down. The average value of u_1 is then $> u_0$, whereas eqn. (5) makes $\bar{u}_1 = u_0$.

3·3. The Webster* approximation to the conversion efficiency of a klystron

We consider two gaps separated by a drift tube of length s. The arrangement is shown in fig. 3·1. The beam current and voltage are I_0, V_0. The h.f. voltage impressed on the first gap is $V_1 \sin \omega t$ and on the second $V_2 \cos(\omega t_2 - \gamma)$, where γ is an arbitrary phase angle. The time origin is the centre of the first gap which we now call t_0.

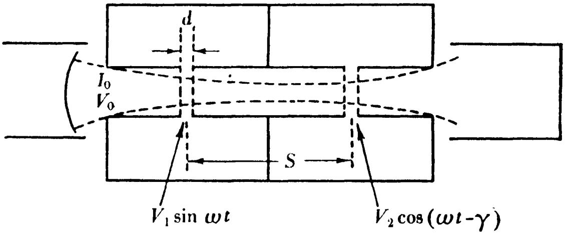

Fig. 3·1. Diagram explaining symbols used in text.

The time of arrival at the centre of the second gap t_2 is given by

$$t_2 = t_0 + \frac{s}{u_0\left(1 + \dfrac{e\beta V_1}{mu_0^2}\sin \omega t_0\right)}, \tag{18}$$

using eqn. (17). Continuing to make the assumption $V_1/V_0 \ll 1$ we can expand this by the binomial theorem

$$t_2 \doteqdot t_0 + \frac{s}{u_0} - \frac{se\beta V_1}{mu_0^3}\sin \omega t_0$$

or

$$\omega t_2 \doteqdot \omega t_0 + \frac{\omega s}{u_0} - \frac{\omega se\beta_1 V_1}{mu_0^3}\sin \omega t_0. \tag{19}$$

---

* Webster, *J. Appl. Phys.* 10 (1939), 501.

We now introduce some notations so as to reduce the factors involved to dimensionless quantities. First, $\omega s/u_0$ is the transit angle of an unmodulated reference electron through the drift tube. We then put $\omega s/u_0 = S$. Also $V_1/V_0 = \alpha_1$, $V_2/V_0 = \alpha_2$, where α_1 and α_2 are the depths of modulation at the gaps. Finally, we remember that $u_0^2 = 2eV_0/m$. When these symbols are introduced we find that we can write eqn. (19) as

$$\omega t_2 - S = \omega t_0 - \frac{S\alpha_1\beta}{2}\sin\omega t_0. \tag{20}$$

Now the current through the system is continuous, which requires that

$$i_0\,dt_0 = i_2\,dt_2,$$

or we can use eqn. (12) to obtain the same result. Then

$$i_0 = i_2\frac{dt_2}{dt_0}. \tag{21}$$

But from eqn. (19)

$$\frac{dt_2}{dt_0} = 1 - \frac{S\alpha_1\beta}{2}\cos\omega t_0, \tag{22}$$

therefore

$$i_2 = \frac{i_0}{1 - \frac{1}{2}S\alpha_1\beta\cos\omega t_0}. \tag{23}$$

Eqn. (23) gives the law of variation of the bunched current at the second gap. We next expand i_2 as a Fourier series in the angle $\omega t_2 - S$, i.e. we write

$$\begin{aligned} i_2 = a_0 &+ a_1\cos(\omega t_2 - S) + a_2\cos 2(\omega t_2 - S) + \dots \\ &+ b_1\sin(\omega t_2 - S) + b_2\sin 2(\omega t_2 - S) + \dots. \end{aligned} \tag{24}$$

Then, in the usual way, we have, using eqn. (20),

$$\left.\begin{aligned} a_n &= \frac{i_0}{\pi}\int_0^{2\pi}\cos n\left(\omega t_0 - \frac{S\alpha_1\beta}{2}\sin\omega t_0\right)d(\omega t_0), \\ &= 2i_0 J_n\left(n\frac{S\alpha_1\beta}{2}\right), \\ a_0 &= 1, \end{aligned}\right\} \tag{25}$$

$$b_n = \frac{i_0}{2\pi}\int_0^{2\pi}\sin n\left(\omega t_0 - \frac{S\alpha_1\beta}{2}\sin\omega t_0\right)d(\omega t_0) \tag{26}$$

$$= 0. \tag{27}$$

Thus

$$i_2 = i_0\left[1 + 2\sum_{n=0}^{\infty} J_n\left(n\frac{S\alpha_1\beta}{2}\right)\cos n(\omega t_2 - S)\right]. \tag{28}$$

The catcher current therefore consists of a d.c. component plus all the harmonics of the modulating frequency, the amplitudes of the harmonics being proportional to the Bessel coefficients

$$J_1\left(\frac{S\alpha_1\beta}{2}\right), \quad J_2\left(\frac{2S\alpha_1\beta}{2}\right), \text{ etc.}$$

Now the most important uses of the klystron are as an amplifier or oscillator, in which case the catcher resonator is tuned to resonance with the applied frequency and because the eigenvalues of the catcher resonance equation certainly do not lie in a geometric progression, the catcher will present a very low impedance to any harmonic except the fundamental. The fundamental power taken from the beam by the catcher is given by the time average of the product $i_2 . V_2$,

$$Pb = \frac{2i_0}{2\pi}\int_0^{2\pi} \beta V_2 \cos(\omega t_2 - \gamma) J_1\left(\frac{S\alpha_1\beta}{2}\right)\cos(\omega t_2 - S)\, d(\omega t_2) \quad (29)$$

$$= i_0 \beta V_2 J_1\left(\frac{S\alpha_1\beta}{2}\right)\cos(S-\gamma). \quad (30)$$

If all the beam current reaches the gap $i_0 = I_0$. Cos $(S-\gamma)$ is a phase factor which can be adjusted by varying the d.c. voltage and the phase of the coupling between the resonators. It can therefore be made equal to unity. When this is done, we can obtain the conversion efficiency by dividing eqn. (30) by $I_0 V_0$ which is the d.c. power input. Then

$$\eta_{\text{conv.}} = \beta\alpha_2 J_1\left(\frac{S\alpha_1\beta}{2}\right). \quad (31)$$

It is often assumed that the greatest possible value of $\beta\alpha_2$ is 1. This assumption will be criticized later on, but we use it for the moment. This gives

$$\eta_{\text{conv.}}(\text{max.}) = \frac{J_1(S\alpha_1\beta)\,(\text{max.})}{2}.$$

The largest maximum of $J(z)$ is 0·584 at $z = 1{\cdot}84$. This is the basis of the often repeated statement that the maximum efficiency available in a klystron oscillator is 58·4 %. Fig. 3·2 shows $J_0(z)$, $J_1(z)$, $J_2(z)$ plotted as functions of z.

We now pause for a moment to consider some of these results.

First of all we have derived a phase condition in Chapter 1 from purely qualitative considerations. This condition was

$$S = \phi + (4n-1)\tfrac{1}{2}\pi \quad (n = 0, 1, 2, 3, \text{etc.}),$$

where ϕ = angle between buncher and catcher field, but $\phi = \gamma + \frac{1}{2}\pi$ in our present notation, therefore

$$S - \gamma = 2n\pi, \tag{32}$$

so

$$\cos(S-\gamma) = 1. \tag{33}$$

Eqn. (33) is, of course, in agreement with the foregoing analysis. In most practical tubes the buncher and catcher either oscillate in phase with one another or 180° out of phase. For the in-phase case we have

$$S = (4n-1)\tfrac{1}{2}\pi, \tag{34}$$

and modes 3, 7, 11, etc., are excited. In antiphase

$$S = (4n+1)\tfrac{1}{2}\pi, \tag{35}$$

and modes 1, 5, 9, etc., are excited. These relations allow the distance between the resonator centres to be determined when the mode number and voltage desired are known or the voltage for a given mode if the distance has been fixed.

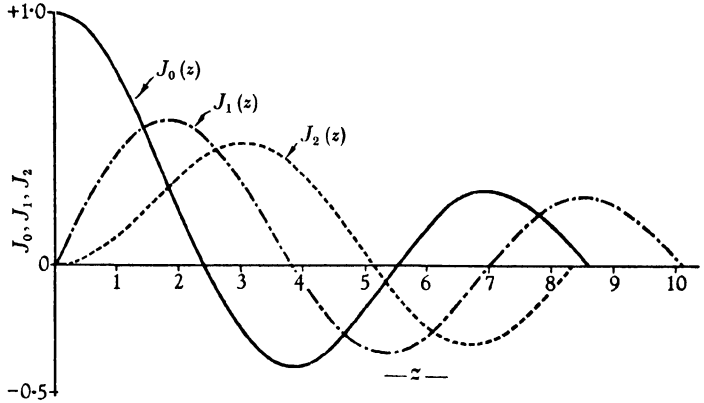

Fig. 3·2. The Bessel functions J_0, J_1 and J_2.

Secondly, we must remember that we have only calculated the conversion efficiency as yet. The relations given above only state that if the 'bunching parameter' $(\frac{1}{2}S\alpha_1\beta)$ is adjusted to 1·84 and if the phase condition is obeyed, the amount of energy transferred from the h.t. source to the h.f. field will be 58·4 % of the input. What is much more interesting is to find out how this should be done so as to achieve the greatest output power: should it be done with a long tunnel and correspondingly large S, or by raising α_1? The first case corresponds to a high amplification factor, while in the second the voltage swing is large. The answers to these questions can be obtained by evaluating the output efficiency, that is, the ratio of the useful power output to the power input.

Before we make the small signal output calculation we should mention that the catcher resonator may be designed to operate on one of the harmonics of the impressed frequency, in which case the klystron will act as a frequency multiplier. The conversion efficiencies are given by the maxima of $J_n(\frac{1}{2}nS\alpha_1\beta)$. For instance, the maximum conversion efficiency of a klystron tripler is 43 %. Actually it is very difficult to realize good efficiencies with klystron frequency multipliers, probably because the space-charge repulsion forces acting on the bunch reduce the harmonics of the current wave much more than the fundamental. We shall return to this topic later in the book.

3·4. Small signal theory of the output efficiency of a klystron oscillator

The output power which can be coupled out of the catcher into a load is less than the power converted by the following amounts:

(1) The power lost in bunching the beam.

(2) The power lost in exciting the buncher resonator, i.e. the ohmic and dielectric losses in the buncher.

(3) The power lost in demodulating the beam.

(4) The losses in the catcher resonator.

In the present section we assume that the signals are small enough to allow us to neglect the bunching and debunching powers. We consider that the circuits act as two tightly coupled low-loss resonant circuits, that is, the complete system has two resonant frequencies; at one frequency the primary and secondary are in phase and 180° out of phase at the other. The relative magnitude of V_s/V_p depends on the coupling coefficient and the tuning of one circuit.

Let P_0 = useful output power, $P_{\text{conv.}}$ = conversion power, P_r = power lost in resonators. Then

$$\eta_0 = \frac{P_0}{i_0 V_0} = \frac{P_{\text{conv.}} - P_r}{i_0 V_0}. \tag{36}$$

Since V_1 and V_2 are peak values of the resonator voltage

$$P_r = \frac{V_1^2}{2Z_1} + \frac{V_2^2}{2Z_2}, \tag{37}$$

if Z_1, Z_2 = shunt impedances of the resonators.

We put $V_1/V_2 = \alpha_1/\alpha_2 = g$. This quantity measures the voltage step-down from catcher to buncher. It is usual for the buncher and catcher to be identical in physical form, so that it is reasonable to write

$$Z_1 = Z_2,$$

therefore

$$P_r = \frac{V_2^2}{2Z_1}(1 + g^2). \tag{38}$$

Putting eqns. (31) and (38) into (36) we have

$$\eta_0 = \frac{i_0 \beta V_2 J_1(\frac{1}{2} S \alpha_1 \beta) \cos(S - \gamma) - (V_2^2/2Z_1)(1 + g^2)}{i_0 V_0} \tag{39}$$

$$= \beta \alpha_2 J_1(\tfrac{1}{2} S \alpha_1 \beta) \cos(S - \gamma) - \frac{\alpha_2^2 V_0}{2 i_0 Z_1}(1 + g^2). \tag{40}$$

Eqn. (40) shows that, to minimize the circuit losses, the beam current should be made as large as possible at the working voltage, or in other words the d.c. beam impedance should be very small compared with the resonator impedance. If this is the case the load impedance has to be matched to the beam impedance for maximum power transfer, and the output efficiency can approach 58·4 % instead of the 29·2 % which is the most that is available if the load has to be matched to the resonator.

We now introduce a very valuable simplification due to Milner of the B.T.H. Co. Milner realized that the circuit losses are not direct observables, but that the minimum beam current which would just maintain oscillation of vanishingly small amplitudes could serve as an equally useful measure. We first consider the starting current when the load is removed, then

$$i_{S_0} \beta V_2 \left(\frac{S \alpha_1 \beta}{4}\right) \cos(S - \gamma) = \frac{V_2^2}{2Z_1}(1 + g^2), \tag{41}$$

because as $\alpha_1 \to 0$, $J_1(\frac{1}{2}S\alpha_1\beta) \to \frac{1}{4}S\alpha_1\beta$, as can be seen from the series expansion of $J_1(z)$, therefore

$$i_{S_0} = \frac{2V_0}{S\beta^2 Z_1} \sec(S-\gamma)\left(\frac{1}{g}+g\right). \tag{42}$$

This expression can be minimized with respect to g and S, corresponding to the physical processes of adjusting the coupling between the resonators and the voltage for minimum starting current.

The first condition yields $g = 1$, which is otherwise obvious. The second condition requires a little more discussion. We have to minimize $\sec(S-\gamma)/S$, where $S = \omega s/u_0$. As u_0 changes, near the point of minimum starting current, ω changes so as to maintain $\sec(S-\gamma) = 1$, $S-\gamma = 2n\pi$ ($n = 0, 1, 2$, etc.). Furthermore, S should be as large as possible. The minimum starting current then becomes

$$i'_{S_0} = \frac{4V_0}{S\beta^2 Z_1}. \tag{43}$$

Let us define the starting current parameter $F = \dfrac{i'_{S_0}}{i_0}$.

Then
$$F = \frac{4V_0}{i_0 S\beta^2 Z_1}. \tag{44}$$

From eqn. (44)
$$\frac{1}{2Z_1} = \frac{S\beta^2}{8} F \frac{i_0}{V_0}. \tag{45}$$

Eqn. (38) then becomes

$$P_r = V_2^2 \frac{S\beta}{8} F \frac{i_0}{V_0}(1+g^2). \tag{46}$$

Putting eqn. (46) into (40) we have

$$\eta_0 = \beta\alpha_2 J_1\left(\frac{S\alpha_1\beta}{2}\right)\cos(S-\gamma) - \alpha_2^2 \frac{S\beta^2}{8}(4g^2)F. \tag{47}$$

We now consider that the phase angle $(S-\gamma)$ has been correctly adjusted by some means or other, and consider the optimum value of η_0 obtained by adjusting the load coupling and the coupling between the resonators. These physical operations correspond to the mathematical operations of maximizing η_0 with respect to α_1 and α_2. Strictly speaking we should make a third optimization with respect to S, but the values resulting from this procedure differ very little from the mode values and we shall neglect this refinement for the moment. Further to save writing we put

$$\frac{S\alpha_1\beta}{2} = \phi. \tag{48}$$

Then
$$\frac{\partial\eta_0}{\partial\alpha_2} = \beta J_1(\phi) - F\frac{S\alpha_2\beta^2}{4} = 0, \tag{49}$$

$$\frac{\partial\eta_0}{\partial\alpha_1} = \beta\alpha_2\frac{S\beta}{2}J_1'(\phi) - F\frac{S\alpha_1\beta^2}{4} = 0. \tag{50}$$

From eqn. (49)
$$\alpha_2 = \frac{4J_1(\phi)}{FS\beta}, \tag{51}$$

whence
$$\left(\frac{F}{2}\right)^2 = \frac{J_1(\phi)}{\phi}\left[J_0(\phi) - J_1\frac{(\phi)}{\phi}\right], \tag{52}$$

where we use the fact that $J_1'(\phi) = J_0(\phi) - J_1(\phi)/\phi$. Using eqn. (52) we can compute the F value belonging to a given ϕ. If we have already assumed a mode number this is equivalent to calculating the ϕ value belonging to a given $\alpha_1\beta$. We have now enough information to compute α_2 from eqn. (51) which would complete the determination of the necessary quantities for insertion into eqn. (47) to give the output efficiency. It happens that we can convert these relations to more simple forms by making the well-known substitution

$$J_1(\phi) = \tfrac{1}{2}\phi(J_0(\phi) - J_2(\phi)). \tag{53}$$

Eqn. (52) then becomes

$$F = [J_0^2(\phi) - J_2^2(\phi)]^{\frac{1}{2}}. \tag{54}$$

Making this substitution and a substitution for α_1/α_2 in eqn. (47) we can arrive at an expression for η_0 after a little algebra,

$$\eta_0 = \frac{\phi_1^2}{S}J_2(\phi)\left[\frac{J_0(\phi) + J_2(\phi)}{J_0(\phi) - J_2(\phi)}\right]^{\frac{1}{2}}. \tag{55}$$

The computational procedure is to assume values of ϕ and to calculate corresponding values of F and η_0 from eqns. (54) and (55). For every S we can then plot a curve of η_0 against F.

At present we are still concerned with the assumption α_2 max. $\beta = 1$. The above equations are then only valid if

$$\frac{4J_1(\phi)}{SF} \leqslant 1; \tag{56}$$

when this is given a value > 1 we have to put $\alpha_2 = 1$ in eqn. (50). Then

$$F = S\beta\left[\frac{J_0(\phi)}{\phi} - \frac{J_1(\phi)}{\phi^2}\right], \tag{57}$$

a form which does not lead to a particularly simple expression for η_0. For each F value we now have a value of ϕ and α_2. S is assumed to be known so we can calculate $\alpha_1\beta$ from eqn. (48). Milner has plotted these curves which are of the form shown in figs. 3·3 and 3·4. Fig. 3·3 shows that F should be as small as possible for an efficient valve, and that for a given F smaller mode numbers are preferable to larger ones. On the other hand, eqn. (44) shows that F is inversely proportional to S, so that one has to calculate the F values for various S and then determine the best conditions from the curves. We shall give a fuller treatment, allowing for the power lost in bunching, in the chapter on Klystron Oscillators. We can, though, make some interesting generalizations even on the present results.

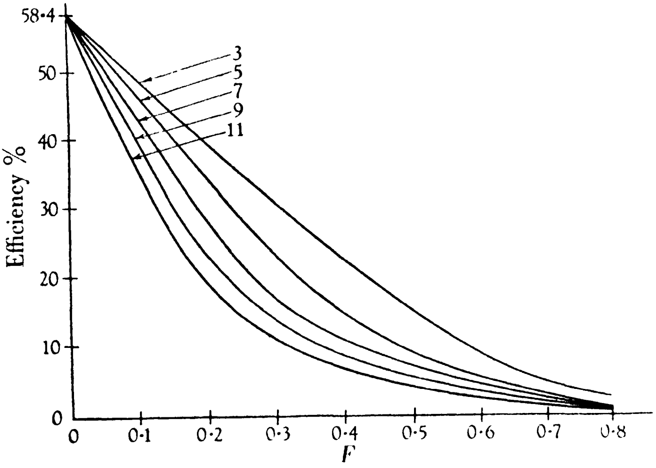

Fig. 3·3. Efficiency versus Milner's parameter F.

First, the form of the parameter F shows that it is necessary to make the beam impedance as small as possible, the resonator impedance as large as possible, S and β^2 as large as possible for an efficient valve. At a fixed voltage these requirements mean that the length between gap centres should be great and that the current should be as large as possible. These requirements are directly contradictory as it is found that the maximum current is a function of $(d/l)^2$, where d is the tunnel diameter and l the tunnel length. It might be thought that the way out of this dilemma is to increase d, but this means using a resonator with much capacitance at the centre and correspondingly low R. In practice it also means high h.f. series resistance because the grids contribute much more to this term than does the body of the resonator. What is usually done is to select a voltage which must not be exceeded, fix the gap spacing by requiring that $\beta^2 > 0{\cdot}6$, and then make a study of the impedance of a family of resonators. The maximum current is fixed by assuming that the tunnel length is twice the depth of one resonator, and it is then possible to determine the best compromise open to one.

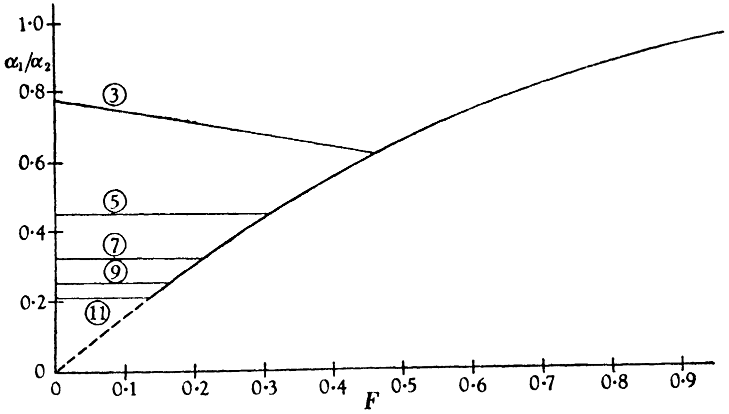

Fig. 3·4. Voltage ratio versus F.

3·5. The velocity-modulation action of a gap. Second-order approximation

We return to the study of a modulating gap in order to obtain an expression for the power gained by the beam in passing through the gap.

As before we have

$$\ddot{Z} = \frac{eV_1}{md}\sin\omega t, \tag{13}$$

$$\dot{Z} = -\frac{eV_1}{\omega dm}\cos\omega t + c_1, \tag{14}$$

and

$$Z = Z_0 + c_1 t - \frac{eV_1}{md\omega^2}\sin\omega t. \tag{58}$$

The boundary conditions are that

$$Z = 0 \text{ at } t = t_0, \quad \dot{Z} = u_0 \text{ at } t = t_0.$$

Then
$$c_1 = u_0 + \frac{eV_1}{md\omega}\cos\omega t_0,$$

and
$$Z = \left(u_0 + \frac{eV_1}{md\omega}\cos\omega t_0\right)(t - t_0) + \frac{eV_1}{md\omega^2}(\sin\omega t_0 - \sin\omega t). \quad (59)$$

We put $V_1/V_0 = \alpha$, $\phi = \omega Z/u_0$, $\phi_0 = \omega d/u_0$ as before, but instead of putting $t_1 = t_0 + d/u_0$, we introduce a correction factor to represent the effect of the changing voltage. That is, we now take

$$t = t_0 + \frac{Z}{u_0} + \frac{\delta}{\omega}. \quad (60)$$

δ is assumed to be a small quantity.

We can now proceed in either one of two ways. The most direct method would be to calculate the velocity of exit from the gap, average the gain in energy over all possible phases of entry to the field, and multiply by the number of electrons to obtain the total power absorbed by the beam. A second method is to apply the equation of continuity to the first gap in the same way that we applied the equation of continuity to the first and second gaps to calculate the degree of bunching. We shall adopt this method because it gives us the reactive part of the beam impedance as well as the resistive part. We have

$$i = \frac{i_0 dt_0}{dt} = \frac{i_0 d(\omega t_0)}{d(\omega t)}. \quad (61)$$

But
$$\frac{d(\omega t_0)}{d(\omega t)} = 1 - \frac{d(\delta)}{d(\omega t)} \quad (62)$$

from eqn. (60), therefore

$$i = i_0\left(1 - \frac{d(\delta)}{d(\omega t)}\right). \quad (63)$$

We next establish a relationship between δ and ωt by means of eqn. (59). We approximate by assuming that $\cos(\omega t - \phi - \delta)$ and $\sin(\omega t - \phi - \delta)$ can be replaced by $\cos(\omega t - \phi)$ and $\sin(\omega t - \phi)$. Then

$$Z = Z + \frac{u_0\delta}{\omega} + \cos(\omega t - \phi)\left[\frac{\alpha_1 Z}{2\phi_0 u_0} + \frac{\alpha_1\delta}{2\phi_0\omega}\right]$$
$$+ \frac{\alpha_1 u_0}{2\phi_0\omega}[\sin(\omega t - \phi) - \sin\omega t]. \quad (64)$$

But the product $\alpha_1\delta$ is $\ll 1$, so we neglect it. Multiplying by ω/u_0 we have

$$\phi = \phi+\delta+\frac{\alpha_1\phi}{2\phi_0}(\cos\omega t\cos\phi+\sin\omega t\sin\phi)$$
$$+\frac{\alpha_1}{2\phi_0}(\sin\omega t\cos\phi-\cos\omega t\sin\phi-\sin\omega t), \tag{65}$$

therefore

$$\delta = \frac{\alpha_1}{2\phi_0}[\sin\omega t(1-\cos\phi-\phi\sin\phi)+\cos\omega t(\sin\phi-\phi\cos\phi)]. \tag{66}$$

Then finally

$$i_1 = i_0\Bigg[1-\frac{\alpha_1}{2\phi_0}\sin\omega t(\sin\phi-\phi\cos\phi)$$
$$+\frac{\alpha_1}{2\phi_0}\cos\omega t(\cos\phi-1+\phi\sin\phi)\Bigg]. \tag{67}$$

This quantity has to be averaged over all the electrons in the gap at time t, and we initially chose V_1 a sinusoidal voltage, so that the component of i_1 in phase with the voltage is

$$\frac{i_0\alpha_1}{2\phi_0}(\sin\phi-\phi\cos\phi).$$

The average in-phase current is then

$$\mathbf{I}_1 = \frac{i_0\alpha_1}{2\phi_0^2}\int_0^{\phi_0}(\sin\phi-\phi\cos\phi)\,d\phi = i_0\alpha_1\left[\frac{1-\cos\phi_0}{\phi_0^2}-\frac{\sin\phi_0}{2\phi_0}\right]. \tag{68}$$

The average power lost in bunching is therefore

$$Pb = \frac{V_1^2}{2R_0}\left[\frac{1-\cos\phi_0}{\phi_0^2}-\frac{\sin\phi_0}{2\phi_0}\right]; \tag{69}$$

similarly, the average reactive part of the current is

$$\mathbf{I}_r = \frac{i_0\alpha_1}{2\phi_0^2}\int_0^{\phi_0}(\phi\sin\phi-1+\cos\phi)\,d\phi \tag{70}$$

$$= i_0\alpha_1\left[\frac{\sin\phi_0}{\phi_0^2}-\frac{1+\cos\phi_0}{2\phi_0}\right]. \tag{71}$$

The beam therefore applies an admittance $G+jB$, where

$$G = \frac{1}{R_0}\left[1-\frac{\cos\phi_0}{\phi_0^2}-\frac{\sin\phi_0}{2\phi_0}\right] \tag{72}$$

and

$$B = \frac{1}{R_0}\left[\frac{\sin\phi_0}{\phi_0^2}-1+\frac{\cos\phi_0}{2\phi_0}\right] \tag{73}$$

to the terminals of the gap.

It should be remembered that this analysis could be equally well applied to the catcher gap, in which case we should find that the field gains power because of the bunching and loses power because of the beam loading to an extent given by eqn. (69) but with V_1 replaced by V_2.

In its present form the analysis is distinctly unsatisfactory because it gives no indication of how severe the limitation imposed on its validity by the approximation is likely to be. A further approximation shows, in fact, that Pb contains a small term in α^4 which decreases rapidly as ϕ_0 increases. Apart from the standard assumptions detailed earlier in the chapter and the approximations made in the working, the only assumptions which are implicit in the expressions just given, are that the field is bounded by perfect grids and that no electrons are turned back in the gap. The first order approximation gave sufficiently good information for the bunching calculation and even the output efficiency for high impedance beams, but the second approximation was necessary before the beam loading could be evaluated. The beam loading becomes a large effect if the beam impedance is low, and the depths of modulation great or in other words it is important in high-power tubes. In the next section we proceed to remove one restriction by making the calculation for generalized fields and incidentally gain some more information about the validity of the present analysis.

3·6. The general expression for power interchange at a gap

We next consider the general problem of a gap without grids, in which the field is some, as yet undetermined, function of the axial and radial co-ordinates.

This problem has been solved by slightly different methods by Petrie, Strachey and Wallis* of S.T.C. and Watson of A.S.E. We here adopt the rather more direct method of Watson, but carry his calculations somewhat further to reach the important general formulae first established by the S.T.C. workers.

The equation of motion in a general field is

$$\frac{md^2z}{dt^2} = eE(z)\sin\omega t. \tag{74}$$

We put $\theta = \omega t, \quad \theta_0 = \omega t_0, \quad Z = \frac{\omega z}{u_0} = \frac{2\pi z}{S_0},$

---

* Now published in *J. Instn Elect. Engrs*, 93, pt. IIIA, no. 5 (1946), 875.

where S_0 is the distance travelled per cycle of oscillation by an electron of velocity u_0 and t_0 is the time of entry to the field. The field extends from $Z = 0$ to $Z = \infty$, so we can normalize the field by writing

$$G(Z) = \frac{E(Z)}{\int_{-\infty}^{+\infty} E(Z)dZ}$$

when the depth of modulation α becomes $\frac{1}{V_0}\int_0^\infty E(Z)\,dZ$. Then

$$\frac{d^2Z}{d\theta^2} = \frac{\alpha}{2}G(Z)\sin\theta. \tag{75}$$

Although eqn. (75) can be solved exactly for several fields it is not in general soluble, and we have to find an approximate solution subject to the conditions

$$\theta = \theta_0,\ \frac{dZ}{d\theta} = 1 \quad \text{at} \quad Z = 0.$$

The first approximation is obtainable by supposing that $G(Z) = 0$ and we then get $\theta_1 = \theta_0 + Z$. The second approximation is obtained by solving

$$\frac{d^2Z}{d\theta^2} = \frac{\alpha}{2}G(Z)\sin(\theta_0+Z) \quad \text{and so on.} \tag{76}$$

If we call the solution of eqn. (76) θ_2 and number further solutions accordingly, we have

$$\frac{d^2Z}{d\theta_{n+1}^2} = \frac{\alpha}{2}G(Z)\sin\theta_n,\quad \theta_{n+1} = 0,\quad \frac{dZ}{d\theta_{n+1}} = 1 \quad \text{at} \quad Z = 0.$$

For the second approximation we have

$$\frac{d^2Z}{d\theta^2} = \frac{\alpha}{2}G(Z)\sin(\theta_0+Z),$$

therefore $$\left(\frac{dZ}{d\theta_2}\right)^2 = 1+\alpha\int_0^Z G(W)\sin(\theta_0+W)\,dW,$$

therefore

$$\theta_2 = \theta_0 + \int_0^Z \left[1+\alpha\int_0^V G(W)\sin(\theta_0+W)\,dW\right]^{-\frac{1}{2}} dV. \tag{77}$$

Now the power gained or lost by the beam is the input power times the average gain or loss of kinetic energy per electron. If we define the 'diode efficiency' of the gap as this quantity divided by the input power, we have

$$\eta_D = \frac{1}{2\pi}\int_0^{2\pi}\left[\left(\frac{dZ}{d\theta}\right)^2 - 1\right] d\theta_0, \tag{78}$$

where the quantities are evaluated at exit from the field $Z = \infty$. An approximation to η_D is given by

$$\frac{\alpha}{2\pi}\int_0^{2\pi}\int_0^{\infty} G(Z)\sin\theta_n\, d\theta_0\, dZ. \tag{79}$$

From eqn. (77) expanding by the binomial theorem we have

$$\theta_2 = \theta_0 + Z - \frac{\alpha}{2}\int_0^{\infty}\int_0^{V} G(W)\sin(\theta_0 + W)\, dW\, dV + O(\alpha^2),$$

$$\sin\theta_2 = \sin(\theta_0 + Z) - \frac{\alpha}{2}\cos(\theta_0 + Z)$$

$$\times\int_0^{\infty}\int_0^{V} G(W)\sin(\theta_0 + W)\, dW\, dV + O(\alpha^3).$$

Thus

$$\eta_D = \frac{\alpha}{2\pi}\int_0^{2\pi}\int_0^{\infty} G(Z)\left\{\sin(\theta_0 + Z) - \frac{\alpha}{2}\cos(\theta_0 + Z)\right.$$

$$\left.\times\int_0^{X}\int_0^{V} G(W)\sin(\theta_0 + W)\, dW\, dV\right\} dZ\, d\theta_0 + O(\alpha^3).$$

Integrating with respect to θ_0 we have

$$\eta_D = \frac{\alpha^2}{4}\int_0^{\infty}\left\{G(Z)\sin Z\int_0^{X}\int_0^{V} G(W)\cos W\, dW\, dV\right.$$

$$\left. - G(Z)\cos(Z)\int_0^{X}\int_0^{V} G(W)\cos W\, dW\, dV\right\} dX.$$

The double integrals can be evaluated by integration by parts. We require to integrate

$$\int_0^{A}\int_0^{B} \phi(W)\, dW\, dV = \left[B\int_0^{B}\phi(W)\, dW\right]_0^{A} - \int_0^{A} V\phi(V)\, dV$$

$$= A\int_0^{A}\phi(V)\, dV - \int_0^{A} V\phi(V)\, dV,$$

therefore

$$\eta_0 = \frac{\alpha^2}{4}\int_0^\infty G(Z)\cos Z\,dZ\int_0^\infty ZG(Z)\sin Z\,dX - \int_0^\infty G(Z)\sin Z\,dZ\int_0^\infty ZG(Z)\cos Z\,dX.$$

In this form it is easy to see that it is quite permissible to shift the origin of Z to the centre of the gap if we take the limits of integration to be $-\infty$ to $+\infty$.

But
$$\int_{-\infty}^{+\infty} G(Z)\sin Z\,dZ = 0,$$

because $G(Z)$ must be an even function of Z and $\sin Z$ is certainly an odd function of Z, therefore

$$\eta_D = \frac{\alpha^2}{4}\int_{-\infty}^{+\infty} G(Z)\cos Z\,dZ\int_{-\infty}^{+\infty} ZG(Z)\sin Z\,dZ = \frac{\alpha^2\beta\gamma}{4}+O(\alpha^3), \tag{80}$$

where
$$\beta = \int_{-\infty}^{+\infty} G(Z)\cos Z\,dZ, \quad \gamma = \int_{-\infty}^{+\infty} ZG(Z)\sin Z\,dZ. \tag{81}$$

From the form of γ it is clear that it is very closely allied with β. In fact, if we had followed the S.T.C. writers and made the assumption that the electrons enter the modulating field with a velocity u not necessarily that of the reference electrons, we should have found

$$\beta = \int_{-\infty}^{+\infty} G(Z)\cos\left(\frac{Z}{u}\right)dZ, \tag{82}$$

$$\gamma = \int_{-\infty}^{+\infty} G(Z)\sin\frac{Z}{u}\,dZ = u^2\frac{d(\beta)}{du}. \tag{83}$$

γ therefore measures the rate of change of β with respect to the velocity at input to the gap, and it provides the mathematical formulation of an idea which has already been mentioned, viz. that an accelerated electron gains more energy from the field than is given up to the field by an electron entering at an instant in the cycle when the field is of the same magnitude but in the reverse direction.

The above expression has neglected terms of the order α^3 and higher powers of α. Since it is assumed that α is rather small this is permissible. Later numerical results will show that in most practical cases the above analysis will be adequate up to $\alpha = \frac{1}{2}$ at least.

We now apply these results to a gridded gap. Using the notation of this section

$$\beta = \frac{1}{L}\int_{-\frac{1}{2}L}^{\frac{1}{2}L} \cos Z\,dZ = \frac{2}{L}\sin\tfrac{1}{2}L$$

$$= \frac{\sin\frac{1}{2}L}{\frac{1}{2}L}, \tag{84}$$

$$\gamma = \frac{1}{L}\int_{-\frac{1}{2}L}^{+\frac{1}{2}L} Z\sin Z\,dZ = \frac{1}{L}\left[\sin Z - Z\cos Z\right]_{-\frac{1}{2}L}^{+\frac{1}{2}L},$$

$$\gamma = \frac{\sin\frac{1}{2}L}{\frac{1}{2}L} - \cos\tfrac{1}{2}L. \tag{85}$$

Using these expressions for β and γ in eqn. (80) we can derive the expression for power lost in bunching. After a little reduction it yields the expression we found in eqn. (69) by a quite different method. The methods of § 5 are justified, though the derivation obscures the degree of approximation. It should be remembered that a positive value of η_D represents a transfer of power from the field to the beam, while a negative value means gain of power by the field. η_D is in fact negative over a range of values of D and oscillators have been made using this principle, but the efficiencies are very low. This matter will be taken up in more detail later on.

3·7. The calculation of β and γ

We consider the gap system shown in fig. 3·5. We look for a general solution of Maxwell's equations in normalized cylindrical co-ordinates

$$Z = \frac{2\pi z}{S_0}, \quad R = \frac{2\pi r}{S_0}.$$

Such a solution is found by combining scalar wave functions of the form

$$\psi_n = e^{jn\theta} J_n(kR)\, e^{j\gamma z}\, d\gamma,$$

where $k^2 = (\omega^2/c^2) - \gamma^2$ and remembering that the Neumann functions are inadmissible because of the singularity at $R = 0$. Moreover, in the cases that concern us, the functions are independent of θ so that $n = 0$. Then

$$G(Z, R) = \int_{-\infty}^{+\infty} A(\gamma) J_0(kR)\, e^{j\gamma z}\, d\gamma,$$

where $A(\gamma)$ is an arbitrary function of γ. $G(Z, R)$ is normalized so that $\int_{-\infty}^{+\infty} G(Z, R)\, dZ = 1$, as in the last section.

This solution for the field is correct for the case in which there is propagation, and therefore power transfer, along the drift tube. But we require to prevent any such leakage of power, and so in practical designs the drift tube is always much smaller than the critical diameter above which propagation can take place. In this case we require a solution satisfying Laplace's equation, which is obtained by neglecting ω^2/c^2 in the expression for k. Then

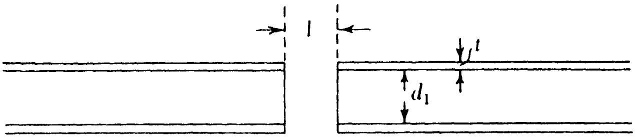

Fig. 3·5. Cylindrical gap notation.

$$G(Z, R) = \int_{-\infty}^{+\infty} a(k)\, I_0(kR)\, e^{jkz}\, dk, \tag{86}$$

where $I_0(kR)$ is a modified Bessel function of the first kind and of order zero.

Now
$$\beta(u) = \int_{-\infty}^{+\infty} G(Z, R) \cos \frac{Z}{u}\, dZ$$

for the case in which the velocity of entrance is different from the velocity u_0. We also know from physical reasoning that $G(Z, R)$ must be symmetrical about the centre line of the gap. Thus

$$\int_{-\infty}^{+\infty} G(Z, R) \sin \frac{Z}{u}\, dZ = 0,$$

and we can write

$$\begin{aligned} \beta(u) &= \int_{-\infty}^{+\infty} G(Z, R)\, e^{jz/u}\, dZ \\ &= \int_{-\infty}^{+\infty} \int_{-\infty}^{+\infty} a(k)\, I_0(kR) \exp[jz(k + 1/u)]\, dk \quad \text{using eqn. (86)} \\ &= \frac{1}{2\pi}\, a\left(\frac{1}{u}\right) I_0\left(\frac{R}{u}\right). \end{aligned}$$

Putting $R = 0$ we get

$$[\beta(u)]_{R=0} = \frac{1}{2\pi}a\left(\frac{1}{u}\right)$$

or

$$[\beta(u)]_R = [\beta(u)]_0\, I_0\left(\frac{R}{u}\right). \tag{87}$$

If we can determine β for any particular R value eqn. (85) allows us to calculate any other value of β.

In starting current calculations we require the mean value of β^2 averaged over the beam, which is supposed to be uniform over its cross-section. Let the beam radius be R_0, then

$$\begin{aligned}\beta^2(u) &= \frac{1}{\pi R_0^2}\int_0^{R_0}\beta^2(u)_R\, 2\pi R\, dR\\ &= \beta^2(u)_0\,[I_0^2(R_0/u) - I_1^2(R_0/u)]\end{aligned}$$

or

$$\beta(u)_{\text{r.m.s.}} = \beta(u)_0[I_0^2(R_0/u) - I_1^2(R_0/u)]^{\frac{1}{2}}. \tag{88}$$

We now require to find a value of β for some particular R value. This can be done by considering the factor at the edge of the gap. Referring again to fig. 3·5 it is clear that, if the ratio t/d is large, that is, the tunnel walls are very thick in comparison with the diameter, the field at the edge of the gap will be linear and

$$\beta(u)_{R=R_1} = \frac{\sin\phi/2u}{\phi/2u}.$$

Then

$$\beta(u)_0 = \frac{1}{I_0(R_1/u)}\sin\frac{\phi/2u}{\phi/2u}, \tag{89}$$

and the r.m.s. value can be calculated from eqn. (88).

Another particular solution for the edge field is known. This is the case when t is very small compared with d and the gap length tends to zero. In this case the potential in the gap is given by

$$V = \frac{1}{\pi}\sin^{-1}\frac{2Zu}{\phi},$$

$$\begin{aligned}\beta(u)_{R=R_1} &= \int_{-\frac{1}{2}\phi}^{+\frac{1}{2}\phi}\frac{\partial V}{\partial Z}\cos Z\,dZ\\ &= \int_0^1 \cos(\phi/2u\sin\pi V)\,dV\\ &= J_0(\phi/2u).\end{aligned}$$

We can now obtain $\beta(u)_0$ as before,

$$\beta(u)_0 = \frac{1}{I_0(R_1/u)} J_0(\phi/2u). \tag{90}$$

A series of careful experiments on electrolytic trough models was undertaken at Bristol to test the range of validity of the expressions for the edge β. The results show that for most practical arrangements, at any rate above 3 cm. wave-length, $\beta = J_0(\phi/2u)$ is a very good approximation to the correct value. At lower wave-lengths t/α_1 is generally greater than 0·05, and it becomes better to take the mean of $J_0(\phi/2u)$ and $\dfrac{\sin\phi/2u}{\phi/2u}$. In no real case is the sine form a better approximation than the Bessel function.

The results given above have been deduced for conditions in which the velocity at entrance to the h.f. field is not necessarily equal to the velocity corresponding to the applied potential and the beam does not necessarily fill the tunnel. Usually $u = 1$, but it is rather unusual for the beam to fill the tunnel, although for simplicity in design calculations it is assumed to do so. If we put $R_0 = R_1 = R$, then

$$\beta_{\text{r.m.s.}} = J_0(\tfrac{1}{2}\phi)\left(\frac{I_0^2(R) - I_1^2(R)}{I_0^2(R)}\right)^{\frac{1}{2}}. \tag{91}$$

γ can be found using eqn. (83). Using eqn. (88) with (90) inserted for β_0 we obtain

$$\bar{\gamma} = \frac{u^2\beta(u)}{2}\left[\frac{\phi}{u^2}\frac{J_1(\phi/2u)}{J_0(\phi/2u)} - \frac{2/u I_0(R/u)\, I_1^2(R/u) + 2R/u^2\, I_1(R/u)\, I_0^2(R/u) - 2R/u^2\, I_1^2(R/u)}{I_0(R/u)\,(I_0^2(R/u) - I_1^2(R/u))}\right].$$

Writing $u = 1$ and rearranging slightly we have

$$\gamma = \frac{\beta}{2}\left[\phi\frac{J_1(\frac{1}{2}\phi)}{J_0(\frac{1}{2}\phi)} - \frac{2I_1^2(R)}{I_0^2(R) - I_1^2(R)} + \frac{2RI_1(R)}{I_0(R)}\right]. \tag{92}$$

We shall see in later chapters that $\bar{\beta}$ and $\bar{\gamma}$ are usually required in the form $\bar{\beta}^2$ and $2\bar{\gamma}/\bar{\beta}$. Figs. 3·6, 3·7 and 3·8 show plots of these quantities as functions of L and R.

The expressions given above are strictly correct only for a magnetically focused tube, in which the h.f. field cannot deflect the electrons. In the electrostatic case the electrons are deflected as well as accelerated, because of the curvature of the h.f. field which is essentially the same as that due to an ordinary cylindrical electron lens. The deflexion of the beam introduces two fresh factors into the discussion, first the expression for the gap efficiency is changed,

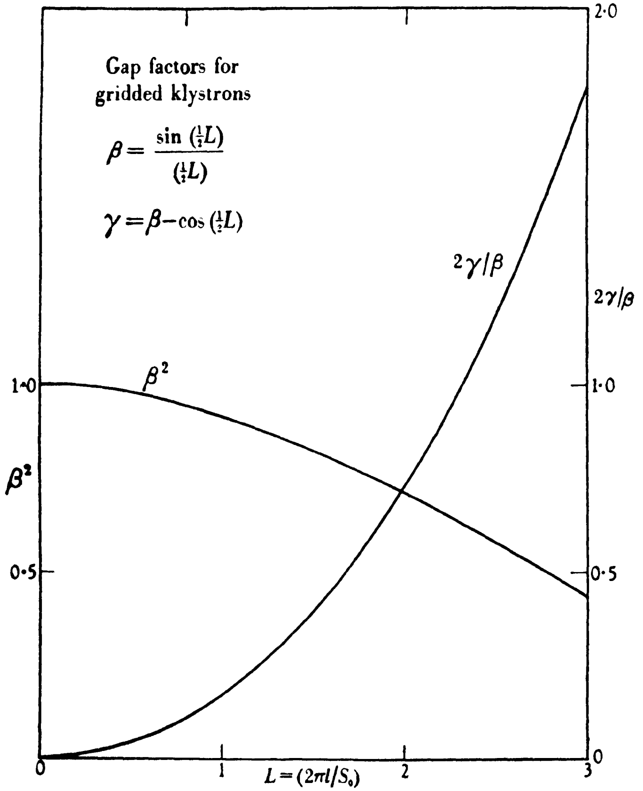

Fig. 3·6. Gap factors β and γ for gridded gaps.

and secondly a periodic variation in beam diameter is set up. Any calculation of the deflexion power is certain to be very much less accurate than the calculation of the bunching power, because we have assumed that the electrons have no velocity perpendicular to the direction of motion, which is not the case in any real electrostatically focused beam. It is clear that the true value of the deflexion power will depend on the relative magnitude of the velocities perpendicular to the direction of motion and the h.f. field. It would seem best to evaluate the deflexion loss graphically, for a definite focusing structure. Feenberg has extended the results of this section to cover the deflexion loss. His expression for the total beam loss, including both deflexion and acceleration effects, is

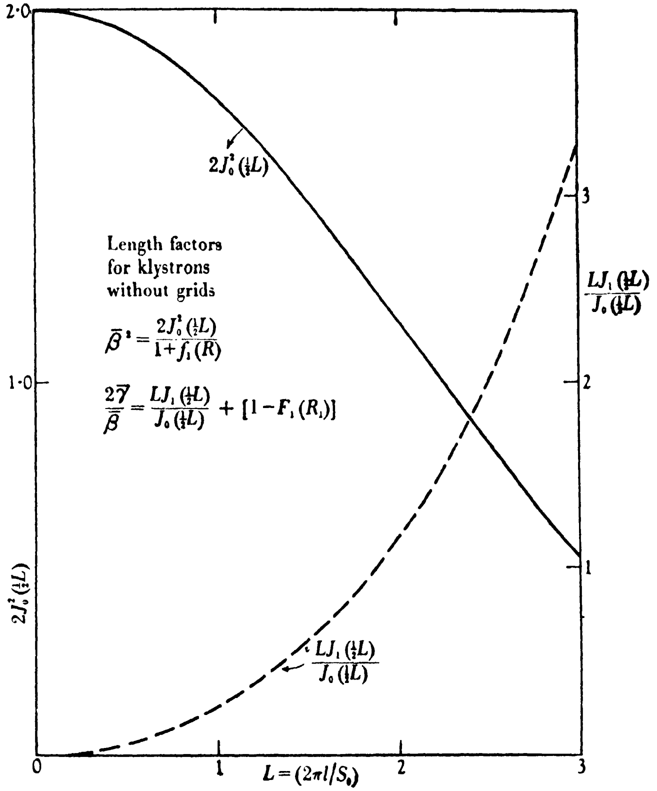

Fig. 3·7. Length factors for gaps without grids.

$$2\frac{R_0}{Rb} = g^2(1)\left[\frac{2}{A}\left(1+\frac{BI_1(B)}{I_0(B)}\right)\frac{I_0(A)\,I_1(A)}{I_0^2(B)} - \left(\frac{I_0(A)}{I_0(B)}\right)^2 - \left(\frac{I_1(A)}{I_1(B)}\right)^2\right] - \frac{I_0(A)\,I_1(A)}{A^2 I_0(B)}\left(\frac{d}{du}g^2(u)\right)_{u=1}. \qquad (93)$$

Here $g(u) = \beta$ at edge of gap, A = beam radius, B = tunnel radius. This expression uses the average β and not the r.m.s. β as we have done.

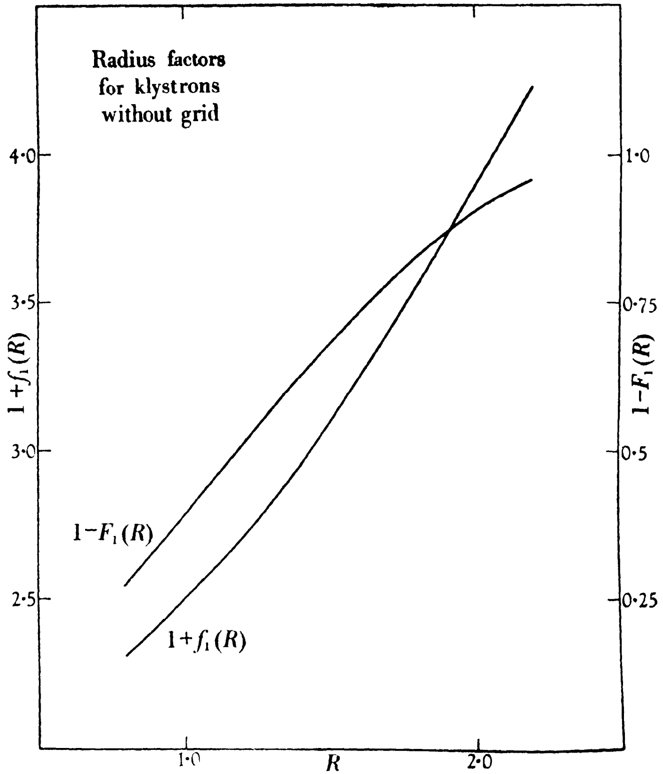

Fig. 3·8. Radius factors for gaps without grids.

3·8. Non-sinusoidal bunching

We conclude our general survey by considering what improvement in the conversion efficiency of a V.M. tube can be obtained by using different time functions for the buncher voltage; it should be remembered that, since the catcher is an impulsively excited high Q circuit, the output wave form will be sinusoidal whatever the buncher wave form. It is physically obvious that the best condition occurs when all the electrons which passed through the buncher in one cycle arrive simultaneously at the centre of the catcher gap. To achieve this we must have a saw-tooth variation in the transit time, and in the approximation of very small signals the buncher voltage should be saw-toothed and the conversion efficiency would approach 100 %. Before we discuss the problem in detail we shall deepen our understanding of the form of the catcher current.

In fig. 3·9 we show the time of arrival at the catcher centre plotted against time at the buncher centre for three different values of bunching factor $\frac{1}{2}S\alpha_1\beta_1$. The catcher gap is supposed to extend over the time interval between the dotted lines. When $\theta = \frac{1}{2}$ the number of electrons in the catcher gap at the time when the catcher voltage is at the negative maximum is $(I_0/u_0)\Delta_2 t_1$. For $\theta = 1$ it is $(I_0/u_0)\Delta_4 t_1$ and for $\theta = 1{\cdot}84$ it is $(I_0/u_0)(\Delta_1 t_1+\Delta_2 t_2+\Delta_3 t_1)$. As $\Delta_4 t_1$ is greater than $\Delta_1 t_1+\Delta_2 t_1+\Delta_3 t_1$ it might appear that $\theta = 1$ gives the best bunching factor, but although the current peak is greatest for this case, many more electrons arrive with unfavourable phases than is the case for $\theta = 1{\cdot}84$, as has been shown by our formal analysis in § 3·3 where we found that the fundamental component of the current is greatest for this value of θ. The mathematical analysis has performed the summation $\Sigma\Delta_n t_1$ automatically and has taken account of the fact that if $\theta > 1$, dt_2/dt_1 becomes negative for some values of t_1. The physical reason for this is that negative values of dt_2/dt_1 do not mean that electrons are moving backwards but only that electrons which passed through at $-t_1'$ (fig. 3·9), etc., have been caught up by those that passed through at $+t_2'$ and passed by all those between, so that the direction of relative motion has changed. This diagram makes it obvious that the requirement for

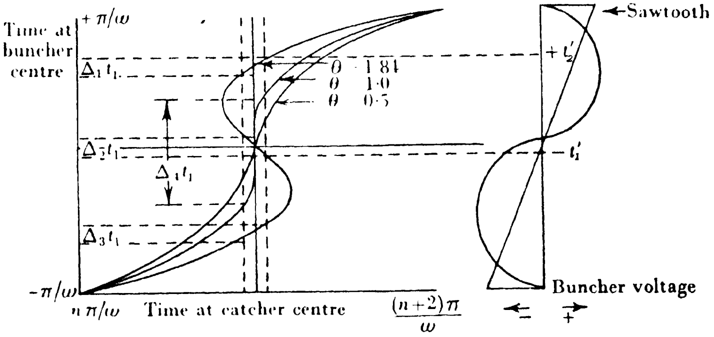

Fig. 3·9. Sinusoidal and ideal bunching.

100 % efficiency is that all the electrons should arrive simultaneously at the centre of the catcher gap, as shown by the vertical full line.

The theoretical basis for the study of non-sinusoidal bunching has been given by Feenberg, and Warnecke* and his co-authors whose treatment we reproduce below. When the phase is optimized the conversion efficiency is

$$\eta_{\text{conv.}} = \beta \frac{V_2}{V_0} \frac{1}{2\pi} \int_0^{2\pi} \frac{dt_1}{dt_2} \cos \omega t \, d(\omega t).$$

If we put $\omega t = \phi$ and $\omega t_2 = \phi + \tau(\phi)$ we can write

$$\eta_{\text{conv.}} = \beta \frac{V_2}{V_0} \frac{1}{2\pi} \int_1^{2\pi} \cos(\phi + \tau(\phi)) \, d\phi. \tag{94}$$

The integral is maximized by writing, for all ϕ,

$$\cos(\phi + \tau(\phi)) = 1, \quad \phi + \tau(\phi) = 2\pi n. \tag{95}$$

Now, for drift-tube conversion $\tau(\phi) = \omega s / u_1(\phi)$. Thus the optimum condition becomes

$$\phi + \frac{Su_0}{u_1(\phi)} = 2k\pi.$$

If we expand $\tau(\phi)$ in a Fourier series we find that

$$\tau(\phi) = (2k-1)\pi + 2\left[\sin\phi + \frac{\sin 2\phi}{2} + \ldots + \frac{\sin n\phi}{n} + \ldots\right],$$

which we recognize as a trapezoidal wave form, thus agreeing with our physical intuition. Now we have the approximate relation

$$\left(\frac{u_1(\phi)}{u_0}\right)^2 = \frac{V_0 + V(\phi)}{V_0} \quad \text{or} \quad \left(\frac{S}{\tau(\phi)}\right) = \frac{V_0 + V(\phi)}{V_0},$$

so that a relation between $\tau(\phi)$ and $V(\phi)$ has formally, at any rate, been established. Computation shows that if a second harmonic component is added to the bunching voltage, an efficiency of about 74 % can be obtained. Increasing the number of harmonics introduced only causes small increases in the efficiency.

It has been proposed to make use of this effect by locating a second harmonic resonator very close to the catcher gap, the necessary driving power being extracted from a second harmonic catcher beyond the fundamental catcher. Feenberg has proposed the more practical alternative of using multiresonator tubes with the resonators tuned to various harmonics of the required frequency. No experimental results on either of these systems have been given.

---

* Warnecke, *J. Phys. Radium*, 4 (1943), pts. 5 and 6.

To conclude this chapter we should note that a radically different approach to these problems has been made by Hahn* and Ramo†; they study the propagation of waves along the electron beam, which is a similar situation to that encountered in the study of waves on dielectric rods. The method is not suitable for large signals, nor is it as simple as the ballistic method, so we refer interested readers to the original papers.

---

* Hahn, *Gen. Elect. Rev.* 42 (1939), 258; 497.
† Ramo, *Proc. Inst. Radio Engrs, N.Y.*, 27 (1939), 757.

Chapter 4

HEAVY CURRENT ELECTRON BEAMS

The mathematical analysis of the last chapter has shown that the problem of focusing as many electrons as possible through the tunnel is of primary importance in klystron design. In this chapter we shall derive expressions for the maximum current which can be passed through tunnels of given dimensions, using either magnetic or electrostatic focusing at a fixed voltage.

That there is a maximum current can be seen from the following argument. In the electrostatic case we assume that we are able to design a gun which produces any desired radial electric field, which is at first adjusted so that a low-current beam just clears the edges of the tunnel at entrance. In the field free space inside the tunnel the resultant inward radial acceleration is destroyed by the outward space-charge field so that the beam eventually reaches a position of minimum diameter, known as the throat, where all the electrons are travelling parallel to the axis. Clearly the beam profile is symmetrical about the plane of the throat. If the current is increased, by some means, keeping the entrance pupil constant, the throat will move nearer to the centre of the tunnel and increase in diameter. If the process is continued the throat will eventually reach the centre of the tunnel, and because of the symmetry property just mentioned the beam will also graze the tunnel at exit. Any further increase in cathode current will then cause a current to the tunnel walls and a decrease in current through the tunnel. In the magnetic case the beam is kept parallel by means of an axial magnetic field. As we shall see, space charge now manifests itself by a lowering of the potential inside the beam. If the current is gradually increased the potential inside the beam falls until finally electrons are repelled out of the tunnel. By analogy with other types of space-charge flow we should expect these maximum currents to vary with the $\frac{3}{2}$ power of the voltage, and this expectation is in fact correct. The current should also be proportional to the tunnel area in the electrostatic case. We shall see that these considerations impose very drastic limits on the length of klystrons, and therefore on the amplification factors and power output which can be obtained.

4·1. Electrostatic focusing in a cylindrical tunnel

This calculation has been made by several authors. The basic calculation was first made by Watson,* whose work was extended by Thompson and Headrick.† Spangenberg, in an unpublished report, first calculated the maximum current through a circular tunnel, and Guénard‡ has recently published a similar result. We reproduce the analysis of Guénard here.

To formulate the expressions for this case we consider the spreading of a beam from a plane A in fig. 4·1, where the beam is supposed to be of uniform density, monochromatic and the individual electrons are supposed to travel parallel to the axis.

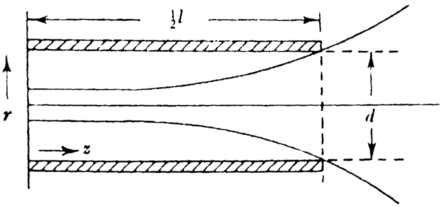

Fig. 4·1. Spreading of an electron beam from the 'throat'.

Let the beam current and voltage be I_0, V_0 and the beam radius at plane A be r_0. By an integration of the divergence conditions we find that the radial electric field is given by

$$E_r = \frac{\rho r}{2\epsilon_0}. \tag{1}$$

But $$\rho = \frac{I_0}{u_0 \pi r^2} \quad \text{and} \quad dz = u_0\,dt,$$

while $$u_0 = (2e/m)^{\frac{1}{2}}\,V_0^{\frac{1}{2}}.$$

The equation of radial motion is then

$$\frac{d^2r}{dz^2} = \frac{1}{4\pi\epsilon_0(2e/m)^{\frac{1}{2}}}\,\frac{I_0}{V_0^{\frac{3}{2}}}\,\frac{1}{r}. \tag{2}$$

Integrating this by multiplying both sides by $2dr/dz$ we obtain

$$z = \int_{r_0}^{r} \frac{dr}{(\frac{1}{2}K \log_e r/r_0)^{\frac{1}{2}}},$$

---

* Watson, *Phil. Mag.* 3 (1927), 849.

† Thompson and Headrick, *Proc. Inst. Radio Engrs, N.Y.*, 28 (1940), 318.

‡ Guénard, *Ann. Radioélect.* 1 (1945), 74.

or changing the variables to $R = \dfrac{r}{r_0}$, $Z = \left(\dfrac{K}{2}\right)^{\frac{1}{2}} \dfrac{z}{r_0}$,

$$Z = \int_1^R \frac{dR}{(\log_e R)^{\frac{1}{2}}}. \tag{3}$$

This equation can be integrated graphically to give the curve in fig. 4·2. The maximum current can be calculated as follows. For the moment we consider that r_0 is unity, which is permissible since it only occurs as a scale factor in R and Z. We next plot the point $(r, \frac{1}{2}l)$ on fig. 4·2. The point will not, in general, fall on the curve, but by adjusting $(\frac{1}{2}K)^{\frac{1}{2}}$ (which varies as $I_0^{\frac{1}{2}}$) correctly it can be brought on to the line. The maximum current can then be deduced from the condition that the tangent at the point representing the exit conditions shall go through the origin. This occurs for $R = 2{\cdot}4$, $Z = 2{\cdot}65$.

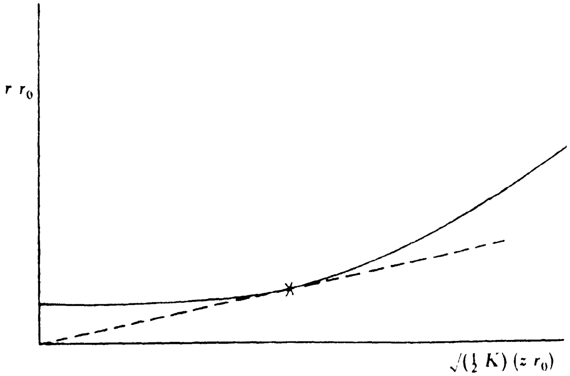

Fig. 4·2. Universal beam spreading curve-electrostatic focusing.

Then
$$r_0 = \frac{r}{2{\cdot}4} = \frac{d}{4{\cdot}8},$$

$$2{\cdot}65 = \left(\frac{K}{2}\right)^{\frac{1}{2}} \frac{l}{2r}$$

$$= \left(\frac{K}{2}\right)^{\frac{1}{2}} \frac{2{\cdot}4l}{d} \tag{4}$$

But
$$K = \frac{1}{\pi\epsilon_0(2e/m)^{\frac{1}{2}}} I_0 V_0^{-\frac{3}{2}}$$

$$= 6{\cdot}04 \times 10^4 I_0 V_0^{-\frac{3}{2}}. \tag{5}$$

Squaring eqn. (4) and inserting (5) we finally obtain as the expression for the maximum current

$$I_{0\,\mathrm{max.}} = 38{\cdot}9 \times 10^{-6} V_0^{\frac{3}{2}} \left(\frac{d}{l}\right)^2. \tag{6}$$

If $d/l = \frac{1}{6}$ and $V_0 = 1$ kV. the maximum current is around 34 mA. These dimensions are reasonable for a gridless 10 cm. klystron oscillator. If an amplifier has a gridded tunnel 1 cm. diameter and 10 cm. long the current is only 12·3 mA. The corresponding beam impedances are about 30 kΩ and about 90 kΩ, so, when it is remembered that a resonator for 10 cm. is not likely to have an impedance greater than 100 kΩ and if dielectric is sealed into it, as little as 70 kΩ, it is obvious that circular tunnels longer than a few centimetres are quite out of the question with electrostatic focusing, unless very high voltages are allowable.

4·2. Electrostatic focusing in rectangular and annular apertures

Convenient analytical expressions for the rectangular tunnel are easily derived for the case in which the height of the tunnel is much greater than its breadth. The analysis is similar to that given above, and in unpublished work Beck has shown that the maximum current per unit length which can be focused through a rectangular aperture is

$$I_{\mathrm{max.}} = 83{\cdot}3 \times 10^{-4} \frac{t}{l^2} V_0^{\frac{3}{2}} \,\mathrm{amp./m.}, \tag{7}$$

where t = breadth of tunnel, and the other symbols have their usual meanings.

This expression is applicable to two other important cases; those of the annular tunnel and the annular beam in a circular tunnel. While eqn. (7) is rigorously correct for an annular tunnel, it is only accurate for the annular beam in a circular tunnel when the mean beam diameter is large in comparison with the beam breadth. If the beam breadth is again t and the mean diameter of the annulus is P we obtain

$$I_{\mathrm{max.}} = 26{\cdot}2 \times 10^{-3} \frac{tP}{l^2} V_0^{\frac{3}{2}}. \tag{8}$$

Eqn. (8) shows that the maximum current in the case of an annular tunnel is about 70 % greater than in that of a circular tunnel of the same area.

4·3. Magnetic focusing in circular tunnels

In this case the beam is prevented from spreading by the application of a steady magnetic field parallel to the beam axis. We consider that the tunnel is long enough to allow us to consider the conditions at the centre of the tunnel without reference to any effects due to the ends. This means simply that the tunnel length is greater than its diameter. When the current inside the tunnel is small, the potential on the axis is substantially that of the walls, but as the current is increased, the potential starts to fall. It might be thought that the axis potential could be steadily forced down to zero before electrons start to be reflected, but the analysis shows that the axis potential can only be depressed about 80 % below the value on the walls. Any further increase in current causes an abrupt transition to a state with a virtual cathode and reflected electrons. The calculation has been given by Smith and Hartman,* and by Guénard.† We again follow Guénard.

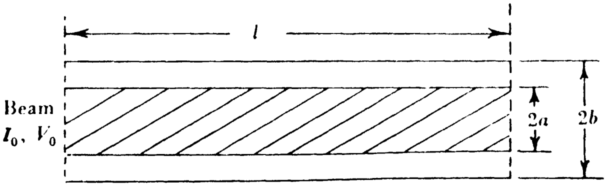

Fig. 4·3. Notation for magnetic focusing.

The potential variation inside the beam is given by integrating Poisson's equation, which in cylindrical co-ordinates reads

$$\frac{d^2V_1}{dr^2}+\frac{1}{2}\frac{dV_1}{dr}=\frac{\rho}{\epsilon_0}. \tag{9}$$

Outside the beam, in the case where it does not fill the tunnel (fig. 4·3), the potential is given by Laplace's equation

$$\frac{d^2V_2}{dr^2}+\frac{1}{2}\frac{dV_2}{dr}=0. \tag{10}$$

The boundary conditions are that

$$V_1=V_2,\quad \frac{dV_1}{dr}=\frac{dV_2}{dr}\quad \text{at}\quad r=a,$$

$$V_2=0\qquad\qquad \text{at}\quad r=b.$$

---

* Smith and Hartman, *J. Appl. Phys.* 11 (1940), 220.

† Guénard, *J. Phys. Radium*, 6 (1945), 43.

If the current density is J we have that

$$\rho = \frac{J}{u_0} \quad \text{and} \quad u_0 = (2e/m)^{\frac{1}{2}} V^{\frac{1}{2}}.$$

Then using the dimensionless co-ordinates

$$\Phi = \frac{V}{V_m} \quad \text{and} \quad R = r\left[\frac{J}{\epsilon_0(2e/m)^{\frac{1}{2}}}\right]^{\frac{1}{2}} V_m^{-\frac{3}{4}},$$

where V_m is the potential on the axis we obtain

$$\frac{d_2\Phi_1}{dR^2} + \frac{1}{R}\frac{d\Phi_1}{dR} = \Phi_1^{-\frac{1}{2}}, \tag{11}$$

$$\frac{d_2\Phi_2}{dR^2} + \frac{1}{R}\frac{d\Phi_2}{dR} = 0. \tag{12}$$

And at a we have

$$\begin{aligned} R_a &= a\left[\frac{J}{\epsilon_0(2e/m)}\right]^{\frac{1}{2}} V_m^{-\frac{3}{4}} \\ &= K^{\frac{1}{2}}\Phi_m^{\frac{3}{4}}, \end{aligned} \tag{13}$$

where $K = \dfrac{I_0 V_0^{-\frac{3}{2}}}{\pi\epsilon_0(2e/m)^{\frac{1}{2}}}$ as before and $\Phi_b = V_0/V_m$. Writing $k = b/a$ we get $R_b = kK^{\frac{1}{2}}\Phi_b^{\frac{3}{4}}$.

Since we are interested only in the maximum current we limit ourselves to the case in which the beam fills the tunnel, i.e. $k = 1$. Eqn. (11) has then to be integrated graphically or numerically up to the point of maximum current. The point of maximum current is reached when the value of R given by eqn. (13) falls on the curve representing the solution of eqn. (11). That is

$$R = K^{\frac{1}{2}}\Phi^{\frac{3}{4}}, \quad \frac{dR}{d\Phi} = \tfrac{3}{4}K^{\frac{1}{2}}\Phi^{-\frac{1}{4}}, \quad \text{or} \quad \Phi = \tfrac{3}{4}R\frac{d\Phi}{dR}. \tag{14}$$

Guénard's paper contains a table giving the integral of eqn. (11) which has been plotted in fig. 4·4, and this shows that the maximum current is reached when $R = 5\cdot12$, $\Phi = 5\cdot65$. Then

$$K_{\text{max.}} = \frac{5\cdot12^2}{5\cdot65^{\frac{3}{2}}} = 1\cdot90$$

and

$$I_{0\,\text{max.}} = 32\cdot5 \times 10^{-6} V_0^{\frac{3}{2}}. \tag{15}$$

It is interesting that eqn. (15) is independent of the size of the aperture and the length of the tunnel, but the magnetic field required to prevent the beam from spreading is proportional to the current. The currents given by eqn. (15) are greater than those given by electrostatic focusing, while the ratio of diameter to length is less than 0·9. Unfortunately, the full current cannot be utilized in V.M. tubes because of the large depression of the potential inside the beam which is objectionable; first, because of the resulting departure from the desired bunching conditions, and secondly because of the reduction in the β factor and increase in the loading at the gaps. If the depression of potential is limited to 10 % the maximum current is reduced to $6{\cdot}25 \times 10^{-6} V_0^{\frac{3}{2}}$. This last figure represents a much fairer basis of comparison for our purposes, and we can say that for usual tube structures magnetic focusing will give about ten times as much current as electrostatic. The decisive factor is usually the weight, size and cost of the focusing magnet.

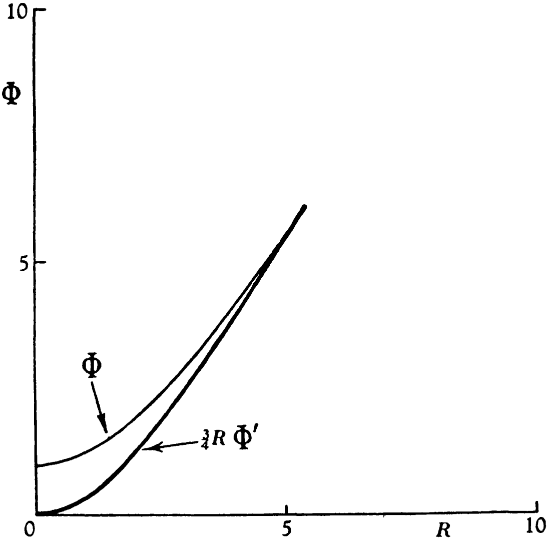

Fig. 4·4. Determination of maximum current in the magnetic case.

4·4. Magnetic focusing in rectangular tunnels

A similar analysis can be applied to the case of a rectangular beam. The result is that

$$J_{0\max.} = 18{\cdot}5tV_0^{\frac{3}{2}}, \tag{16}$$

where J_0 = current density. The corresponding depression of potential is 80 % on the axis. If this is limited to 10 % the current density is given by $J = 3{\cdot}9tV_0^{\frac{3}{2}}$ amp./m.

4·5. Conclusion

The results given in this chapter show that space-charge effects constitute a very grave limitation to the amount of current which can be forced through any tunnel. We shall see in later chapters that the maximum frequency which can be generated by a V.M. tube is determined by the condition that the starting current must not exceed the running current. For this reason current limitations become more and more important as the frequency of operation rises. For a more general survey the reader is referred to an excellent paper by J. R. Pierce.*

* Pierce, *Bell. Syst. Tech. J.* 24 (1945), 305.

Chapter 5

VELOCITY-MODULATION AMPLIFIERS AND FREQUENCY MULTIPLIERS

The velocity-modulation amplifier is a particularly important application of the principle because it is the one of two known ways of obtaining a power gain at wave-lengths lower than about 8 cm., where present-day triodes become inoperative. The second method is by the travelling-wave tube of Kompfner. For this reason it will be of importance in communication and television systems, though it has found no application in radar technique. This statement must be taken as referring only to power amplifiers and not to signal amplifiers which, although they can have a reasonable voltage gain, reduce the signal-to-noise ratio of the system.

The general theory set out in Chapter 3 would appear to show that, if circuit losses are neglected, one could obtain a very high power gain by making the tube long so that $\frac{1}{2}S\alpha_1\beta$ is about 1·84 for vanishingly small values of α_1. The theory of beam production has shown that this would mean for the electrostatic case a very high voltage or a very low current, or in the magnetic case a very large magnetic field over a long gap. Obviously if the current is too low the circuit losses cannot be neglected, so we can say that a long tube requires either high voltage or intense magnetic field. These are not the only objections to increasing the length, although we have as yet made no calculation of the degree to which longitudinal space-charge forces set up in the beam by the bunching can reduce the amplitudes of the a.c. components at the output gap. In fact, this is not an easy calculation to make, but we shall try to obtain upper and lower bounds so as to make a fair estimate of the maximum length. We shall find that the simple amplifier is not capable of very large gains, but that by coupling extra resonators on to the same beam, the gain can be increased by a large factor. We commence this study by taking the simplest case, that of the power amplifier.

5·1. Velocity modulation power amplifiers

We consider two resonators with parameters ω_0, Q_0 and Z_0, coupled to a beam of current I_0 at a voltage V_0 and spaced by s m. from gap centre to gap centre. The h.f. voltages on the gaps are V_1 and V_2, and we write $V_1/V_0 = \alpha_1 V_2/V_0 = \alpha_2$ as usual. An unpublished Bristol report by Beck gives the following analysis.

To drive the input resonator to an amplitude V we require

$$W_i = \frac{V_1^2}{2Z_0} + \frac{I_0 V_0 \alpha_1^2}{4}\overline{\beta\gamma}. \tag{1}$$

The first term represents the circuit loss and the second the power lost in bunching. An extra term quadratic in α_1 has to be added if there is deflexion loss.

We can write eqn. (1) as

$$W_i = \frac{I_0 V_0 (\alpha_1 \bar{\beta})^2 P}{8}; \tag{2}$$

here

$$P = \frac{4V_0}{I_0 Z_0 \bar{\beta}^2} + \frac{2\bar{\gamma}}{\bar{\beta}}, \tag{3}$$

and turns out to be of fundamental significance in V.M. tube design. Following the same reasoning the output power is

$$W_0 = I_0 V_0 \left[\alpha_2 \bar{\beta} J_1\left(\frac{S\alpha_1 \bar{\beta}}{2}\right) - (\alpha_2 \bar{\beta})^2 \frac{P}{8}\right]. \tag{4}$$

The $\cos(S-\gamma)$ term does not appear because the phase of the catcher adjusts itself so as to extract the maximum power from the beam. We now consider the maximum power output which is obtained by increasing the excitation and correctly adjusting the coupling to the load. Putting $\partial W_0/\partial \alpha_1 = 0$ for a maximum yields $J_1'(\tfrac{1}{2}S\alpha_1\bar{\beta}) = 0$ or

$$\tfrac{1}{2}S\alpha_1\bar{\beta} = 1{\cdot}84; \tag{5}$$

$\partial W_0/\partial \alpha_2 = 0$ gives

$$P = \frac{4J_1(\tfrac{1}{2}S\alpha_1\bar{\beta})}{\alpha_2\bar{\beta}}. \tag{6}$$

Inserting eqn. (5) into (6) we get

$$\alpha_2 \bar{\beta}_{\text{opt.}} = \frac{2{\cdot}36}{P}, \tag{7}$$

which finally gives

$$W_{0\,\text{max.}} = \frac{0{\cdot}63 I_0 V_0}{P}, \tag{8}$$

$$\eta_{0\,\text{max.}} = \frac{0{\cdot}63}{P}. \tag{8a}$$

If we suppose that the condition for maximum voltage swing on the output grid is $\alpha_1\bar{\beta}+\alpha_2\bar{\beta} = 1$, we can see from eqns. (5) and (7) that $3{\cdot}68/S+2{\cdot}36/P = 1$ is a condition for the validity of the analysis. For a practical case in which S is $\frac{7}{2}\pi$ radians, about the shortest length which one would use, the minimum value of P is about 3·5, which is only likely to be found in a very high power tube. Although electrons are reflected when the catcher voltage gets too large, it is probable that the efficiency would still increase slowly beyond this point. We shall return to this point later on. Having seen that our analysis does not violate any basic requirements of the theory, we can go on to consider the power gain.

The power amplification, for the optimum conditions, using eqns. (2), (5) and (8), becomes

$$G_{p\,\text{opt.}} = 0{\cdot}402\left(\frac{S}{P}\right)^2. \tag{9}$$

When $\alpha_2\bar{\beta}$ is optimized, but the input amplitude is varied

$$G_p = \frac{16}{P^2}\,\frac{J_1(\frac{1}{2}S\alpha_1\bar{\beta})}{(\alpha_1\bar{\beta})^2}. \tag{10}$$

As $\alpha_1 \rightarrow 0, J_1(\frac{1}{2}S\alpha_1\bar{\beta}) \rightarrow \frac{1}{4}S\alpha_1\bar{\beta}$, and eqn. (10) then gives

$$G_{p\,\text{max.}} = \left(\frac{S}{P}\right)^2. \tag{11}$$

The last equation shows that for very small signals the power amplification has increased by a factor of just under 2·5. Fig. 5·1 shows curves relating the optimum amplification and efficiency for various values of S, all of the form $S = (2n+1)\frac{1}{2}\pi$, so that the phase difference between input and output is either 0° or 180°, and corresponding to the modes of oscillator theory.

The results derived in this section show that we require S to be large and P small for good performance. These requirements, at least in the electrostatic case, are contradictory; the larger we make S the smaller I_0 becomes. Even in the magnetic case, increasing S means increasing the distance over which a large field has to be maintained constant. The designer must therefore use any data which he may have been given, such as a maximum voltage rating, to establish broad limits for his design, and then calculate a series of particular cases to determine the final solution. We should observe that if in a gridded tube each grid absorbs n % of the electrons, the current in the first gap is then $I_0(1-n/100)$ and in the second gap $I_0(1-n/100)^3$. We should therefore repeat the above calculations with different P factors for each gap. It is often good enough to use the geometric mean of the P factors unless n is very large.

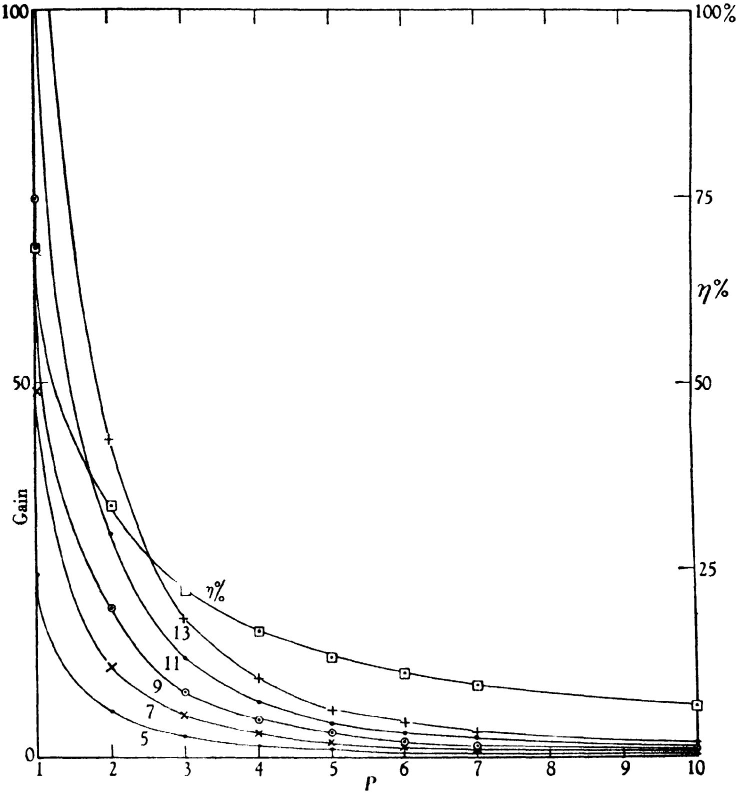

Fig. 5·1. Gain and efficiency against corrected starting current parameter P.

5·2. Webster's debunching theory

In this section we proceed to calculate the debunching field which would result from the electron concentration near the centre of the bunch, assuming that the bunch is a section of a plane parallel sheet of electrons extending to infinity. This is a very big assumption, because although the bunch is certainly infinitely bigger than an electron, the real point is the size of the bunch in relation to the size of the tunnel and the distance between bunches. We should consider the forces set up in a cylinder of electrons in which the centre is at rest and the ends are contracting towards the centre with a velocity equal to the maximum velocity modulation. A simple calculation shows that the length of the cylinder is of the same order as its diameter which makes the case far different from the Webster assumption. We give a derivation of Webster's result in the form due to Saveliev.*

The time co-ordinate of a point s in the drift space for the ith electron is

$$t_i' = t_i + \int_0^s \frac{ds}{u_i},$$

therefore

$$\frac{dt_i'}{dt_i} = 1 + \int_0^s \frac{ds}{u_i^2}\frac{du_i}{dt_i'}\frac{dt_i'}{dt_i}. \tag{12}$$

du_i/dt_i' is the acceleration of the ith electron in the space-charge field. Now the concentration of current is causing a field whose magnitude can be calculated as follows. At s the current is I, so the excess space charge is $\dfrac{I-I_0}{u_i A}$. But $\dfrac{dE}{ds} = -\dfrac{\rho}{\epsilon_0}$, therefore

$$E = -\frac{i_0}{\epsilon_0 A}\int_0^s \frac{I-I_0}{u_i I_0}. \tag{13}$$

Now $du_i/dt_i = eE/m$ and $I/I_0 = dt_i/dt_i'$, whence we obtain

$$\frac{dt_i'}{dt_i} - 1 = \frac{eI_0}{m\epsilon_0 A}\int_0^s \frac{ds'}{u_i^2}\frac{dt_i'}{dt_i}\int_0^s \left(\frac{dt_i}{dt_i'} - 1\right)\frac{ds''}{u_i}. \tag{14}$$

Eqn. (14) is rigorous for the situation studied, and we now approximate by assuming that the modulation is small, and putting $u_i = u_0$. Also as the resonator is near the point of formation of the first bunch dt_i'/dt_i can be taken as constant over the integration. Then

$$\frac{dt_i'}{dt_i} - 1 = \frac{eI_0}{m\epsilon_0 A u_0^3}\int_0^s ds \int_0^s \left(\frac{dt_i'}{dt_i} - 1\right) ds''. \tag{15}$$

Differentiate twice with respect to s and put

$$Y(s) = \frac{dt_i'}{dt_i} - 1 = -\left[\frac{I-I_0}{I}\right] \quad \text{and} \quad h^2 = \frac{eI_0}{m\epsilon_0 A u_0^3} = \frac{3\pi \times 10^4 I_0}{A V_0^{\frac{3}{2}}}.$$

---

* Saveliev, *J. Tech. Phys. U.S.S.R.* 10 (1940), 1365.

Then
$$\frac{d^2Y(s)}{ds^2}+h^2Y(s) = 0, \tag{16}$$

or
$$Y(s) = A\sin hs+B\cos hs. \tag{17}$$

The boundary conditions are $Y(s) = 0$, $s = 0$, and evaluating eqn. (12) at $s = 0$,

$$\frac{dY(s)}{ds} = -\frac{\omega V_1}{2u_0V_0}\cos\omega t \quad (s = 0).$$

Then
$$Y(s) = -\frac{\omega V_1}{2u_{\iota}V_0}\,\frac{\sin hs}{s}\cos\omega t$$

or
$$dt_i' = dt_i-\frac{\omega V_1}{2u_0V_0}\,\frac{\sin hs}{s}\cos\omega t$$

and
$$t_i' = t_i+\frac{s}{V_0}-\frac{sV_1}{2u_0V_0}\,\frac{\sin hs}{hs}\sin\omega t. \tag{18}$$

Comparing this with eqn. 3 (19) we see that the velocity modulation after s m. is reduced by $\dfrac{\sin hs}{hs}$ by the debunching field. Since s appears in the modified form $\dfrac{\sin hs}{h}$, there is an optimum s which is found by evaluating $hs = \frac{1}{2}\pi$, therefore

$$\begin{aligned} s_{\text{opt.}} &= \frac{\pi}{2h} \\ &= 5{\cdot}01\times10^{-3}\frac{A^{\frac{1}{2}}V_0^{\frac{3}{4}}}{I_0^{\frac{1}{2}}}. \end{aligned} \tag{19}$$

For the following figures, taken from a 10 cm. klystron, $I_0 = 0{\cdot}1$ amp., $V_0 = 2000$ V., beam diameter $= 0{\cdot}005$ m., $s_{\text{opt.}} = 0{\cdot}021$ m.

If the Webster debunching analysis is correct, the maximum drift distance is very much shorter than we should have anticipated from any of our foregoing work. The question is difficult to check experimentally with ordinary tubes; for instance, the tube whose parameters were given above agreed very well with the theory given in § 5·1, but as $\dfrac{\sin hs}{hs} = 0{\cdot}65$ in this case, the check is not very reliable, for the effect of the smaller s value could have been masked by a low estimate of the resonator impedance. Experimental evidence does, on the whole, lead to the conclusion that the Webster theory greatly overestimates the debunching effect.

5·3. Other calculations of debunching

Warnecke and his co-authors* have made a calculation of the debunching in a magnetically focused beam, small in comparison to the tunnel diameter, this last assumption being made to ensure that the potential does not vary across the beam. It would have been more realistic to assume that the beam filled the tunnel and the current was kept small enough to fulfil the condition on the potential, which is that the variation in potential across the beam should only be of the order of $(\alpha_1\beta)^2$. The authors deduce an expression for the acceleration of the electron in the drift tube, as a function of the bunching and of an action potential. This action potential is that due to a disk of charge, and to simplify calculations the mean value across the beam is taken to be an exponential function $e^{-1\cdot 18\zeta/a}$, where ζ = distance to centre of bunch, and a = beam radius. The acceleration is then given by

$$\ddot{Z} = Kj\omega u_0 \sum_{n=1}^{\infty} \frac{n}{n^2+p^2/a^2} J_n\left(n\frac{S\alpha\beta}{2}\right) e^{jn(\omega t-S)},$$

where $$K = \frac{2h^2u_0^2}{\omega^2}, \quad A = \frac{\omega a}{u_0}, \quad p = 1\cdot 18.$$

This leads to a transit time

$$\bar{\tau} = \frac{4K}{(\alpha_1\bar{\beta})^2}\int_0^{\frac{1}{2}S\alpha_1\bar{\beta}} dy \int_0^y \sum_1^{\infty} \frac{n}{n^2+p^2/a^2} J_n(nx)\sin(nx\sin\phi - n\phi)\,dx$$

with $x = \frac{1}{2}\alpha_1\bar{\beta}u_0$, $y = \frac{1}{2}\alpha_1\bar{\beta}t$. $\bar{\tau}$ can be expressed as a Fourier sine series, the coefficients being somewhat complicated. Approximate forms are

$$a_1 = \frac{1}{12}\frac{1}{1+p^2/a^2}\left(\frac{S\alpha_1\bar{\beta}}{2}\right)^3 \quad (0 < \tfrac{1}{2}S\alpha_1\bar{\beta} < 1\cdot 4).$$

a_1 remains practically constant at its value for $\frac{1}{2}S\alpha_1\bar{\beta} = 1\cdot 4$, for $1\cdot 4 < \frac{1}{2}S\alpha_1\bar{\beta} < 2$ and then decreases.

a_2 is negligible for $\frac{1}{2}S\alpha_1\bar{\beta} < 1\cdot 2$,

$$a_2 = 0\cdot 7 - 0\cdot 2S\alpha_1\bar{\beta}, \quad \tfrac{1}{2}S\alpha_1\bar{\beta} > 1\cdot 6, \quad p^2/a^2 = 1.$$

---

* Warnecke, *J. Phys. Radium*, 4 (1943), pts. 5 and 6.

The time co-ordinate at S is now given by

$$t_2 = S - \frac{S\alpha_1\bar{\beta}}{2}\sin\omega t + \frac{4K}{(\alpha_1\bar{\beta})^2}(a_1\sin\omega t + a_2\sin 2\omega t + \ldots),$$

and if

Case 1. $\frac{4K\,|\,a_2\,|}{(\alpha_1\bar{\beta})^2}$ is of the same order as the $\frac{S\alpha_1^2\bar{\beta}^2}{4}$ term in the expansion for the time at the catcher.

$$i_2 = I_0\left[1 + 2J_n\left(\frac{nS\alpha_1\bar{\beta}}{2} - \frac{4Ka_1}{(\alpha_1\bar{\beta})^2}\right)\begin{smallmatrix}\sin\\ \cos\end{smallmatrix}\, n(\omega t - S)\right]. \qquad (20)$$

or if

Case 2. $\left(\frac{4K\,|\,a_2\,|}{(\alpha_1\bar{\beta})^2}\right)^{\frac{1}{2}} \leqslant \frac{S\alpha_1^2\beta^2}{2}$. The fundamental amplitude is now given by

$$i_2 = I_0\left[1 + 2J_1(B) + \frac{K}{(\alpha_1\bar{\beta})^2}\sum_{p=2}^{\infty} a_p[J_{p+1}(B) + (-1)^p J_{p-1}(B)]\right],$$

where $$B = \frac{S\alpha_1\bar{\beta}}{2} - \frac{4Ka_1}{(\alpha_1\bar{\beta})^2}.$$

These rather complicated results lead to some rather simple general conclusions. In case 1, as in the Webster approximation, we find that the conversion efficiency can be maintained at its maximum value. The debunching merely means that the effective value of S is less than its geometric value. In the second case, since a_2 is negative, the conversion efficiency is decreased somewhat, but the bunch still occurs at the phase $(\omega t - S)$.

In some discussion, the authors point out that their results reduce to those of Webster in the case of an infinitely wide beam, and when $\frac{\sin hs}{hs}$ can be put equal to $1 - \frac{1}{6}(hs)^2$. In the author's development, if we put $p/a = 1$, which is of the correct order for practical cases, s is only reduced to $s(1 - \frac{1}{12}(hs)^2)$, and, moreover, this is an overestimate, because Warnecke especially states that he has used an overestimate for the average value of the action function. Although at first glance it appears likely that space-charge debunching should be a big effect, a little more consideration shows that though the forces tending to disintegrate a single bunch are fairly large, yet a beam containing a number of bunches would exhibit much smaller effects, because of the rebunching action of one bunch on another. Furthermore, it is clear that the magnetically focused case, in which radial motion can play no part in reducing the space-charge forces, is worse than the electrostatic case. A similar calculation has been made by Borgnis and Ledinegg.*

Strachey of S.T.C. has also considered the finite beam using the assumption that a magnetic field is used to prevent radial motion, and that the current density in the beam varies as $\rho_0+\rho\cos kz$, which limits the range of α_1, for which his results are valid. However, the form of the results should be unchanged. Strachey's work is especially valuable because it includes the effects of the walls of the tunnel. In all cases it is found that the Webster debunching expression has to be multiplied by a correction factor which is small unless the beam diameter is large in comparison with S_0, the distance travelled by an unmodulated electron per cycle of the h.f. oscillation.

In view of these results we shall omit any explicit consideration of debunching forces in our later work, but noting that certain designs may have to be checked from this point of view.

5·4. Multiresonator klystron amplifiers

We next consider tubes which have one or more extra resonators interposed between buncher and catcher and coupled to the same beam. It is found that if the extra resonators are tuned, but not loaded, a very large increase in gain results. Clearly this system is very much the same as using two or more tubes in cascade, except that one unloaded resonator performs the functions of the catcher for the first tube and buncher for the second. However, particularly at large drive powers, there are differences due to the fact that the intermediate bunchers are working on a current which is already bunched. We confine ourselves here to a small signal theory, and take the three-resonator tube as an explicit example. Consider the system drawn in fig. 5·2. The velocity at exit from the first gap is

$$u_1 = u_0\left(1+\frac{\beta V_1}{2V_0}\sin\omega t_1\right). \tag{21}$$

The velocity at exit from the second gap, using the same assumptions, is

$$u_2 = u_0\left(1+\frac{\beta V_1}{2V_0}\sin\omega t_1+\frac{\beta V_2}{2V_0}\sin(\omega t_2-\delta_2)\right). \tag{22}$$

---

* Borgnis and Ledinegg, *Ann. Phys., Lpz.*, 43 (1943), 296.

The time of arrival at the centre of the second gap is

$$t_2 = t_1 + \frac{s_1}{u_0(1+\bar{\beta}V_1/2V_0 \sin \omega t_1)}$$

$$\doteqdot t_1 + \frac{s_1}{u_0} - \frac{s_1\bar{\beta}V_1}{2u_0V_0}\sin \omega t_1;$$

similarly,

$$t_3 = t_2 + \frac{s_2}{u_0} - \frac{s_2\bar{\beta}V_1}{2u_0V_0}\sin \omega t_1$$

$$= t_1 + \frac{s_1+s_2}{u_0}\left(1-\frac{\bar{\beta}V_1}{2V_0}\sin \omega t_1\right) - \frac{s_2\bar{\beta}V_2}{2u_0V_0}\sin(\omega t_2 - \delta_2). \qquad (23)$$

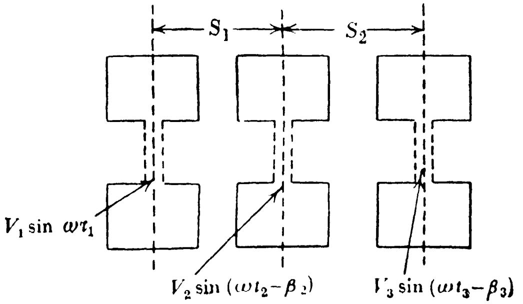
S_1
S_2
$V_1 \sin \omega\tau_1$
$V_2 \sin(\omega t_2 - \beta_2)$
$V_3 \sin(\omega t_3 - \beta_3)$

Fig. 5·2. Notation for three-resonator klystron amplifier.

Now if V_1/V_0 is small we can write

$$\sin(\omega t_2 - \delta_2) = \sin(\omega t_1 + S_1 - \delta_2)$$

without much error. Then

$$\omega t_3 = \omega t_1 + S_1 + S_2 - a\sin(\omega t_1 + \gamma),$$

where
$$a^2 = \left\{\left[(S_1+S_2)\frac{\alpha_1\bar{\beta}}{2}\right]^2 + \left(\frac{S_2\alpha_2\bar{\beta}}{2}\right)^2 + (S_1+S_2)\left(\frac{S_2\alpha_1\alpha_2\bar{\beta}^2}{2}\right)\cos(S_1-\delta_2)\right\}, \qquad (24)$$

$$\tan\gamma = \frac{S_2\alpha_2\bar{\beta}\sin(S_1-\delta_2)}{(S_1+S_2)\tfrac{1}{2}\alpha_1\bar{\beta} + \tfrac{1}{2}S_2\alpha_2\bar{\beta}\cos(S_1-\delta_2)}. \qquad (25)$$

Since the second resonator is running without any coupling except that due to the beam, the phase will adjust itself so as to extract the maximum amount of power from the beam if it is tuned to the frequency of the driver. But from the results of Chapter 3 we can see that this gives $\cos(S_1-\delta_2)=0$ which reduces a below its maximum value. If the second resonator is slightly detuned, however, the phase of V_2 will change much more rapidly than the amplitude. There will then be a certain value of the detuning which will maximize a. This value can easily be determined by a numerical calculation, or analytically if we make the assumption that the resonator parallel impedance remains constant. Since the phase will have changed by $\pm\frac{1}{2}\pi$ at the points for which $G=|B|$, we shall be working within the range used for measuring Q and the assumption is justified.

From eqn. (4) of this chapter we see that α_2 is given by

$$J_1\left(\frac{S_1\alpha_1\bar{\beta}}{2}\right)\sin(S-\delta_2)=(\alpha_2\bar{\beta})\frac{P}{8}$$

or

$$\alpha_2\bar{\beta}=\frac{8}{P}J_1\left(\frac{S_1\alpha_1\bar{\beta}}{2}\right)\sin(S_1-\delta_2)$$

$$=2\frac{S_1\alpha_1\bar{\beta}}{P}\sin(S_1-\delta_2)\quad\text{for }\alpha_1\ll 1. \tag{26}$$

The last term of a is then maximized by the condition that $\sin(S_1-\delta_2)\cos(S_1-\delta_2)$ is a maximum, or that $S_1-\delta_2=\frac{1}{4}\pi$. If this is done, from eqns. (25) and (26),

$$a^2=\left\{\left[\left(\frac{S_1+S_2}{2}\right)\alpha_1\bar{\beta}\right]^2+\frac{1}{2}\left(\frac{S_1S_2\alpha_1\bar{\beta}}{P}\right)^2+\frac{(S_1+S_2)\,S_1S_2(\alpha_1\bar{\beta})^2}{2P}\right\}.$$

The maximization of a leads to a transcendental equation, but the above cannot be very different from the desired result. The output power is

$$W_0=I_0V_0[\alpha_3\bar{\beta}J_1(a)-(\alpha_3\bar{\beta})^2P/8]$$

$$=I_0V_0\frac{2J_1^2(a)}{P},$$

if the load coupling is correctly adjusted, the power amplification then becoming

$$G_p=\frac{16J_1^2(a)}{P^2(\alpha_1\bar{\beta})^2}. \tag{27}$$

This relation does not admit of a simple expression for the overall gain, but we can evaluate the approximate value of the maximum amplification for small signals. In this case

$$G_{p\,\max.} = \frac{4a^2}{P^2(\alpha_1\bar{\beta})^2}$$

$$= \frac{4}{P^2}\left[\left(\frac{S_1+S_2}{2}\right)^2 + \frac{1}{2}\left(\frac{S_1S_2}{P}\right)^2 + \frac{1}{2}\left(\frac{S_1S_2}{P}\right)(S_1+S_2)\right]. \quad (28)$$

The amplification of a two-resonator klystron of the same length is, to the same order,

$$G_{p\,\max.} = \frac{4}{P^2}\left[\left(\frac{S_1+S_2}{2}\right)^2\right]. \quad (29)$$

This makes the large increase in gain very obvious. At this point we should mention that since P varies approximately as $1/\bar{\beta}^2$ the amplification varies at least as $\bar{\beta}^4$ and can vary as $\bar{\beta}^8$ if S_1S_2/P is the predominating term. It is therefore much more important to use a high β factor in an amplifier than it is in an oscillator. Since the uncertainties in β calculation are rather large, especially for gridless tubes, it is difficult to obtain good agreement between theoretical amplification factors and measured ones. However, the theory developed above does give a reasonable agreement with practice, and in spite of the approximations in the derivation gives better results than the theories given by Feenberg (Sperry) and Tomlin (S.T.C.).

Feenberg has calculated the gain for n resonators and has also paid considerable attention to the large signal case and to cases in which the middle resonator is running on a harmonic. This work is of very considerable interest because of its bearing on the problem of saw-tooth bunching, but we have no space to discuss it further.

The multiresonator amplifier will be of great value in the development of stable frequency microwave communication systems, because power amplifications of the order of several thousand can be realized in a single tube. This leads directly to the possibility of using lightly loaded high Q cavities in bridge stabilizing circuits. It is also possible to use frequency modulation with a stabilized mean frequency in a straightforward way, with a reflex klystron as frequency modulator, if high-gain amplifiers are available.

5·5. Signal-to-noise ratio in klystron amplifiers

We conclude our work on amplifiers with a brief discussion of signal-to-noise ratio. We can make some calculations on the theoretical signal-to-noise ratio of klystron amplifiers, but the calculation does not agree with experiment, the noise being much greater than theory predicts. The matter is discussed in more detail in Chapter 8 where we deal with V.M. mixers.

If the amplifier is to be useful, it must have a reasonable power gain so that the noise generated in the next stage is unimportant, as well as a reasonable signal-to-noise ratio. We have already calculated the power gain under various conditions, so we can proceed to enumerate the various sources of noise. These are given below:

(1) Thermal noise of the loaded first resonator.

(2) Thermal noise of the loaded output resonator.

(3) Shot noise in the beam which induces a voltage across the first resonator which is then amplified.

(4) Shot noise in the beam induces a voltage across the output resonator.

Additional resonators introduce additional components of resonator noise and amplified shot noise. Division noise also makes a contribution, but in a carefully designed tube without grids, the current interception can be kept down to a few per cent of the total.

Following Herold* we assume that the aerial of radiation resistance R_a is coupled by means of a lossless line and transformer to the input resonator. The voltage step-up of the transformer is μ and the aerial temperature is T_a. The output resonator is loaded for maximum power output, and the succeeding stage has a noise resistance referred to the input side equal to R_n ohms. The space-charge smoothing factor is F^2. The load resistance giving optimum power output is, from eqns. (4) and (5),

$$R_L = \frac{8J_1^2(\frac{1}{2}S\alpha_1\bar{\beta})}{P^2\bar{\beta}^2}\frac{V_0}{I_0}$$

$$= \frac{\alpha_1^2 G_p V_0}{2I_0},$$

---

* Herold, *Proc. Inst. Radio Engrs, N.Y.*, 31 (1943), 501.

using eqn. (10). The noise resistance of the output resonator is then

$$R_n' = R_n + \frac{R_L Z_0}{R_L + Z_0} = R_n + Z_L.$$

The mean-square noise voltage across the output resonator becomes

$$\bar{e}_2^2 = 4kTR_n'\Delta f + 2eI_0\bar{\beta}^2 Z_L'^2 F^2 \Delta f,$$

where $Z_L' = Z_L$ in parallel with the beam-loading resistance. This quantity is equivalent to a noise voltage of $\bar{e}_2^2/G_p$ in the input resonator, or an equivalent noise resistance $R_{\text{eq.}} = \dfrac{\bar{e}_2^2}{G_p 4kT\Delta f}$. These conditions lead to the noise-equivalent circuit for the input resonator shown in fig. 5·3. If we now put $g_a = 1/\mu^2 R_a$, $g_1 = 1/Z_1$, $g_b = 1/R_0$, where R_0 = beam-loading resistance, the total square noise current is

$$\bar{i}_{nL}^2 = 4kT_a g_a \Delta f + 4kTg_1\Delta f + 2eI_0\bar{\beta}^2F^2\Delta f + 4kTR_{\text{eq.}}(g_a + g_1 + g_b)^2\Delta f,$$

therefore

$$\left(\frac{S}{N}\right)^2 = \frac{e_a^2}{4kTR_a\Delta f}\,\frac{1}{\dfrac{T_a}{T} + \dfrac{g_1}{g_a} + \dfrac{2e}{4kT}\left(\dfrac{I_0\bar{\beta}^2F^2}{g_a}\right) + \dfrac{R_{\text{eq.}}}{g_a}(g_a + g_1 + g_b)}. \qquad (30)$$

But $\dfrac{e_a^2}{4kTR_a\Delta f}$ is the $\left(\dfrac{S}{N}\right)^2$ of the aerial alone if it is at room temperature. We therefore write

$$\left(\frac{S}{N}\right)^2_{\text{receiver}} = \left(\frac{S}{N}\right)^2_{\text{aerial}} \times \frac{1}{\text{N.F.}}, \qquad (31)$$

where N.F. = noise factor of the receiver. When N.F. is minimized with respect to g_a we get

$$\text{N.F.}_{\text{min.}} = \frac{T_a}{T} + \frac{2R_{\text{eq.}}}{Z_1'} + 2\left\{\left(\frac{R_{\text{eq.}}}{Z'}\right)^2 + g_1R_{\text{eq.}} + 20I_0\bar{\beta}^2F^2R_{\text{eq.}}\right\}^{\frac{1}{2}}, \qquad (32)$$

where we have put $Z_1' = 1/g_1 + g_b$ and $2e/4kT = 20\,\text{V.}^{-1}$. When the aerial is matched to the resonator $Z_1' = 1/g_a$ and

$$\text{N.F. matched} = 1 + \frac{T_a}{T_1} + \frac{4R_{\text{eq.}}}{Z_1'} + (20\bar{\beta}I_0F^2 - g_b)Z_1'. \qquad (33)$$

These expressions are not very suitable for the determination of optimum conditions. If G_p is large enough for us to neglect $R_{\text{eq.}}$ and g_b is also assumed to be very small,

$$\text{N.F. matched} = 1 + \frac{T_a}{T} + 1{\cdot}6 I_0 Z_1', \tag{34}$$

when we put in reasonable values for $\bar{\beta}^2$ and F^2 and it is obvious that I_0 must be kept very small if N.F. is to be at all reasonable; but this means that P is made small and therefore the tube must be long if G_p is to be large. This forces one to the conclusion that a very long tube with magnetic focusing would be necessary. Such a tube would hardly be a technical possibility.

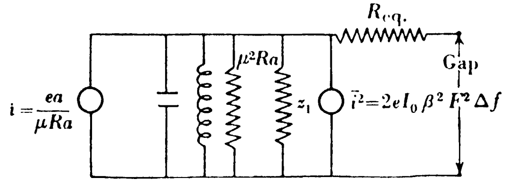

Fig. 5·3. Equivalent circuit for calculation of noise input.

In the case of the three-resonator amplifier, an extra contribution is made to $R_{\text{eq.}}$, but the gain can certainly be made so high that the middle resonator is the only important noise source beyond the input grid. The analysis can easily be applied to this case, and the conclusions are much the same. We have made no practical tests of the theory given above, but if mixer experience is anything to go by, the noise factor will be underestimated. Herold assumes that $F^2 = 1$, instead of $F^2 \doteqdot 0{\cdot}1$ as one would expect in a space-charge limited beam, apparently because of division noise due to current taken by the focusing electrodes and grids. However, the extra noise appears to exist in tubes without grids and with vanishingly small division noise, so this has merely the status of an *ad hoc* assumption.

We therefore conclude that the klystron does not show much promise as a signal-level amplifier, but that the best line of approach would be a three-resonator tube with a high-voltage gain between first and second resonators, using the minimum beam current consistent with a reasonable overall gain.

5·6. Klystron frequency multipliers

The expression for the alternating current at the catcher gap, which was derived in Chapter 3, shows that, neglecting debunching, the current wave contains all the harmonics of the input frequency with amplitudes proportional to $J_n(\frac{1}{2}nS\alpha\beta)$. It is very easy to extend the results of the first section of this chapter to cover the frequency multiplier. We consider an input resonator excited at an angular frequency ω_1 and an output resonator whose fundamental resonance is $n\omega_1$. We shall take the case of a klystron tripler as an example. The P values of the buncher and catcher are

$$P_1 = \frac{4V_0}{I_0 Z_1 \bar{\beta}_1^2} + \frac{2\bar{\gamma}_1}{\bar{\beta}_1}, \tag{35}$$

$$P_2 = \frac{4V_0}{I_0 Z_2 \bar{\beta}_2^2} + \frac{2\bar{\gamma}_2}{\bar{\beta}_2}. \tag{36}$$

Then the input power to obtain a depth of modulation α_1 is $\frac{1}{8}I_0 V_0 P_1(\alpha\bar{\beta}_1)^2$ as usual. The power output

$$W_0 = I_0 V_0\left[\alpha_2\bar{\beta}_2 J_3\left(\frac{3S_1\alpha_1\bar{\beta}_1}{2}\right) - (\alpha_2\bar{\beta}_2)^2\frac{P_2}{8}\right].$$

Minimizing W_0 with respect to α_1 and α_2 yields

$$J_3'\left(\frac{3S_1\alpha_1\bar{\beta}_1}{2}\right) = 0$$

or

$$\frac{S_1\alpha_1\bar{\beta}_1}{2} = 0{\cdot}467$$

and

$$\alpha_2\bar{\beta}_2 = \frac{4J_3\left(\frac{3S_1\alpha_1\bar{\beta}_1}{2}\right)}{P_2},$$

therefore

$$W_0 \text{ matched} = \frac{I_0 V_0 2J_3^2\left(\frac{3S_1\alpha_1\bar{\beta}_1}{2}\right)}{P_2},$$

and

$$W_{0\,\text{max.}} = \frac{0{\cdot}377 I_0 V_0}{P_2},$$

$$\eta_{0\,\text{max.}} = \frac{0{\cdot}377}{P_2}.$$

The power amplification at maximum output is

$$G'_p = \frac{3{\cdot}46 S_1^2}{P_1 \times P_2}$$

and
$$G_p = \frac{16}{P_1 P_2} \frac{J_3^2\left(\frac{3S_1\alpha_1\beta_1}{2}\right)}{(\alpha_1\beta_1)^2}.$$

the output efficiency is about 60% of that of an amplifier with $P_1 = P_2$. If we write $S_2 = s\omega_2/u_0 = 3S_1$, G_p becomes

$$G'_p = \frac{0{\cdot}384 S_2^2}{P_1 P_2},$$

which is very slightly less than an amplifier of the same length, working at ω_2. These predictions, unfortunately, do not agree very well with practice, because the debunching, which we have neglected so far, introduces a much greater percentage diminution of the harmonics than it does of the fundamental. Using Warnecke's debunching theory the fundamental amplitude is reduced to $J_1(a-b)/J_1(a)$ of its original value, while the third harmonic is reduced to $J_3(a-b)/J_3(a)$, and for small arguments these functions are $(1-b/a)$ and $(1-b/a)^3$, which illustrates the point rather forcibly. However, though the power output and the efficiency are low, the klystron frequency multiplier is a workable device, even when the multiplication is large. For instance, the Sperry Company has made tubes giving an elevenfold frequency multiplication. Tubes of this type are of interest in stable-frequency systems where the stability is obtained by using a crystal-controlled oscillator at a frequency of a few megacycles. Conventional multiplying circuits are used to bring the frequency up to a few hundred megacycles, and the klystron then multiplies into the decimetre band in a single stage, thereby eliminating a large number of rather complicated stages in a region which is not well covered either by conventional valves or by V.M. tubes.

Chapter 6

KLYSTRON OSCILLATORS

In Chapter 3 we have calculated the output efficiency of a klystron oscillator as a function of the ratio of starting current to running current, but making no allowance for power loss to the beam. In the present chapter we refine these calculations, but we first consider some of the circuit details.

6·1. Equivalent circuit of a klystron oscillator*

The equivalent circuit of a loop-coupled klystron is shown in fig. 6·1, where the load is lumped into R and C. The loop equations are

$$Z_1 I_1 - j\omega M_1 I_3 = 0, \tag{1}$$

$$Z_3 I_3 - j\omega M_1 I_1 - j\omega M_2 I_2 = 0, \tag{2}$$

$$Z_2 I_2 - j\omega M_2 I_3 = \frac{i_2'}{j\omega C_2} = e. \tag{3}$$

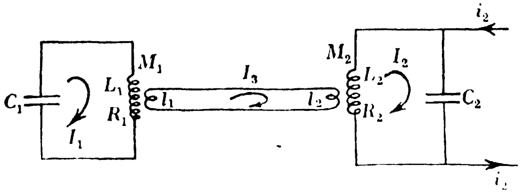

Fig. 6·1. Equivalent circuit of two coupled resonators. Coupling by mutual inductance.

We first determine the possible resonant frequencies of the system. These are determined by the condition that $Z_2' = e/I_2$ should be real. Eliminating I_3 between eqns. (1) and (2) we have

$$I_1 = \frac{-\omega^2 M_1 M_2}{Z_1 Z_3 + \omega^2 M_1^2} I_2. \tag{4}$$

Then from eqns. (1), (3) and (4)

$$Z_2' = \frac{Z_1 Z_2 Z_3 + \omega^2 M_1^2 Z_2 + \omega^2 M_2^2 Z_1}{Z_1 Z_3 + \omega^2 M_1^2}. \tag{5}$$

---

* Webster, *J. Appl. Phys.* 10 (1939), 864.

This is too complicated to evaluate in general. We therefore put

$$M_1 = M_2 = M, \quad K = M^2/2Ll,$$

$$L_1 = L_2 = L, \quad \omega_1 = \frac{1}{(L_1C_1)^{\frac{1}{2}}} = \omega_0(1+\tfrac{1}{2}a),$$

$$l_1 = l_2 = l, \quad \omega_2 = \frac{1}{(L_2C_2)^{\frac{1}{2}}} = \omega_0(1-\tfrac{1}{2}a),$$

and we also neglect the circuit losses, that is, we put $R_1 = R_2 = 0$. This is clearly not correct for R_2, but we desire to obtain a general picture. Eqn. (5) then yields

$$(1-2K)\,\omega^4 - 2(1+\tfrac{1}{4}a^2)\,(1-K)\,\omega^2\omega_0^2 + \omega_0^4(1-\tfrac{1}{4}a^2)^2 = 0.$$

Neglecting terms of the order of K^2, a^2 and less we obtain

$$\omega^2 = \omega_0^2\{1+K \pm (K^2+a^2)^{\frac{1}{2}}\} \tag{6}$$

or

$$\frac{\omega_1'^2 \sim \omega_2'^2}{\omega_0^2} = 2(K^2+a^2)^{\frac{1}{2}}. \tag{7}$$

Eqn. (7) shows that the coupled resonances are $2K\omega_0$ megacycles apart when $(L_1C_1)^{\frac{1}{2}} = (L_2C_2)^{\frac{1}{2}}$, and any alteration of C_1 or C_2 will increase this frequency separation.

We next wish to deduce the ratio $V_1/V_2 = \alpha_1/\alpha_2$. Now $V_1 = I_1/j\omega C_1$, and since $I_2 \gg i_2'$, $V_2 = I_2/j\omega C_2$, so we have from eqn. (4)

$$\frac{V_2}{V_1} = -\frac{C_1}{C_2}\,\frac{Z_1Z_3+\omega^2M^2}{\omega^2M^2}$$

$$= -\frac{C_1}{C_2}\left[1+\frac{\left(\dfrac{\omega_1^2-1}{\omega^2}\right)+\dfrac{j}{Q_1}}{K}\right]. \tag{8}$$

As Q_1 tends to infinity when our assumptions are made, eqn. (8) shows that V_1 and V_2 are either in phase or 180° out of phase. If the line connecting l_1 and l_2 has substantial electrical length, some phase change will result, but we are most interested in short loops. Substituting for ω we obtain

$$\frac{V_2}{V_1} = -\frac{C_1}{C_2}\left[1+\frac{\dfrac{\omega_0^2}{\omega^2}\left(1+\dfrac{a}{2}\right)^2-1}{K}\right]$$

$$= -\frac{C_1}{C_2}\left[1+\frac{(1+\frac{1}{2}a)^2\{1-K\mp(K^2+a^2)^{\frac{1}{2}}\}-1}{K}\right] \quad \text{using (6)}$$

$$= -\frac{C_1}{C_2}\left[-\frac{a}{K}\pm\left\{1+\left(\frac{a}{K}\right)^2\right\}^{\frac{1}{2}}\right]. \tag{9}$$

When $a = 0$, $|V_1/V_2| = C_2/C_1$, so to obtain a desired value of $|V_1/V_2|$ some detuning will in general be necessary. It can also be seen that the oscillations on one set of modes will be at ω_1' and on the other set at ω_2'. If we call the higher frequency $(\omega_0^2[1+K+(K^2+a^2)^{\frac{1}{2}}])$ we see from eqn. (9) that the voltages are in phase, while at the lower frequency they are out of phase. Modes 3, 7, 11, etc., therefore appear at a higher frequency than modes 5, 9, etc.

Owing to the assumption of small losses, these results should not be taken as more than an indication of the behaviour to be expected in a real tube. The main difference is that eqn. (9) would lead one to believe that the voltage condition can be satisfied for any K, however small, by correct tuning. In fact, if one varies the coupling, retuning to get the best efficiency for each K, one finds that the efficiency increases quite rapidly at first and then goes through a rather flat maximum. The coupling should therefore be made tight enough to obtain full efficiency but not too large, as this may restrict the overall tuning range of the tube. That the assumption of small losses is in error may be seen from the fact that a particular 30 W. output klystron had a power amplification of 6 used as an amplifier at the same output level. 6 W. were therefore fed back when it was used as an oscillator.

Loop coupling is objectionable for several reasons. First, it is difficult to manufacture the loops and insert them so that the results are repeatable. Secondly, there is an upper limit to the size of loop which may be employed because of self-resonance in the loop. Coupling by means of a circumferential slot overcomes both these difficulties. The coupling is a function of the angular length of the slot and not of the width. The equivalent circuit is shown in fig. 6·2, where L is a large inductance. If the slot is too narrow some capacitance is connected as shown by the dotted capacitator, but if the slot is fairly wide this can be neglected. An analysis similar to that given for the loop case shows that one resonant frequency is independent of the degree of coupling, but the other is displaced from it by an amount depending on the coupling coefficient. This behaviour is observed in practice.

To summarize this section, we observe that the two-resonator klystron will oscillate on two sets of modes at different frequencies. This may be inferred from the fact that there are two coupled meshes. If the loop is short and the losses low, the resonators must oscillate either in phase or in antiphase, but in either case a fixed value of d.c. voltage can be chosen for best efficiency on a particular mode. If the loops are coupled by a long line, the phase relationships will be different, but again some choice of d.c. voltage will give an optimum efficiency. The required ratio between α_1 and α_2 can in all cases be obtained by adjusting the value of the coupling and the tuning of one resonator with respect to the other. Losses will, in general, introduce phase shift even when the coupling device is electrically short, which means that a real klystron will not oscillate best at the voltage corresponding to exact inphase or antiphase conditions, and the departure from the ideal conditions will be greater for high-power oscillators than for low-power.

A somewhat different approach is given in a paper by Bernier, Guènard and Lortie.*

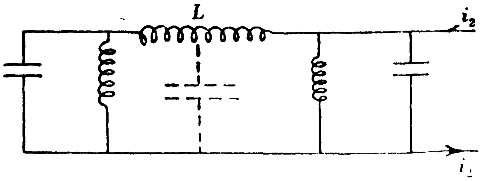

Fig. 6·2. Equivalent circuit of slot coupling.

6·2. The conversion efficiency

From the results of Chapter 3 we can calculate an expression for the conversion efficiency, of the form

$$\eta_{\text{conv.}} = \alpha_2\bar{\beta}_2 J_1\left(\frac{S\alpha_1\bar{\beta}_1}{2}\right)\cos(S-\gamma) - \tfrac{1}{4}\alpha_2^2\overline{\beta_2\gamma_2}, \tag{10}$$

or writing it in full for a gridded klystron, optimizing the phase factor

$$\eta_{\text{conv.}} = \alpha_2\frac{\sin\frac{1}{2}\phi}{\frac{1}{2}\phi}J_1\left(\frac{S\alpha_1\bar{\beta}_1}{2}\right) - \tfrac{1}{4}\alpha_2^2\frac{\sin\frac{1}{2}\phi}{\frac{1}{2}\phi}\left(\frac{\sin\frac{1}{2}\phi}{\frac{1}{2}\phi} - \cos\tfrac{1}{2}\phi\right), \tag{11}$$

where ϕ is the transit angle of the second gap. This comes from using the Webster approximation for the bunching and the second-order approximation for the power lost in bunching. We must now inquire into the validity of this expression, particularly for large α_1. By an extension of the methods used in § 3·6, Strachey, Petrie and

---

* Bernier, Guénard and Lortie, *Bull. Soc. fr. élect.* (Feb. 1944).

Wallis calculated that the 'starting current efficiency', i.e. the efficiency as $\frac{1}{2}S\alpha_1\bar{\beta}_1 \to 0$, is given to terms in α_1^2 by

$$\eta_{\text{conv.}} = -\tfrac{1}{4}\alpha_1^2\overline{\beta_1\gamma_1} + \tfrac{1}{4}\overline{\beta_1\beta_2}S\cos(S-\gamma) + \tfrac{1}{4}(\overline{\beta_1\gamma_2}+\overline{\beta_2\gamma_1})\sin(S-\gamma) - \tfrac{1}{4}\alpha_2^2\overline{\beta_2\gamma_2}. \quad (12)$$

Varying the phase for a maximum we obtain

$$S-\gamma = \tfrac{1}{2}\pi - \lambda, \quad \text{where} \quad \lambda = \tan^{-1}\frac{\overline{\beta_1\beta_2}S}{\overline{\beta_1\gamma_2}+\overline{\beta_2\gamma_1}}.$$

Clearly, the results are no different from those earlier obtained if

$$\overline{\beta_1\gamma_2}+\overline{\beta_2\gamma_1} \to 0.$$

Warnecke* calculated the change of velocity of an electron proceeding through both gaps and found the change of kinetic energy retaining terms in α_2^2 but not in α_1^2. This yields

$$\eta_{\text{conv.}} = \alpha_2\bar{\beta}_2 J_1\left(\frac{S\alpha_1\bar{\beta}_1}{2}\right)\sin(S-\psi) - \tfrac{1}{4}\alpha_2^2\overline{\beta_2\gamma_2} + \tfrac{1}{4}\alpha_2^2 J_2(S\alpha_1\bar{\beta}_1)\frac{\phi-\sin\phi}{\phi^2}\sin 2(S+\psi), \quad (13)$$

where $\alpha_2 = (V_2/V_0)\sin(\omega t+\psi)$ so as to agree with the conventions which we calculated as the second-order approximation for a single gap. Let us examine the third term; dividing it by the first, we have

$$\frac{\alpha_2 J_2(S\alpha_1\bar{\beta}_1)}{4\bar{\beta}_2 J_1(\frac{1}{2}S\alpha_1\bar{\beta}_1)}\,\frac{\phi-\sin\phi}{\phi^2} \doteqdot \frac{\alpha_2\phi J_2(S\alpha_1\bar{\beta}_1)}{24\bar{\beta}_2 J_1(\frac{1}{2}S\alpha_1\bar{\beta}_1)}, \quad \phi < \tfrac{1}{2}\pi.$$

If $\frac{1}{2}S\alpha_1\bar{\beta}_1$ is near 1·8 so that J_1 is near the maximum, J_2 is near its negative maximum of $-0{\cdot}30$. At $\phi = \frac{1}{2}\pi$ this makes the third term about $4\alpha_2$ % of the first. The maximum obtained by varying the phase will not shift markedly from $S+\psi = \frac{1}{2}\pi$ if $0{\cdot}08\alpha_2 < 0{\cdot}15$, because the maximum condition to be obeyed is that

$$\cos(S+\psi) - 0{\cdot}08\alpha_2\cos 2(S+\psi) = 0.$$

$S+\psi$ is then $> \frac{1}{2}\pi$, $\sin 2(S+\psi)$ is negative and the third term represents a small gain in efficiency. For instance if $\alpha_2 = 1{\cdot}5$ the phase correction is about 6·5° and the maximum efficiency is about ½ % greater than the value of the first term. This represents the worst case, because we have used an approximation for

---

* Warnecke, *Ann. Radiodiffusion*, 4 (1944), 1.

$(\phi-\sin\phi)/\phi^2$ which overestimates the value, and a very large α_2. For values of $\frac{1}{2}S\alpha\bar{\beta}_1$ which cause $J_2(S\alpha_1\bar{\beta}_1)$ to be near its first maximum α_2 is certain to be very small, and this case needs no further examination. We therefore conclude that the numerical value of eqn. (13) does not differ materially from the value of eqn. (11), but that a small phase change is introduced.

We have a further check on this conclusion in that many studies of the conversion efficiency have been made by using a differential analyser and by graphical means. The S.T.C. workers using the Manchester differential analyser came to the same conclusion as we have done, and by using the published results of Warnecke and Bernier,* obtained by graphical means, we can demonstrate that eqn. (11) agrees very well with this method. Fig. 6·3 shows eqn. (11) plotted for $\frac{1}{2}S\alpha_1\bar{\beta}_1 = 1{\cdot}84$ and $\alpha_2 = 1$, with ϕ as variable (curve *a*), and also the curve for $\alpha_2\bar{\beta}_2 = 1$, which is a somewhat fairer comparison. The crosses are Warnecke's points. The agreement is to better than 10 % in the worst case, which is excellent considering the inevitable errors of the graphical method and the large values of α_2. This comparison, taken with the theory of Chapter 3, shows

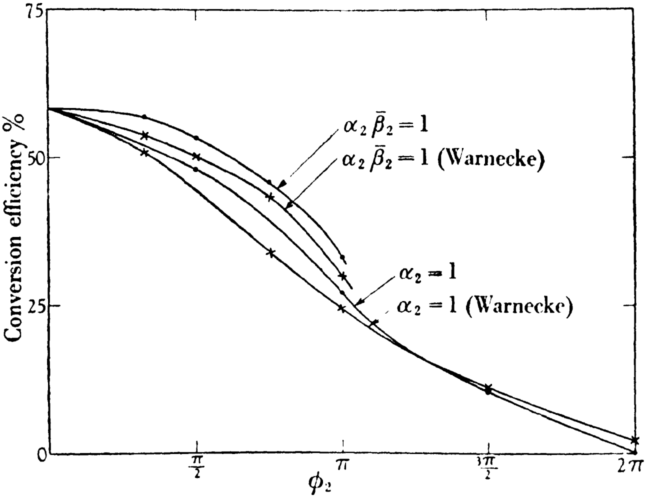

Fig. 6·3. Curves showing Warnecke's graphical values for conversion efficiency and those given by the theory of this chapter.

---

* Warnecke and Bernier, *Rev. Gén. Élect.* 101 (1942), 117.

that in place of $\frac{1}{4}\alpha_2^2\beta\gamma$ we should have $\frac{1}{4}\alpha_2^2(\overline{\beta\gamma}+f(\alpha_2))$, where $f(\alpha_2)$ is almost independent of ϕ for the range studied. Warnecke and Bernier give a curve of the power lost in bunching for $\alpha_2 = 1$ which agrees well with our results between $\frac{1}{2}\pi < \phi < \pi$ and is greater than our results for $\phi < \frac{1}{2}\pi$. However, the graphical method is highly inaccurate for small interchanges of energy because it involves the subtraction of two nearly equal areas in this case.

We should note, however, that Warnecke's graphical analysis does not give any further check of the validity of the $J_1(\frac{1}{2}S\alpha_1\bar{\beta}_1)$ term for the bunching efficiency than we have already gained in discussing the second approximation to this term, because S was considered to be large and α_1 very small in his work. This was not the case in the differential analyser studies in which $\alpha_1 = 0{\cdot}3$ and $0{\cdot}6$.

We shall therefore use eqns. (10) or (11) as expressions for the conversion efficiency, knowing that the errors involved by this assumption are only of the same order of magnitude as the experimental uncertainties in the determination of circuit constants.

6·3. Maximum amplitude conditions

If the field in the catcher is very thin, so that $\bar{\beta}_2$ is large, electrons are reflected when

$$\alpha_1\bar{\beta}_1+\alpha_2\bar{\beta}_2 = 1, \tag{14}$$

because the slowest electron has a velocity of $1-\alpha_1\bar{\beta}_1$. In more practical cases this condition has to be modified. There are three conditions to be studied: transmission of all electrons, the condition in which some electrons are brought to rest and start backwards but eventually penetrate through the gap, and lastly the condition in which some electrons are reflected. Warnecke and Bernier* also studied this question graphically. Their result is shown in fig. 6·4, where κ is the maximum value that can be given to $\alpha_1\bar{\beta}_1+\alpha_2$ plotted as a function of ϕ. We note that α_2 appears instead of $\alpha_2\bar{\beta}_2$, because the equation of motion was solved graphically and not by the approximation methods leading to small changes in velocity. For $\phi_2 > \frac{1}{2}\pi$ the condition for complete transmission is that

$$\alpha_2\bar{\beta}_1+\alpha_2 < \phi_2. \tag{15}$$

The paper referred to above also shows that when $\frac{1}{2}S\alpha_1\bar{\beta}_1 \ll 1$ the efficiency starts to fall sharply directly some of the electrons

---

[*] Warnecke and Bernier, *Rev. Gén. Élect.* 101 (1942), 117.

perform convoluted paths. In the more practical case in which the electrons arriving at the catcher have a considerable spread in the velocity, it seems more probable that the efficiency will continue to rise after α_2 has reached the limit given by the applicable condition. This is because in the case of the small signal theory no electrons at all can get through the catcher gap during the time in which the voltage is above the limit, while in an actual high-power oscillator only the electrons with less than the required amount of energy are

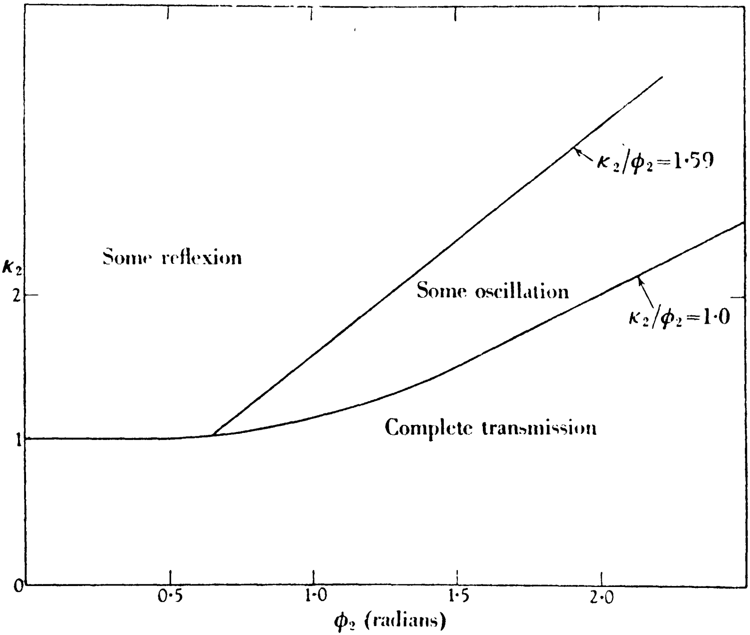

Fig. 6·4. Penetration through large fields for large transit angles.

turned back; and furthermore, if bunching is complete, these electrons tend to arrive after the maximum value of the catcher voltage has been passed. It seems hardly practicable to make the calculation in this case, and we shall limit ourselves to the consideration of the minimum efficiency which can be obtained from a given tube geometry when various optimum conditions are fulfilled.

6·4. The output efficiency of a klystron oscillator

We are now in a position to calculate the output efficiency, including the bunching and debunching losses. The calculation was first given for the Heil tube, in which α_1 is constrained to be equal to α_2 by Fremlin, Petrie, Strachey and Wallis of S.T.C. Beck then extended the results to the two-resonator valve with $\alpha_1 \neq \alpha_2$. Using eqn. (11) we can write, for the large signal-beam efficiency, omitting the deflexion loss,

$$\eta = -\tfrac{1}{4}\overline{\beta_1\gamma_1}\alpha_1^2 - \tfrac{1}{4}\overline{\beta_2\gamma_2}\alpha_2^2 - \alpha_2\bar{\beta}_2 J_1(\tfrac{1}{2}S\alpha_1\bar{\beta}_1)\sin(S+X),$$

where X = phase angle between the fields.

We put $\theta = \frac{1}{2}S\alpha_1\bar{\beta}_1$ to save writing. For the antiphase modes

$$\eta = -\tfrac{1}{4}\overline{\beta_1\gamma_1}\alpha_1^2 - \tfrac{1}{4}\overline{\beta_2\gamma_2}\alpha_2^2 + \alpha_2\bar{\beta}_2 J_1(\theta)\sin S, \tag{16}$$

and for the inphase modes

$$\eta = -\tfrac{1}{4}\overline{\beta_1\gamma_1}\alpha_1^2 - \tfrac{1}{4}\overline{\beta_2\gamma_2}\alpha_2^2 - \alpha_2\bar{\beta}_2 J_1(\theta)\sin S, \tag{17}$$

but $\sin S$ is then negative, so in each case the last term represents a gain in power.

The output efficiency is equal to the beam efficiency minus the circuit losses divided by I_0V_0. Assuming the resonators to have the same impedance Z_0

$$\eta_0 = \eta - \frac{V_0}{2Z_0W}(\alpha_1^2 + \alpha_2^2). \tag{18}$$

Using eqn. (16), (18) becomes

$$\eta_0 = \alpha_2\bar{\beta}_2 J_1(\theta)\sin S - \alpha_1^2\left(\frac{V_0^2}{2Z_0W} + \tfrac{1}{4}\beta_1\gamma_1\right) - \alpha_2^2\left(\frac{V_0^2}{2Z_0W} + \tfrac{1}{4}\overline{\beta_2\gamma_2}\right) \tag{19}$$

$$= \alpha_2\bar{\beta}_2 J_1(\theta)\sin S - (\alpha_1\bar{\beta}_1)^2\frac{P_1}{8} - (\alpha_2\bar{\beta}_2)^2\frac{P_2}{8}, \tag{20}$$

where $P_1 = \dfrac{4V_0}{I_0Z_0\bar{\beta}_1^2} + \dfrac{2\bar{\gamma}_1}{\bar{\beta}_1}$ and a similar expression gives P_2. We optimize with respect to S and the depths of modulation α_1 and α_2.

$$\frac{\partial\eta_0}{\partial S} = \alpha_2\beta_2 J_1(\theta)\cos S + \alpha_2\bar{\beta}_2\sin S\left(\frac{J_1(\theta)-\theta J_2(\theta)}{\theta}\right)\frac{\alpha_1\bar{\beta}_1}{2}$$

$$= 0, \text{ for a maximum.}$$

Making use of a standard expression for $J_1(\theta)/\theta$ we obtain

$$S\cot S = \frac{J_2(\theta)-J_0(\theta)}{J_2(\theta)+J_0(\theta)}, \tag{21}$$

$$\frac{\partial\eta_0}{\partial\alpha_1} = -\alpha_1\bar{\beta}_1^2\frac{P_1}{4} + \alpha_2\bar{\beta}_2\sin S\left(\frac{J_1(\theta)-\theta J_2(\theta)}{\theta}\right)\frac{S\bar{\beta}_1}{2} = 0,$$

therefore
$$\frac{\alpha_1\bar{\beta}_1}{\alpha_2\bar{\beta}_2}P_1 = S\sin S(J_0(\theta)-J_2(\theta)), \tag{22}$$

$$\frac{\partial\eta_0}{\partial\alpha_2} = -\alpha_2\bar{\beta}_2^2\frac{P_2}{4}+\bar{\beta}_2J_1(\theta)\sin S = 0,$$

therefore
$$\frac{\alpha_2\bar{\beta}_2}{\alpha_1\bar{\beta}_1}P_2 = S\sin S(J_0(\theta)+J_2(\theta)). \tag{23}$$

Multiplying and dividing eqn. (22) by (23) we get

$$(P_1\times P_2)^{\frac{1}{2}} = S\sin S(J_0^2(\theta)-J_2^2(\theta))^{\frac{1}{2}}, \tag{24}$$

$$\frac{P_2}{P_1}\left(\frac{\alpha_2\bar{\beta}_2}{\alpha_1\bar{\beta}_1}\right)^2 = \frac{J_0(\theta)+J_2(\theta)}{J_0(\theta)-J_2(\theta)}. \tag{25}$$

Eliminating $\alpha_2\bar{\beta}_2$, P_1 and P_2 from the right-hand side of eqn. (20) we obtain

$$\left(\frac{P_2}{P_1}\right)^{\frac{1}{2}}\eta_{0\,\text{max.}} = \theta^2\frac{\sin S}{S}J_2(\theta)\left(\frac{J_0(\theta)+J_2(\theta)}{J_0(\theta)-J_2(\theta)}\right)^{\frac{1}{2}}. \tag{26}$$

The solution of eqn. (26), subject to eqns. (21), (22) and (23), appears difficult, but we can find an easy way of obtaining the solution if we put $P_1 = P_2 = P$ which implies that $\bar{\beta}_1 = \bar{\beta}_2$, $\bar{\gamma}_1 = \bar{\gamma}_2$, i.e. the gaps are geometrically similar. Then we have

$$P = S\sin S(J_0(\theta)-J_2(\theta)), \tag{27}$$

$$\left(\frac{\alpha_2}{\alpha_1}\right)^2 = \frac{J_0(\theta)+J_2(\theta)}{J_0(\theta)-J_2(\theta)}, \tag{28}$$

$$\eta_{0\,\text{max.}} = \theta^2\frac{\sin S}{S}J_2(\theta)\left(\frac{J_0(\theta)+J_2(\theta)}{J_0(\theta)-J_2(\theta)}\right)^{\frac{1}{2}}. \tag{29}$$

Eqn. (21) still holds, and we also know that $S \doteqdot (2n+1)\frac{1}{2}\pi$. To solve eqn. (29) we first plot $S\cot S$ for a series of n and solve eqn. (21) graphically, over the range $\theta = 0$ to $\theta = 1{\cdot}84$. At $\theta = 1{\cdot}84$ $P = 0$ from eqn. (27). We now know S as a function of θ and eqn. (27) can be solved for P. Eqn. (29) is then solved for pairs of S and θ so that η_0 can be plotted against P. This curve will be correct so long as the value of α_2, which can be computed from eqn. (29), remembering that $\theta = \frac{1}{2}S\alpha_1\bar{\beta}_1$, does not disobey the appropriate maximum amplitude condition. Returning to the case in which $P_1 \neq P_2$ by comparing eqn. (24) with (27), we can see that the efficiency can be determined from the same curves by using the geometric mean of P_1 and P_2 and multiplying the corresponding value of η_0 by $(P_2/P_1)^{\frac{1}{2}}$.

Let us now assign a physical meaning to P. As $\theta \to 0$, which for finite S means $\alpha_1 \to 0$, eqn. (27) shows that

$$P \to S \sin S,$$

and $\sin S$ is very nearly unity in our case, so $P \to S$. We defined a factor F in Chapter 3, §4. F was the ratio of unloaded starting current to running current, and we found

$$F = \frac{4V_0}{I_0 S \bar{\beta}_1^2 Z_1}.$$

Now

$$\frac{P}{S} = \frac{4V_0}{I_0 S \bar{\beta}_1^2 Z_1} + \frac{2\bar{\gamma}_1}{\bar{\beta}_1}. \tag{30}$$

So we identify P as S times the corrected starting current ratio, i.e. the starting current ratio when beam loss is taken into account. P is a more convenient measure of tube performance than F because it is independent of S and using the results given above, the optimum S is easily found.

We next consider what is to be done when the use of the maximum conditions would make α_2 too large. In this case we can still consider S to be optimized, since this is done in the original design. We can easily calculate the minimum efficiency in this case by putting $\alpha_2 \bar{\beta}_2 = 1 - \alpha_1 \bar{\beta}_1$. Then, for $P_1 = P_2$,

$$\eta_0 = (1 - \alpha_1 \bar{\beta}_1) J_1(\theta) \sin S - \tfrac{1}{8} P[(\alpha_1 \bar{\beta}_1)^2 + (1 - \alpha_1 \bar{\beta}_1)^2]. \tag{31}$$

Eqn. (21) still holds and eqn. (28) gives the maximum θ which can be reached for a given P. These relations give the required information for the computation of eqn. (31). The efficiency is the minimum which can be obtained under the assumed conditions, because a slight improvement is possible in most cases by reducing $\alpha_1 \bar{\beta}_1$ by, say, detuning the buncher, because the second term varies very slowly with $\alpha_1 \bar{\beta}_1$ when this quantity is $> 0{\cdot}35$ and $J_1(\theta)$ is insensitive to small changes in θ near its maximum. From the practical point of view it is usually better not to work with reflected electrons because of the possible introduction of unwanted coupling between the resonators and the increase in resonator dissipation. Clearly, eqn. (31) will considerably underestimate the efficiency if $\alpha_2 \bar{\beta}_2$ can be made greater than $1 - \alpha_1 \bar{\beta}_1$ or if the efficiency still increases with increasing α_2, even though electrons are being turned back.

The results of this section are plotted in figs. 6·5, 6·6, 6·7, where the efficiency, optimum S, and value of $\alpha_1\bar{\beta}_1+\alpha_2\bar{\beta}_2$ are plotted as functions of P for modes 5, 7, 9. It should be remembered that these curves are plotted for resonators inphase or antiphase, and as we have seen in the first section of this chapter, this will not, in general, be the case. When $(S+X)\neq S$ the tube will oscillate best around the voltage which makes $\sin(S+X) = 1$. If X can be estimated it is easy to find the required voltage and to obtain the optimum efficiency from the figures by interpolating between the S values. Using slot coupling, modes 5, 9, etc., need a higher voltage for the best operation than that corresponding to their geometrical length, and the working value of S is therefore reduced. The reverse is the case for modes 3, 7, etc.

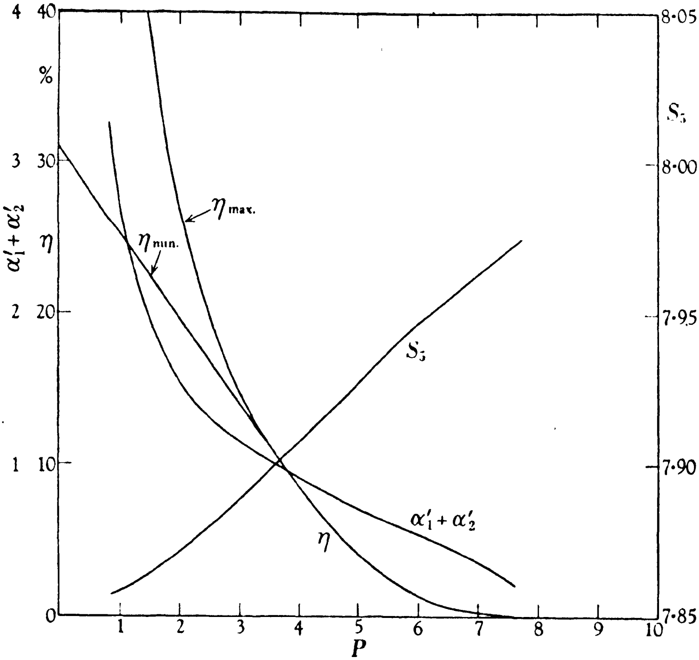

Fig. 6·5. Efficiency, optimum drift length and $\alpha_1\bar{\beta}_1+\alpha_2\bar{\beta}_2$ plotted against P for mode 5 (two-resonator klystron).

The curves for $\eta_{\text{min.}}$ show that at a given P value the output efficiency is larger for larger values of S. For instance, for $P = 2$,

$\eta_5 = 20\,\%$ but $\eta_9 = 30\,\%$. It is, however, more difficult to reach low P values with long drift tubes. The physical reason for the increase in efficiency with increase in S is that the amplification becomes greater and the power fed-back correspondingly less. This effect is much less marked when α_2 is allowed to increase without limit, i.e. on the curve for $\eta_{\text{max.}}$.

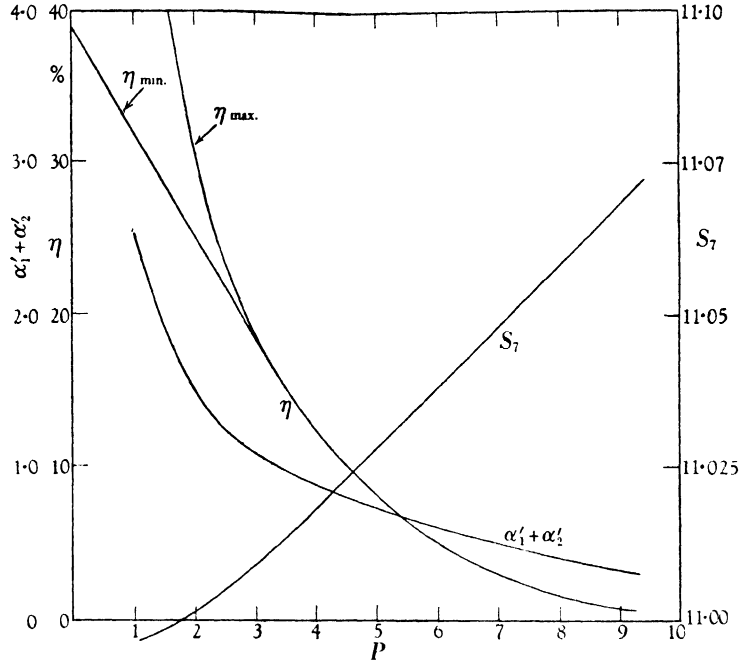

Fig. 6·6. Efficiency, optimum drift length and $\alpha_1\bar{\beta}_1+\alpha_2\bar{\beta}_2$ plotted against P for mode 7 (two-resonator klystron).

It is easy to show that, when the optimum conditions obtain, the optimum load resistance is given by

$$R_{L\,\text{opt.}} = \frac{2R_0}{\bar{\beta}_1^2}\,\frac{\alpha_2}{\alpha_1 S \sin S J_2(\theta)}. \tag{32}$$

We can now plot a modulation characteristic as follows. The tube is assumed to be set up so as to give optimum operation at full current. The maintenance equation is then

$$\alpha_2\bar{\beta}_2 J_1(\theta) - \frac{P}{8}\left[(\alpha_1\bar{\beta}_1)^2 + (\alpha_2\bar{\beta}_2)^2\right] = \frac{\alpha_2^2 R_0}{2R_L}. \tag{33}$$

But the coupling between the resonators has been fixed to a definite value k given by eqns. (25) or (28). We can then rewrite eqn. (33)

$$\frac{J_1(\theta)}{\theta} = \frac{2}{S}\left[\frac{k}{(\overline{\beta_1\beta_2})^2}\frac{R_0}{R_L} + \frac{P}{8}\left(\frac{1+k^2}{k}\right)\right]. \qquad (34)$$

Eqn. (34) can be solved for P by assuming values of θ if we neglect the beam loading and put $R_0 = BP$. The pairs of θ and P thus found

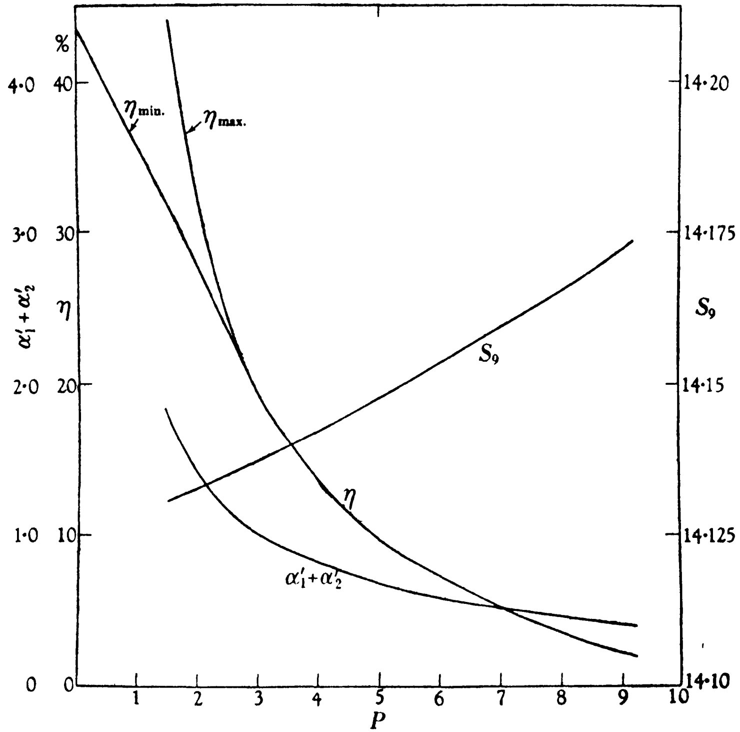

Fig. 6·7. Efficiency, optimum drift length and $\alpha_1\bar{\beta}_1+\alpha_2\bar{\beta}_2$ plotted against P for mode 9 (two-resonator klystron).

can be inserted into the left-hand side of eqn. (33) to give the output as a function of P. This work would only be required in the case of high-power amplitude modulated tube. We can easily see that if we neglect the circuit losses there is some current i_{SL} which will just cause the tube to oscillate because $J_1(\theta)/\theta \rightarrow \frac{1}{2}$ as $\theta \rightarrow 0$. Then

$$\frac{J_1(\theta)}{\theta} = \text{constant} \times \frac{i_r}{i_{SL}}.$$

The power output $$W_0 = \text{constant}\times\theta^2.$$

So $$\frac{J_1(W_0^{\frac{1}{2}})}{W_0} = \text{constant}\times\frac{i_r}{i_{SL}}. \tag{35}$$

Eqn. (35) gives a universal modulation characteristic for all tubes, which is very curved. For this reason amplitude modulation of klystrons is unsuitable for high-quality transmission. Even if the grid characteristic is suitably distorted it is difficult to get linear modulation to a depth greater than 70%. Phase or frequency modulation must therefore be used, and it turns out that frequency modulation is almost ideal provided the circuit band width can be made sufficiently great.

6·5. The output efficiency of single gap-double transit tubes

In this case α_1 is necessarily equal to α_2, but $\overline{\beta_1\gamma_1}$ may not equal $\overline{\beta_2\gamma_2}$. There is also only a single resonator to be excited and both the inphase and antiphase modes are met, the inphase modes in the Heil tube and the antiphase modes in the Samuel tube. Under these circumstances

$$\eta_0 = \alpha\bar{\beta}_2 J_1(\theta)\sin S - \alpha^2\left[\frac{V_0^2}{2Z_0W} + \tfrac{1}{4}(\overline{\beta_1\gamma_1} + \overline{\beta_2\gamma_2})\right]$$

$$= \alpha_2\bar{\beta}_2 J_1(\theta)\sin S - \frac{\alpha^2\overline{\beta_1\beta_2}}{4}P_{II}, \tag{36}$$

where $$P_{II} = \left[\frac{2V_0}{Z_0W\overline{\beta_1\beta_2}} + \frac{\overline{\beta_1\gamma_1} + \overline{\beta_2\gamma_2}}{\overline{\beta_1\beta_2}}\right]. \tag{37}$$

Optimizing this as in §6·4 yields eqn. (21) connecting S and θ, together with

$$P_{II} = -2S\sin SJ_0(\theta) \tag{38}$$

and $$\frac{\beta_1}{\beta_2}\eta_0 = -\theta^2 J_2(\theta)\frac{\sin S}{S}. \tag{39}$$

We shall see, in Chapter 7, that these results also apply to the reflex klystron, if the reflector field is linear and P is suitably redefined.

These results are plotted in figs. 6·6, 6·8, 6·9, 6·10 where the efficiency, optimum S and value of $\frac{1}{2}\alpha\beta$ are plotted as functions of P for modes 5, 7, 9. On the curves the symbol α' has been used for $\alpha\beta$. As the region in which $\alpha\beta > \frac{1}{2}$ is very small, the efficiency for $\alpha\beta = \frac{1}{2}$ has not been computed. The efficiency is seen to be of the same order as the minimum efficiency for the two-resonator tube of the same P. In general, β_1 should be made considerably less than β_2 for best operation. For $\beta_1 = \beta_2$ the efficiency falls off as the mode number increases, unlike the two-resonator case. This is because the h.f. voltage does not build up enough to extract much energy from the bunches when the drift time is long, as is at once obvious from the fact that θ must be near 1·84 if the conversion efficiency is to be tolerable.

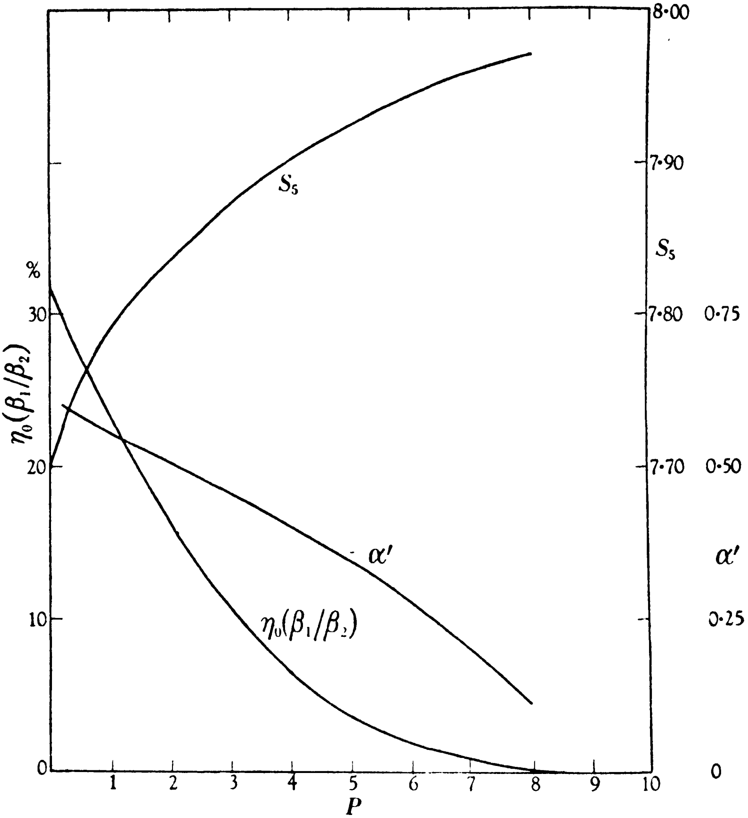

Fig. 6·8. Efficiency, optimum drift length and $\alpha_1\bar{\beta}_1$ plotted against P for mode 5 in a unity coupled klystron.

6·6. Design considerations

The efficiency curves show that P must be made small and S large for high efficiency. In the case of an electrostatic tube the maximum current is inversely proportional to the square of the length, so these requirements are contradictory. In the magnetic case the current is limited by the permissible depression of the potential on the beam axis and the cost of the magnet, in weight, size and money. It is usual to find that the best design, in circumstances

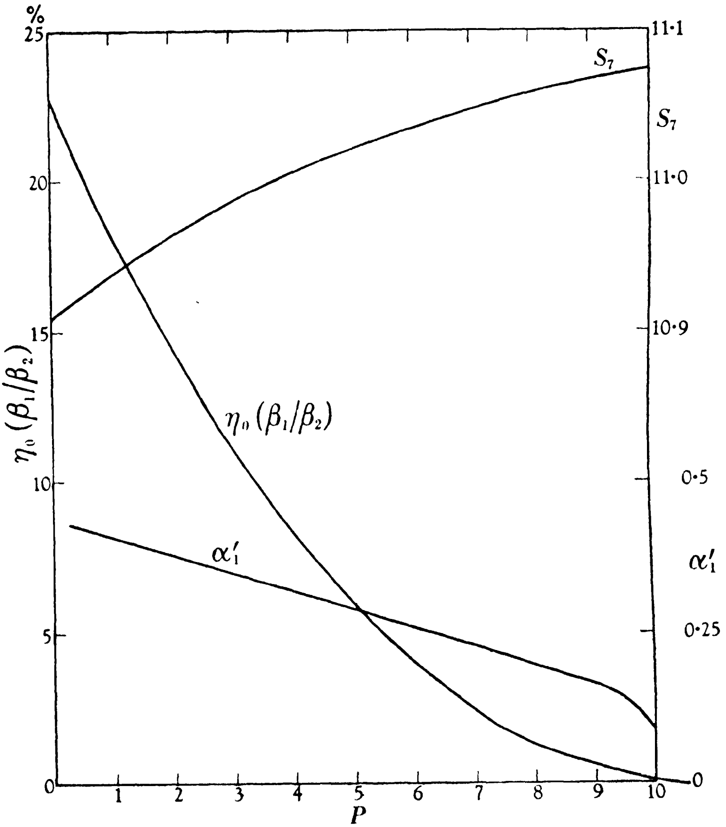

Fig. 6·9. Efficiency, optimum drift length and $\alpha_1\bar{\beta}_1$ plotted against P for mode 7 in a unity coupled klystron.

where voltage is not a major consideration, is that in which the resonators are made just deep enough to get a high Q and are placed so as to share one wall. The gaps are then separated as much as possible. If this design leads to an excessive voltage, one must increase the current, by increasing the tunnel diameter sufficiently to offset the loss in resonator Q. If this first design was without grids, the second will have to use grids.

Gridless tubes are commonly used at high-power levels, because of the difficulty of dissipating large amounts of power on the grid. For instance, a particular type of conduction cooled grid of 8 mm.

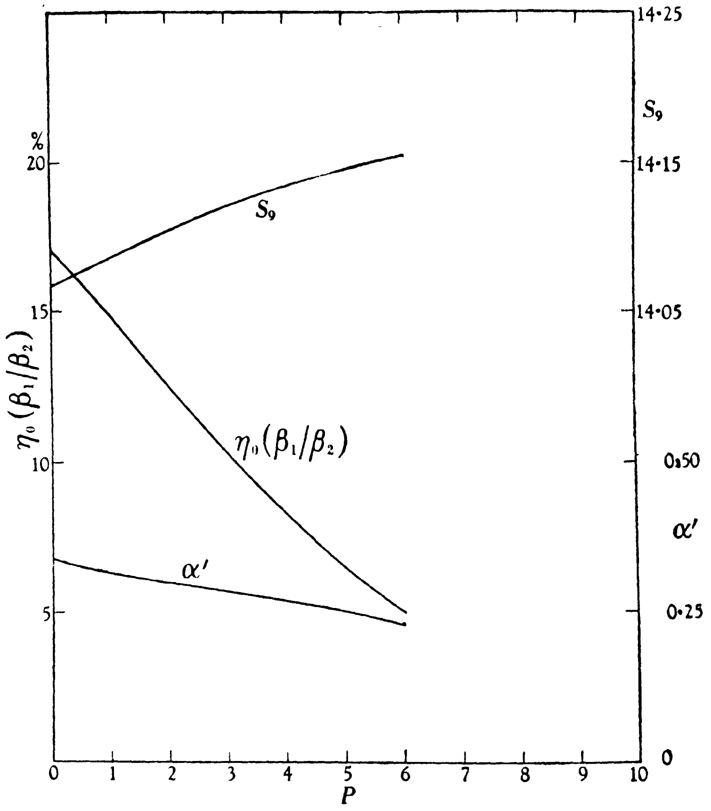

Fig. 6·10. Efficiency, optimum drift length and α_1/β_1 plotted against P for mode 9 in a unity coupled klystron.

diameter will dissipate 10 W. and intercepts about 12 % of the current incident upon it. The input is thus limited to about 80 W. The gridless tube has several disadvantages, one of which, the extra term in the beam loading, has already been mentioned. A second effect is the apparent broadening of the beam by the lens action of the buncher gap. As is well known, a low-voltage ratio cylindrical electrostatic lens has a very long focal length because the transit time in the diverging part of the field is not much different from the transit time in the converging half. In the high-frequency case not only is the lens alternately converging and diverging, but its strength is also much increased. For instance, if an electron enters a gap at the instant the field reaches its negative maximum, it will start to diverge. After the centre line of the system is reached the field would, in the d.c. case, be convergent, but in the h.f. case it is either weakly convergent or divergent according to the actual transit time. Milner and Feenberg have studied this effect, and Milner shows that the beam is broadened by 68 % at the plane of the bunches. In gridless tubes it is therefore necessary to locate the catcher gap where the beam is at least 68 % less than the tunnel diameter. As the minimum beam diameter with maximum current is $d/2{\cdot}4$, this is not difficult to do.

The results of this chapter show that reasonably good output efficiencies can be obtained from klystron oscillators, but a consideration of the means by which they can be obtained indicates that high voltages are necessary. In view of the fact that c.w. magnetrons have considerably greater efficiencies, it is difficult to believe that high-power klystrons will be widely used. It is probable that klystrons will be used to cover the range of powers between 1 and 100 W. where they have several advantages over the magnetron. The calculated efficiencies agree very well with those observed experimentally up to the limit at which $\alpha_1\bar{\beta}_1+\alpha_2\bar{\beta}_2 = 1$. Beyond this limit they are somewhat above the curve for minimum efficiency, but results vary more between individual tubes, presumably because second-order electron optical effects, centring errors and so on influence the voltage at which reflexion sets in. It is, however, true to say that we have here presented a large signal theory of klystron oscillators which is adequate for engineering purposes.

Chapter 7

REFLEX KLYSTRON OSCILLATORS

The reflex klystron is by far the most important type of V.M. tube because it is particularly suitable for use as a local oscillator in superheterodyne receivers. Reflex tubes can be made to operate with voltages available in the ordinary receiver, they are simpler than triodes from the circuit point of view even on wave-lengths at which a triode can be made to oscillate, and lastly, they furnish a simple and direct method of applying A.F.C. to the receiver. Their efficiency is rather low (less than 5 % in present-day tubes), but this is due to the fact that no attempt has been made to design high-power tubes, partly because of the electron optical problem involved, and partly because the d.c. power has to be dissipated from the resonator surface and the cooling problem becomes rather difficult. At present it is roughly correct to say that reflex tubes are used for local oscillators in all sets working below 12 cm. wave-length down to the lowest wave-lengths. As decimetre communication increases in importance it is likely that the necessity for A.F.C. will dictate their use at longer wave-lengths up to the 30–50 cm. region. At this point physical size begins to tell against the V.M. tube.

7·1. The Webster approximation for the reflex klystron

In this section we use the assumptions which have been made in discussing the Webster analysis in Chapter 3, with the additional limitation that we restrict ourselves to the case of a reflector field which varies linearly with distance from the exit grid. This assumption is not far from the truth for many practical tube constructions, but we shall see that it is by no means an optimum field shape. We use it at the moment simply because of the analytical convenience.

By a slight rearrangement of eqn. (17) in Chapter 3 we have for the velocity at exit from the gap on the first transit

$$u_1 = u_0\left(1 - \frac{\alpha_1\beta}{2}\sin\omega t_0\right). \tag{1}$$

The minus sign is chosen so as to bring the analysis into line with that given in Chapter 3, where we calculated the bunching for the electrons which took the shortest time of transit. Here, as we have said in Chapter 1, the slowest electrons take the shortest time. The retarding field is $A = (V_0 - V_2)/d$ V./m. The electrons are brought to rest by this field, turn round and perform a second transit through the gap.

The transit time in the retarding field is

$$\tau = \frac{2u_1 m}{eA}.$$

We put the transit time of an unmodulated electron τ_0, where $\tau_0 = 2u_0 m/eA$. Then the time of return to the centre of the gap is

$$\begin{aligned} t_2 &= t_0 + \tau \\ &= t_0 + \tau_0\left(1 - \frac{\alpha_1 \beta}{2}\sin\omega t_0\right). \end{aligned} \tag{2}$$

Then

$$\frac{dt_2}{dt_0} = 1 - \frac{S\alpha_1\beta}{2}\cos\omega t_0, \tag{3}$$

where we have put $S = \omega\tau_0$, the transit angle in the reflecting field. Eqn. (3) is exactly the same as eqn. (22) of Chapter 3 and gives rise to the same amount of bunching. Since there is only one resonator we must have $\alpha_1 = \alpha_2$, and the reflex klystron with linear reflecting field is seen to behave in exactly the same way as a unity-coupled two-resonator klystron with the exception that the circuit losses are halved. We can therefore use the curves of output efficiencies given for unity-coupled klystrons in Chapter 6 if we redefine P. For the reflex

$$P = 2\left[\frac{V_0}{I_0 Z_0 \beta^2} + \frac{\gamma}{\beta}\right]. \tag{4}$$

There are several observations to be made about the results given above. First, the analysis given above makes the assumption that the electrons emerge directly from the gap into the reflecting field. If they emerge into field-free space before eventually reaching the retarding field some bunching in the opposing phase occurs. We must therefore subtract the transit angle in field-free space from the transit angle in the retarding field to obtain the angle which is to be used in the bunching calculations. The angle to be used in the phase calculation is obviously the sum of the two angles. In most modern tubes there is no field-free space, and we shall not introduce it explicitly as the formulae can easily be rewritten for the cases in which it exists. Secondly, the analysis assumes that the reflecting space is much longer than the gap. This assumption is almost invariably correct in practical cases. Most reflex klystrons have a rather high beam impedance, and it is usually found that the term $\bar{\gamma}/\bar{\beta}$, which represents the effect of beam loading, is a negligible part of P.

If a reflex tube is tested at a fixed anode voltage, the mode being changed by readjustment of the reflector voltage, one finds that the power output increases as the reflector is made more negative. The physical basis for this is the following: The power output is proportional to the peak h.f. voltage multiplied by the h.f. current. The h.f. current reaches its maximum when $\frac{1}{2}S\alpha_1\bar{\beta} = 1{\cdot}84$, therefore α_1 increases as S decreases, and the power output increases also. The final amplitude is, of course, fixed by the condition that the sum of the circuit and load losses, which are a quadratic function of α_1, should just equal the power production. In some cases the penultimate mode is more powerful than the ultimate. The curves show that this is to be expected. Consider a tube for which $P = 5$:

Mode no.	3	7	11	15	19
Efficiency %	Will not start	6·0	6·7	6·25	5·25

When oscillating in mode 7 with the load adjusted for maximum output the depth of modulation will be such that $P = 0{\cdot}275$, so that there is no possibility of any reflexion occurring in the h.f. field, and all our assumptions are well justified. The largest value of P for which $\alpha_1\bar{\beta} \geqslant 0{\cdot}50$ is $P = 3{\cdot}2$ in mode 3, so it is very improbable that any local oscillator will fall outside the scope of our theory. A very clear qualitative description of the reflex klystron with linear reflecting field has been given by J. R. Pierce.[*] Linder[†] has also dealt with more general cases.

7·2. General reflexion field

The numerical results at the end of the last section go a long way towards proving that the only serious deficiency in our analysis is the assumption that the reflector field is linear. In this section we consider the general reflector field by a method due to Barford of E.M.I.

---

[*] Pierce, *Proc. Inst. Radio Engrs, N.Y.*, 33 (1945), 112.

[†] Linder, *Proc. Inst. Radio Engrs, N.Y.*, 35 (1947), 241.

As usual we have to calculate the bunching by means of the expression

$$i_2 = I_0\frac{dt_2}{dt_0}.$$

But
$$\tau = t_2 - t_0,$$

therefore
$$\frac{dt_2}{dt_0} - 1 = \frac{d\tau}{dt_0}, \tag{5}$$

therefore
$$i_2 = \frac{I_0}{1 + d\tau/dt_0}. \tag{6}$$

Now for any reflector field $\tau = f(V_1)$, where V_1 is the h.f. voltage on the gap. We can now expand by Maclaurin's theorem

$$\tau = f(0) + V\left(\frac{df}{dV}\right)_0 + \frac{V^2}{2}\left(\frac{d^2f}{dV^2}\right)_0 + O(V^3)$$
$$= \tau_0 + V\left(\frac{df}{dV}\right)_0 + \frac{V^2}{2}\left(\frac{d^2f}{dV^2}\right) + O(V^3)$$

and
$$\frac{d\tau}{dt_0} = \left(\frac{d\tau}{dV}\right)_0\frac{dV}{dt_0} + V\left(\frac{d^2\tau}{dV^2}\right)\frac{dV}{dt_0} + O(V^2). \tag{7}$$

The modulating voltage is sinusoidal, so we get

$$\frac{dV}{dt_0} = \omega\beta V_1 \cos \omega t_0.$$

Hence neglecting powers of V we get, upon substitution into eqn. (6),

$$i_2 = \frac{I_0}{1 + \omega\beta V_1(d\tau/dV)_0 \cos \omega t_0}. \tag{8}$$

Eqn. (8) gives a general expression for the bunching which is accurate providing the terms in V_1^2 can be neglected.

We next have to evaluate $(d\tau/dV)_0$ from the field configuration. If the reflector field can be expressed as a potential $\phi(z)$, we can write the following equation for the motion of an electron of excess energy V:

$$\tau = 2\left(\frac{2e}{m}\right)^{-\frac{1}{2}}\int_{z_1}^{z_2}\{\phi(z) + V\}^{-\frac{1}{2}}\,dz,$$

where z_1 = co-ordinate of gap centre, and z_2 = co-ordinate of point at which $\phi = V_0 + V$.

We next introduce the dimensionless quantities

$$Q = \frac{\phi(z)}{V_0}, \quad q = \frac{V}{V_0}, \quad Z = \frac{z}{l}, \quad \Delta Z = \frac{\Delta z}{l},$$

where l = the distance from the gap centre to the zero equipotential. Then

$$\tau = 2\left(\frac{2e}{m}\right)^{-\frac{1}{2}} V_0^{-\frac{1}{2}} l \int_{-\Delta Z}^{1} (Q+q)^{-\frac{1}{2}}\, dz, \tag{9}$$

$$\tau_0 = 2\left(\frac{2e}{m}\right)^{-\frac{1}{2}} V_0^{-\frac{1}{2}} l \int_{0}^{1} Q^{-\frac{1}{2}}\, dz, \tag{10}$$

$$\left(\frac{d\tau}{dV}\right)_0 = 2\left(\frac{2e}{m}\right)^{-\frac{1}{2}} V_0^{-\frac{3}{2}} l \frac{d}{dq}\left[\int_{-\Delta Z}^{1} (Q+q)^{-\frac{1}{2}}\, dz\right]_{q=0}. \tag{11}$$

From eqns. (10) and (11) we obtain

$$\left(\frac{d\tau}{dV}\right)_0 = \frac{\dfrac{\tau_0}{V_0}\dfrac{d}{dq}\left[\displaystyle\int_{-\Delta Z}^{1} (Q+q)^{-\frac{1}{2}}\, dz\right]_{q=0}}{\displaystyle\int_{0}^{1} Q^{-\frac{1}{2}}\, dz} \tag{12}$$

$$= \frac{\tau_0}{V_0} R. \tag{13}$$

Here R is to be interpreted as a numerical factor which can be determined graphically from an electrolytic trough measurement. For a linear field long in comparison to the gap R turns out to be $\frac{1}{2}$. The substitution of eqn. (13) in (8) then gives the Webster bunching factor. Instead of a bunching factor $\frac{1}{2}S\alpha_1\beta$ we now have a more general expression $RS\alpha_1\beta$.

Although Barford gave the analysis leading to eqn. (13) he did not fully realize the importance of the relation because he retained separate expressions for $(d\tau/dV)_0$ and τ_0, both of which contain the length $2l$ which makes it impossible to investigate the role of different factors independently.

7·3. Maximum power output and efficiency using the general field

We next proceed to use the expression for the bunching parameter developed above, assuming that it is correct for the largest h.f. voltages we shall meet, and making an allowance for the power lost in bunching and debunching. Following the results of Chapter 6 the expression for the conversion efficiency is

$$\eta_{\text{conv.}} = \tfrac{1}{2}\bar{\beta}\gamma\alpha_1^2 - \alpha_1\bar{\beta}J_1(RS\alpha_1\bar{\beta})\sin S. \tag{14}$$

The phasing condition is $S = (n+\frac{3}{4})\,2\pi$, so that $\sin S$ is itself negative, and the second term represents a gain of energy. The output efficiency is

$$\eta_0 = -\alpha_1\bar{\beta}J_1(RS\alpha_1\bar{\beta})\sin S - \frac{\alpha_1^2}{2}\left(\frac{V_0}{I_0Z_0} + \overline{\beta\gamma}\right). \tag{15}$$

We now optimize η_0 with respect to S, α_1 and R. The physical operations are choice of mode and exact adjustment of reflector voltage in the mode, adjustment of the coupling to the load and lastly correct shape of reflector field. To save writing we put $\theta = RS'\alpha_1\bar{\beta}$ and $\alpha_1\bar{\beta} = \alpha'$:

$$\frac{\partial\eta_0}{\partial S} = -\alpha' J_1(\theta)\cos S - \alpha' \sin S\left[\frac{J_1(\theta) - \theta J_2(\theta)}{\theta}\right]R\alpha'$$

$$= 0 \text{ for a maximum,}$$

therefore
$$S\cot S = \frac{J_2(\theta) - J_0(\theta)}{J_2(\theta) + J_0(\theta)}, \tag{16}$$

$$\frac{\partial\eta_0}{\partial\alpha_1} = -\beta' J_1(\theta)\sin S - \alpha'[J_0(\theta) - J_2(\theta)]\frac{RS\bar{\beta}}{2}\sin S - \alpha\left(\frac{V_0}{I_0Z_0} + \overline{\beta\gamma}\right),$$

therefore
$$2\left[\frac{V_0}{I_0Z_0\bar{\beta}^2} + \frac{\bar{\gamma}}{\bar{\beta}}\right] = -2RS\sin SJ_0(\theta), \tag{17}$$

$$\frac{\partial\eta_0}{\partial R} = -\alpha' J_1'(\theta)\sin S\,.\,S\alpha',$$

therefore
$$\theta = 1{\cdot}84. \tag{18}$$

Using the optimum condition (17) the expression for the output efficiency becomes

$$\eta_0 = -\tfrac{1}{2}\alpha' \sin S\theta J_2(\theta) \tag{19}$$

$$= -\frac{\theta^2}{2R}J_2(\theta)\frac{\sin S}{S}. \tag{20}$$

We proceed as before by solving eqn. (16) for a series of values of θ and inserting the pairs of S and θ thus obtained into eqns. (17) and (20) to get the corresponding values of P and η_0. If this is done for several fixed R values we obtain a family of curves giving η_0 as a function of P with R as parameter. If we then put eqn. (18) into (17) we get

$$R_{\text{opt.}} = \frac{P}{0{\cdot}634S\,|\sin S|}, \tag{21}$$

which allows us to calculate a curve of absolute maximum efficiency, and which is the envelope of the family of curves already plotted.

We can, however, save a great deal of work by observing that eqns. (17) and (20) are the same as the corresponding equations for the unity-coupled two-gap tube, except that the efficiency is divided by $2R$ and the P value at a given θ is multiplied by $2R$. We can therefore still use the curves of Chapter 6 to obtain the efficiency of a reflex with parameter $P = P_1$, $R = R_1$ by reading off the efficiency at $P_2 = P/2R_1$ and dividing the result by $2R_1$. The physical basis for these facts is that although the starting current is

$$i_S \geqslant \frac{V_0}{\beta^2 Z_0 SR}, \tag{22}$$

which is smaller by a factor of $4R$ than in the case of the two-gap tube, the amplitude of oscillation is inversely proportional to R.

7·4. Discussion of design requirements

As in earlier cases we desire P to be as small as possible. This means we must make the beam impedance small, the resonator impedance high and use the correct type of reflector. It is not possible to derive a general expression for the current which can be focused through a reflex tube, and expressions derived for special fields are too restricted to have any general significance. All that can be said is that tubes focus correctly with at least a quarter of the maximum current which could make a single transit through a tunnel of the same dimensions. The resonator is chosen by obtaining a reasonable compromise between tunnel diameter and parallel impedance. The design of the reflector presents several difficulties, because, as is usual in electron optical problems, we have to investigate special cases with the aid of an electrolytic trough. Starting with the simplest case we can say that a flat plate, whose diameter is large compared with that of the exit grid, will give an R value of about $\frac{1}{2}$ or somewhat less when the negative voltage is high so that the transit angle is short. Electrolytic trough plots show that the shape of the exit grid is important in this case, a small amount of the curvature towards the reflector materially increasing R. In the deep cylinder, which is the only other case we have seriously studied, the R value is a rapid function of position varying from about 1·5 near the end-surface to about 5 at the entrance. Space charge can modify the larger values rather markedly, but it is possible to adjust the field to allow for it, using the procedure of relaxation. In any case, we see from the curves that when the reflector is correctly designed in the first place the R value is not nearly as critical as it is in a poorly designed valve working well away from the optimum. We shall have to return to this topic in studying the limitations of V.M. tubes. A detailed discussion of the design of the CV 35 is given by Pearce and Mayo*.

7·5. Frequency control by reflector voltage changes

One of the most important properties of the reflex is the variation in output frequency as the reflector voltage is varied. It is possible to obtain a good general idea of this effect by rather simple methods, and this we proceed to do under the assumptions that small signal theory applies, and that all currents and voltages, except the reflector voltage, are fixed so that the tube is operating correctly on a specified mode when the reflector is adjusted to the middle of the range. If the reflector is then slightly altered, so that the transit time changes, the bunches will no longer arrive back at the gap when the voltage is exactly at its positive maximum. The bunched current can therefore be considered as consisting of a part inphase with the voltage and a reactive part; the beam impedance will also be reactive. Since the frequency of the system as a whole is determined by the condition that the total reactance must vanish, the existence of a reactive component in the beam means that the frequency must change. Fig. 7·1 shows the system which we have to consider.

Let the S value at the centre of the range $= S_0$, h.f. voltage across the gap $= V_1 \sin \omega t_0$, and h.f. current across the gap

$$i_2 = I_0[1 + \theta \cos(\omega t_2 - S)]$$

for the assumption of small signals. But for small ranges of reflector voltage near the optimum we can write

$$i_2 = I_0[1 + \theta \sin(\omega t + \delta)], \tag{23}$$

---

* Pearce and Mayo, *J. Inst. Elect. Engrs*, 93, pt. IIIA, no. 5 (1946), 918.

where $\delta = S - S_0$. The instantaneous power extracted from the beam is then

$$\begin{aligned} W_i &= \beta V_1 I_0 \theta \sin \omega t \sin(\omega t + \delta) \\ &= \beta V_1 I_0 \theta [\sin^2 \omega t \cos \delta + \sin \omega t \cos \omega t \sin \delta]. \qquad (24) \end{aligned}$$

This must be equal to the instantaneous power lost into the circuit. The circuit can be reduced to a loaded parallel resonant equivalent for which the admittance, near resonance, is given by

$$Y_C = \frac{1}{Z'_L} + 2j\Delta\omega C = \frac{1}{Z'_L} + 2j\frac{\Delta\omega}{\omega}\frac{Q}{Z'_L},$$

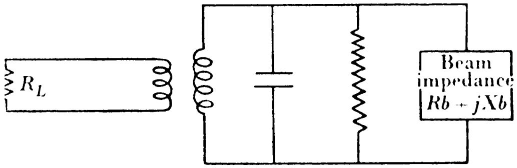

Fig. 7·1. Cavity loaded by reactive beam.

where Z'_L = loaded value of the resonant impedance, and Q = loaded Q of the resonator. Then

$$W_2 = V_1^2\left(\frac{\sin^2 \omega t}{Z'_L} + \frac{2\Delta\omega}{\omega}\frac{Q}{Z'_L}\sin \omega t \cos \omega t\right). \qquad (25)$$

Equating (24) and (25) we have

$$\frac{V_1}{Z'_L} = \beta I_0 \theta \cos \delta, \quad \frac{2\Delta\omega}{\omega}\frac{Q}{Z'_L} V_1 = \beta I_0 \theta \sin \delta. \qquad (26)$$

Dividing we obtain $\qquad \tan \delta = \dfrac{2\Delta\omega}{\omega} Q. \qquad (27)$

Eqn. (27) allows us to calculate the change in angular frequency $\Delta\omega$ resulting from a change of reflector voltage which causes a change of δ in the transit angle. Clearly Q should be small if large frequency shifts are required, as is physically obvious. For an efficient valve this means that C must be kept small. We next require to calculate the maximum frequency deviation which can be obtained.

When δ is made large, the starting current will increase until for a certain value of δ it reaches the running current.

We have

$$\cos\delta_1 = \frac{V_1}{Z'_L \beta I_0 \theta}$$

$$= \frac{V_0}{Z'_L \beta^2 I_0 RS}$$

$$= \frac{i_{SL}}{I_0}, \tag{28}$$

where i_{SL} is the loaded starting current of the tube when $\delta = 0$. Putting this result into the second of eqn. (26) we have

$$\left(\frac{\Delta\omega}{\omega}\right)_{\text{max.}} = \frac{1}{2Q}\frac{I_0}{i_{SL}}\sin\delta_1$$

$$= \frac{1}{2Q}\left(\frac{I_0^2}{i_{SL}^2} - 1\right)^{\frac{1}{2}}. \tag{29}$$

In practical cases eqn. (29) gives values of $\Delta\omega/\omega$ around 1 % which are usually in good agreement with experiment. It is more difficult to say anything about the optimization of eqn. (29). I_0/i_{SL} should be fairly large, but since we are discussing the whole circuit, this cannot be done by decreasing the loading because Q would then increase by the same factor. It is not at all obvious whether the ordinary resonator can be improved on in this respect. It is usually found that the load has to be coupled fairly tightly to the resonator to obtain a nearly linear variation in frequency with reflector voltage. Fig. 7·2 shows types of curves found with light and optimum loading. In conclusion, it should be noted that the reflector field shape does not enter into any of the above results, except in so far as it determines the relation between V_2 and δ.

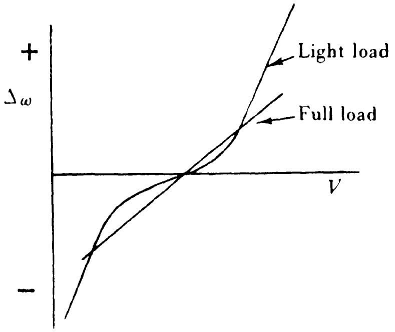

Fig. 7·2. A.F.C. as a function of load.

7·6. Frequency stability and long-line effects

It would be impossible to conclude this chapter without some discussion of effects caused by the load rather than by the beam. It is usual nowadays to carry through this discussion by means of the Rieke diagram, which is a contour diagram showing contours of constant frequency and of constant power output. It is usually plotted on a polar diagram in the reflexion coefficient plane. The diagram is made by setting up a variable load so that the s.w.r. and position of the minimum can be measured simultaneously with the frequency and power output of the generator. The Rieke diagram provides the circuit engineer with all the information needed to apply the valve to any desired end, but it also provides the tube engineer with very valuable data. With a Rieke diagram, taken at constant input voltage and current, one can deduce the driving admittance if a curve of circuit admittance has previously been made. This is done for several powers to give the driving admittance as a function of amplitude, and proves a valuable check on theoretical work. Such a diagram usually shows that the tube will not oscillate at all for certain loads, or has regions in which oscillations are unstable. Another effect, which is not shown by the Rieke diagram, is the type of instability caused by connecting the oscillator to the load by a very long line. If we plot the admittance of such a line as a function of frequency, we may find that it shows the convoluted form of fig. 7·3. If we plot the driving admittance on the same diagram, it may cut the circuit admittance in three places. The two intersections for which B increases as ω increases are stable oscillation points. If such a system is pulsed, for instance, it is found that the oscillations take place on one frequency for a proportion of the pulses, and on the other for the rest. To prevent this, the line should be kept short and care taken to eliminate

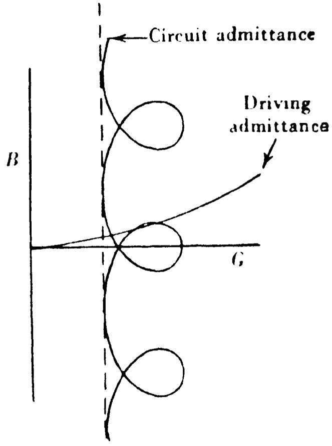

Fig. 7·3. Diagram illustrating frequency jumps in an oscillator connected to a long line.

standing waves; lastly, the tube should be tightly coupled to the line. All these phenomena can be examined in detail, but the development is best done in numerical or graphical form for particular cases rather than in general terms.

7·7. Conclusion

The theory given above is capable of predicting the operating efficiencies of reflex klystrons to a good degree of accuracy. Observed efficiencies agree with theoretical ones to within the errors of measurement of the parallel impedance, reflector factor and so on. This is because the amplitude of oscillation is small enough to make all our assumptions valid, which is not usually the case in power oscillators.

Although the theory shows that for low P values and correct reflector characteristics it is possible to make efficient reflex tubes, it is doubtful whether they would be useful in practice, first, because of the necessity of dissipating the power on the resonator surface, and secondly, because of the difficulty of arranging a smooth control of the reflector characteristics. As a high-current valve approaches the oscillation point, the sudden spreading of the reflector space charge at the onset of oscillation alters the transit time considerably, and may make stable oscillation impossible. However, the reflex has a great role to play in receiver design, and as we shall find later, shows promise of making much higher frequencies available to us.

Chapter 8

MISCELLANEOUS TYPES OF VELOCITY-MODULATION TUBE

Many special types of V.M. tube have been suggested, and some have had a great deal of experimental work done on them. The most important tube in this category is the V.M. mixer, and we shall devote most of this chapter to it, continuing with a section on the monotron and the Müller and Rostas tube, and conclude with some remarks on reactance valves.

8·1. The velocity-modulation mixer

Although the V.M. mixer is not used at present (because of its relatively poor signal-to-noise ratio), there is no doubt that it has several advantages over the crystal mixer which will encourage the carrying out of further research. These advantages are: freedom from danger of burn-out by h.f. power, reduction of radiation from the receiver, and a greater robustness. If the signal-to-noise ratio could be improved, these advantages would cause it to be used in most common T. and R. systems in spite of the fact that power supplies would be needed.

We have already mentioned one type of V.M. mixer and its action in Chapter 1. This is the mode of operation termed velocity discrimination, in which the collector is biased back slightly below cathode potential so that only accelerated electrons can reach it. Two resonators are coupled to the same beam, the resonator nearer to the gun being tuned to and driven by the local oscillator. The signal frequency voltages, small in comparison with the local oscillator voltage, are fed into the second resonator, which is located close enough to the collector to ensure that the V.M. is not destroyed by debunching forces. The collector current pulses which arrive over part of the positive half-cycle of the local oscillator will then vary in amplitude as the signal voltage increases or decreases the velocity of the electrons. The collector current will therefore contain a difference frequency component which can be picked out by a suitably tuned load. In practice it is usually possible to inject both signal and local oscillator into a single resonator because there is ample local oscillator power available to offset the fact that the resonator is tuned to signal frequency.

The second mechanism is that of bunching. In this type of mixer the resonators are put as far apart as possible consistent with current requirements. The signal is fed into the resonator nearer to the gun so that the beam arriving at the second gap is bunched. The collector is biased near cathode potential, and the local oscillator power is adjusted so that the collector is saturated on each half-cycle. However, since the beam is bunched by the time it reaches the second gap the number of electrons in these current pulses will vary and a difference frequency component can once more be detected in the collector current.

In 1940 Bleaney and Cooke of the Clarendon Laboratory gave the analysis for conversion gain and signal-to-noise ratio in an important paper. Experimental results at first bore out their conclusions, but as measurement techniques were refined it was found that there exists a source of noise of far greater magnitude than they had predicted. No explanation of this fact has yet been given, and the whole matter should be reinvestigated, both from the point of view of improving the tubes, and because of the theoretical interest of the extra noise. Their analysis, which we now repeat, must therefore be taken with reserve.

8·2. Velocity discrimination

We consider that the collector has a linear current voltage characteristic of slope g amp./V. and going through the origin. It is clear that we need the maximum velocity modulation of the beam and the minimum shot noise, so the beam impedance will be high and the beam loading of the signal resonator low. We therefore neglect beam loading in our calculation and consider that the collector is near enough to the signal gap to allow us to neglect debunching forces.

A signal input power W_i produces a voltage swing of

$$V_i = (2R_iW_i)^{\frac{1}{2}},$$

where R_i = loaded impedance of signal resonator.

The velocity variation in the beam βV_i produces an average i.f. current of $g\beta V_1/\pi$, and the output power is

$$W_0 = \frac{2g^2\beta^2V_i^2R_c}{\pi^2(\frac{1}{2}R_cg+1)^2}, \tag{1}$$

where we have used the parallel equivalent circuit for the output network. The conversion efficiency is therefore

$$\frac{W_0}{W_i} = \frac{g^2\beta^2R_iR_c}{\pi^2(\frac{1}{2}R_cg+1)^2}. \tag{2}$$

The conversion efficiency given by eqn. (2) is, of course, the maximum theoretical value and cannot be reached in a real valve because of the departure from the ideal discontinuous characteristic. The conversion efficiency is in any case low; if we take the following figures which were obtained for early 10 cm. mixers, we get $W_0/W_i \div 0{\cdot}6$, $g = 0{\cdot}0005$ amp./V., $R_i = 20\,\mathrm{k}\Omega$, $R_c = 5\,\mathrm{k}\Omega$, $\beta^2 = 0{\cdot}6$.

R_c is limited by the band width of the i.f. amplifier and g is limited by the thermal velocities in the electron beam. However, eqn. (2) varies only slowly with g, for instance, increasing g to 0·005 only brings W_0/W_i up to about 1·6.

We next have to consider the sources of noise in the tube. These are

(*a*) Shot noise in the collector current.

(*b*) Thermal noise in the load resistance.

(*c*) Noise in the collector current due to the V.M. caused by thermal noise in the resonator.

(*d*) The shot noise in the beam has a component at the resonator frequency; this causes a voltage across the gap which is imposed on the beam as amplified shot noise.

(*e*) The fluctuations in the ratio in which the electron beam divides between collector and resonator gives rise to one source of division noise, while fluctuations in the currents to other electrodes give rise to other sources. This type of noise is not susceptible to general theoretical treatment, although its magnitude can be assessed in particular cases.

(*a*) As usual we have

$$\overline{i_c^2} = 2F^2eI_c\Delta f, \tag{3}$$

where F^2 = space charge smoothing factor (< 1), and Δf = i.f. band width.

It must be remembered that Δf must be multiplied by 3 when the local oscillator is switched on. That is, if the i.f. amplifier has a band width of 2 Mc./sec. at 45 Mc./sec. and the local oscillator frequency is 3045 Mc., the noise between 44 and 46, between 2999 and 3001 and between 3089 and 3091 Mc./sec. will appear in the output.

(*b*) The thermal noise in the load resistor is

$$\bar{e}_c^2 = 4kTR_c\Delta f \quad \text{or} \quad \bar{i}_c^2 = \frac{4kT}{R_c}\Delta f, \tag{4}$$

where k = Boltzmann's constant

$= 1{\cdot}4 \times 10^{-23}$ W./degree.

(*c*) The mean-square thermal noise voltage in the resonator is

$$\bar{v}_i^2 = 4kTR_i\Delta f.$$

The corresponding noise current in the collector lead is

$$\bar{i}_c^2 = \frac{4g^2kT\beta^2R_i\Delta f}{\pi^2(\frac{1}{2}R_cg+1)^2}, \tag{5}$$

as can be seen by comparison with eqn. (1).

(*d*) The shot noise in the beam at the signal resonator is given by

$$\bar{i}_0^2 = F^2 2eI_0\Delta f. \tag{6}$$

This produces a noise signal in the resonator whose power is

$$\beta^2R_iF^2 2eI_0\Delta f.$$

Again using the reasoning leading to eqn. (1) we have

$$\bar{i}_c^2 = \frac{2eI_0g^2R_i^2F^2\beta^2\Delta f}{\pi^2(\frac{1}{2}R_cg+1)^2}. \tag{7}$$

These relations are very complex and very little can be gained from a general discussion. Numerical examples show that the largest contribution is from the amplified shot noise, the shot noise being of the same order but considerably smaller. The other contributions are usually an order of magnitude smaller.

The theory gives reasonably correct results for the conversion gain or rather loss, but as has already been said, gives much too low an estimate of the tube noise. Experiments made on 10 cm. mixers using i.f. amplifiers with about 2 Mc./sec. band width showed that the noise factor was between 17 and 20 db. below the ideal figure. Under similar conditions a good modern crystal is only 7–10 db. down, conversion loss accounting for about half this figure. The theoretical estimate of noise can be brought into fair agreement with experiment by the formal expedient of putting $F^2 = 1$. There does not appear to be any basis for this procedure, but in view of the confused state of the fundamental postulates of noise theory it is possible that one may be found.

8·3. Frequency conversion by bunching

In making the same calculation in the case of conversion by bunching we may clearly use small signal theory, and the only difficulty which arises is the allowance to be made for space-charge debunching. Bleaney and Cooke used Webster's original expression for the effect of space charge. We have already seen that this overestimates the amount of debunching, so we shall make the calculation first without including a correction and then using the Webster expression.

The current at the second resonator contains, as a result of bunching by the signal, a component of magnitude

$$2I_0J_1(\tfrac{1}{2}S\alpha_1\bar{\beta})\cos(\omega t_2 - S). \quad \text{(Chap. 3, eqn. 28)}$$

The h.t. voltage can be so adjusted that $\cos(\omega t_2 - S) = 1$. Moreover, we assume that since $\alpha \ll 1$ we can take $J_1(\frac{1}{2}S\alpha_1\bar{\beta}) = \frac{1}{4}S\alpha\bar{\beta}$. Then the signal-frequency current at the second resonator is $\frac{1}{2}S\alpha\bar{\beta}_1 I_0$. The r.m.s. i.f. current, if the local oscillator voltage swings the collector up to saturation, is $\dfrac{S\alpha\bar{\beta}_1 I_0}{2(2\pi)^{\frac{1}{2}}}$. Putting in the expression for V_i, we get

$$\frac{W_0}{W_i} = \frac{S^2\beta^2}{4\pi^2}\frac{R_iR_c}{R_0^2}, \tag{8}$$

where $R_0 =$ the beam impedance.

Now, according to Webster, the debunching forces acting over a distance s reduce the bunching by an amount $\sin hs/hs$, where $h^2 = \dfrac{eI_0}{m\epsilon_0 V_0^3 A}$ and $A =$ beam area. Making the substitution we find that

$$\frac{W_0}{W_i} = 2{\cdot}67\beta^2\frac{\sin^2 hs}{\lambda^2}\frac{R_iR_c}{R_0}\frac{A}{V_0^{\frac{1}{2}}}. \tag{9}$$

Putting reasonable numerical values we obtain conversion efficiencies about 10 times smaller than in the case of voltage discrimination. The noise contribution from sources (*a*) and (*b*) remains the same.

(*c*) Thermal noise in the resonator

$$\bar{i}_c^2 = 10{\cdot}68kT\frac{R_i}{R_0}\frac{A}{\lambda^2}\frac{\beta^2\sin^2 hs}{V_0^{\frac{1}{2}}}\Delta f. \tag{10}$$

(*d*) Amplified shot noise

$$\bar{i}_c^2 = 5{\cdot}34kT\frac{R_i^2}{R_0}\frac{A}{\lambda^2}\frac{\beta^4\sin^2 hs}{V_0^{\frac{1}{2}}}\Delta f. \tag{11}$$

In this case the collector current is half the total beam current, and the shot noise in this current is the only important noise source. It turns out to be of the same order as the total noise in the case of velocity discrimination. It was therefore concluded that the bunching conversion mechanism is even less satisfactory than velocity discrimination, but little or no experimental work has been done on mixers of this type to substantiate this conclusion.

8·4. The monotron

Monotron is the name given by Hansen to a single resonator, single-transit type of V.M. tube. A very simple type of monotron is an ordinary gridded V.M. tube in which the gap transit angle has been made much bigger than usual. Eqn. (72) of Chapter 3 gives a beam conductance of

$$G = \frac{1}{R_0}\left[\frac{1-\cos\phi_0}{\phi_0^2} - \frac{\sin\phi_0}{2\phi_0}\right]. \tag{12}$$

If we plot this function we find that it becomes negative as ϕ_0 increases. Negative values of G represent negative resistances across the resonator, and so if $1/G$ can be made small enough, the system will oscillate. The maximum conversion efficiency is about 2·5 % at $\phi_0 = 2{\cdot}3$ radians. Actually we cannot expect the value of G to be given at all exactly by eqn. (12), because it was initially assumed that the velocity of an electron did not change by very much in the gap, whereas the present conditions admit of no such assumption. It is possible to visualize an inhomogeneous electric field which should give much greater efficiency than the linear field treated above. For instance, if the field were strong near the entrance to the system, then weak over a relatively long distance and finally strong again near the exit, the monotron would not be very different from an ordinary klystron. Another idea, suggested by Hansen, is to make the field weak for a considerable distance from the entrance and then to increase it suddenly. If the electrons have a velocity which makes them spend several cycles in the weak field, the gain of velocity in one-half cycle will be more or less cancelled in the next. If the reference electron takes an odd number of quarter cycles in the weak field there will be some net bunching, and energy can be extracted in the later part of the field. Since the bunching would be small, it might be that the voltage across the circuit would build up to a very high value with a correspondingly good efficiency.

In a sense it can be said that the oscillating diode of Llewellyn is an example of this last type of field, because although the h.f. field is linear, the superposed d.c. field produces essentially the same results.

We may very easily make a formal calculation of the monotron efficiency. From the results of Chapter 3 it is clear that we can define a gap efficiency for the monotron of the form

$$\eta_g = \left(\frac{\overline{\beta\gamma}}{4} + \frac{\overline{\delta\mu}}{4}\right)\alpha_1^2,$$

where β, γ are the coefficients belonging to the even part of the field and δ, μ are similar coefficients belonging to the odd part of the field. The output efficiency is, as usual,

$$\eta_0 = \eta_g - \frac{i_s}{i_r}\eta_s$$

and

$$i_s V_0 \eta_s = \frac{V_0^2 \alpha_1^2}{2Z}.$$

Then

$$\eta_0 = \alpha_1^2\left(\frac{\overline{\beta\gamma}}{4} + \frac{\overline{\delta\mu}}{4} - \frac{R_0}{Z}\right). \tag{13}$$

This expression gives us little information, even supposing that we could calculate the four gap coefficients for a particular field. To get a useful theoretical expression we should have to investigate the variation of the coefficients with α_1, when we should find that the amplitude of the oscillation is limited by the non-linearities of the generator in the well-known way. It is probably true to say that graphical methods yield the simplest solution in this particular instance.

Müller and Rostas* have investigated the performance of the plane-field monotron when the h.f. voltage is much greater than the applied d.c. The electrons can only penetrate completely through the h.f. field for certain conditions of transit angle, but the conversion efficiency is much higher than in the low-voltage case. In particular, they find that for $\phi_0 = \frac{2}{5}\pi$, $V_1 = 4V_0$, the conversion efficiency is a maximum and is about 15 %. The practical value of this work is rather dubious because such a tube would require an extremely high starting current, because the oscillator has to build up from low voltages, in which case the starting efficiency is only about 2 %, as we have already said. Other modes exist which are not self-starting.†

8·5. Velocity-modulated reactance valves

A reactance valve is used in frequency modulation technique as a source of variable reactance which can be placed in parallel across a resonant circuit and whose value can be controlled in magnitude by the amplitude of a desired signal. The reactance is achieved by the use of a feedback voltage which is approximately 90° out of phase with the input. Similar results can be obtained by means of V.M. tubes. For instance, consider two reflex tubes whose resonators are tightly coupled together so that they are in phase with one another. The reflector of one tube is set so as to make the system oscillate, then if the reflector of the other tube is set so that the transit angle is 90° different from the correct condition no power is absorbed by the second tube but a large reactance is introduced. If the transit angle is not exactly 90° power absorption is introduced as well as reactance. The same thing would occur if two conventional klystrons were coupled buncher to buncher and catcher to catcher and the voltage on one cathode varied away from the condition for correct phasing. Finally, a single resonator could be used, with the transit angle adjusted so as to maximize $\left[\frac{\sin\phi_0}{\phi_0^2} - \frac{1+\cos\phi_0}{2\phi_0}\right]$ and the beam current used as variable.

The reactance change can be calculated for any desired case by expressing the r.f. admittance as a function of beam current and phase angle so that the conditions for minimum beam susceptance can be evaluated. For instance, in the case of a reflex tube the electronic admittance can be expressed in the form

---

* Müller and Rostas, *Helv. phys. Acta*, 13 (1940), 435.

† Marcum, *J. Appl. Phys.* 17 (1946), 4.

$$Y_e = 2\bar{\beta}^2 RS \frac{I_0}{V_0} \frac{J_1(\theta)}{\theta} e^{-j(S-\frac{1}{2}\pi)}, \tag{14}$$

and it is a simple matter to investigate the performance of a circuit when Y_e is connected across the output terminals.

8·6. The multireflexion tube

This tube, which has recently been developed in the Philips Laboratories,[*] is a modification of the reflex klystron. In the normal reflex steps are taken to minimize the possibility of electrons making more than one transit through the gap because multiple transits introduce the risk of hysteresis and increase noise. In the Philips tube multiple transits are arranged in such a way that the bunch tends to preserve its identity. This is achieved by making the field on the gun side of the resonator parabolic in form. The field on the reflector side is parabolic but with an additional 'step' so that electrons which were accelerated in the gap travel ½ cycle farther than those which were retarded. On the return journey the fast electrons lose their excess energy and fall in with the rest of the bunch. Electrons in a parabolic field retain any density modulation they may have been given, so the bunch remains formed until it has given up energy during several transits. It eventually disperses due to beam spreading, etc. If the bunch makes n transits, the conversion efficiency is increased n times, but it is found that the dropping out of phase occurs suddenly and n cannot be large. The maximum conversion efficiency is 48% against 29·2% for the reflex when $\alpha = 0{\cdot}5$.

A further increase in efficiency is obtained when a focusing magnetic field is used because some electrons return to the cathode and reduce the d.c. input.

Effects of this type were briefly investigated at Bristol in 1941 but it was thought that the increase in output efficiency, though four or five times, did not compensate for the magnets. This work was, however, on local oscillators and not on high-power valves, where the efficiency is more important.

---

[*] Coeterier, *Philips Tech. Rev.* 8 (1946), 275.

8·7. Conclusion

In this chapter we have dealt with the less well-known embodiments of V.M. ideas. There is scope for great improvements in valve mixers for microwave technique, and it is possible that a thorough examination of the production of noise in V.M. tubes will lead to their perfection. The reactance tube has not yet been used to any large extent, but it provides a simple method of frequency modulation which may turn out to be of great value.

Chapter 9

LIMITATIONS AND DEFECTS IN VELOCITY-MODULATION TUBES

It is now time to attempt the difficult task of prophesying the future development and possibilities of the V.M. principle. It is already clear that V.M. tubes are more suitable than triodes for some purposes, even in the region where triodes operate reasonably well. Frequency modulation is an instance. Below this region the only reasonably efficient local oscillators are V.M. tubes, and the only way of obtaining amplification is by the same means. It is clearly of great practical importance to make some estimate of the frequency limit beyond which the V.M. tube will not operate. This, then, becomes our first task. We shall then deal with some of the more common electrical faults which occur, particularly oscillation hysteresis; by which we mean that oscillation starts at a different voltage according as to whether the voltage is being raised or lowered. There are also other types of hysteresis, such as tuning hysteresis, which is exhibited by high-power klystrons.

We have already shown how the efficiency depends on the input power and the circuit constants. The output is only limited by the technical difficulties of dissipating power, but even at very high voltages and currents the klystron self-oscillator cannot compete with the resonator magnetron because of the at least double efficiency of the latter. This remark should be qualified by noting that the technical problems encountered in the development of very high-powered c.w. magnetrons have not yet been overcome, but there is no reason to doubt that they will be. If high-powered amplifiers are required for relay systems or similar purposes, the multiresonator klystron is probably the best answer, though it may prove difficult to obtain sufficient band width for some purposes. In this connexion the circuit engineering problem of providing broad-band resonant circuits and coupling elements is of fundamental importance and has lagged far behind the electronic side.

Another rather specialized circuit problem is that of providing valves with a considerable tuning range; for instance, an octave or more. The triode, used in the 'butterfly' circuit, shows considerable promise in this direction but naturally suffers from a frequency limitation, which will have to be overcome by using V.M. tubes. The reflex klystron is most suitable for this purpose because the transit angle can be varied over a wide range by altering only the reflector voltage. This allows the input power to remain constant, whereas in the Heil or Samuel tubes the anode voltage has to be varied with corresponding variation in input power. Two-resonator tubes are out of the question because of the mechanical complexity involved in correctly ganging the tuning. A concentric line resonator gives the best mechanical solution to the problem, which is then reduced to one of providing a sliding 'contact' which will present a low impedance over the frequency band required. A sliding contact will not remain good for very long, at least not if it is outside the vacuum enclosure, so one has to design a labyrinth filter system to present a high-input impedance over the band. Some moderately successful special solutions have been reached, but they are by no means lossless, nor has a systematic design procedure been evolved. It is lucky that the ± 12 % tuning range available in thermally tuned valves is sufficient for most purposes.

9·1. Maximum frequency of klystron operation

The maximum frequency at which V.M. tubes will operate is reached when the starting current, of the best resonator system possible at the frequency, exceeds the running current which is to be taken as the maximum current which can be focused through the tunnel. It is almost certainly better to base this investigation on a circular tunnel rather than a rectangular or annular one, because the 70 % gain in current at a given voltage is offset by the increased circuit losses. It seems impossible to prove this, but all practical figures lend colour to the argument.

The starting current for a two-resonator klystron is

$$i_{S_0'} \geqslant \frac{4V_0}{S\beta^2 Z_0} \quad \text{(Chapter 3, eqn. (43)).} \tag{1}$$

For the reflex

$$i_{S_0'\,\text{reflex}} \geqslant \frac{V_0}{RS\beta^2 Z_0} \quad \text{(Chapter 7, eqn. (22)).} \tag{2}$$

These relations show that a reflex will have a much smaller starting current than a similar klystron, so we restrict ourselves to the study of eqn. (2). If we now put the starting current equal to the running current and rearrange, we get

$$R_0 \leqslant RS\beta^2 Z_0. \tag{3}$$

The only quantity which shows direct frequency dependence is Z, which varies at least as fast as $f^{-\frac{1}{2}}$ for a family of geometrically similar resonators. We say at least as fast because at very high frequencies surface irregularities increase the resistance above the value given by a skin effect calculation using the resistivity of the bulk metal. Already at 1·25 cm. wave-length this effect is about 20–40 %, depending on the care with which the surface is prepared. The form of eqn. (3) shows that the starting condition can be fulfilled for any Z_0 and R_0 by increasing S and R. We have already seen that the efficiency of a reflex is inversely proportional to R, and we also know that some specific minimum power output is required to work a mixer. If we introduce P by substitution for $\beta^2 Z_0$ in eqn. (3) neglecting $2\bar{\gamma}/\bar{\beta}$, we can write, for starting,

$$\frac{P}{2R} \leqslant S. \tag{4}$$

But $P/2R$ is the 'reduced' P which determines the efficiency when used in conjunction with our curves. We can then proceed as follows. With a certain resonator design calculate P for a number of values of V_0, using the maximum current which can be focused through the system. Then, if the required output is n W., the required efficiency can be calculated for each P. The efficiency corresponding to $P/2R$ is read off for all the likely modes, i.e. those for which eqn. (4) is obeyed, say η_7 for mode 7, etc. Then if $\eta_{n+\frac{3}{4}} \geqslant 2R\eta_0$ for $S(n+\frac{3}{4})$, where we have put η_0 for the required efficiency, the design requirements are met. The problem is then reduced to designing a reflector which will give the assumed value of R for the voltage corresponding to $S(n+\frac{3}{4})$. Other values of R may be investigated to see if they give a better result.

This formulation shows that the main requirement for a good tube is a low P value. There are obvious limits above which one would not increase the voltage, for any given application, so P may be said to depend on I_0 and Z_0, and the product of these quantities must be maximized. We shall not be much in error if we write, for an electrostatic tube, $I_0 = k(l/d)^2$, where k is a constant which may be determined from the best available gun designs. Now $Z_0 = f(l/d)$ and the functional dependence can be determined empirically, so $I_0 Z_0 \propto (l/d)^2 f(l/d)$, and the maximum can, in principle, be determined. For geometrically similar resonators $I_0 Z_0 \propto \lambda^{\frac{1}{2}}$. Using the best extrapolation from present-day figures, i.e. Z_0 a few thousand ohms and R_0 about 40 kΩ for a reasonable resonator, it is possible to forecast that reflex klystrons should be practicable for wave-lengths of a few millimetres*. For shorter wave-lengths a new system of generation will be required.

9·2. Hysteresis

The most common type of hysteresis is that encountered when the reflector voltage of a reflex is altered to vary the frequency. The power output is sometimes found to follow the form of fig. 9·1.

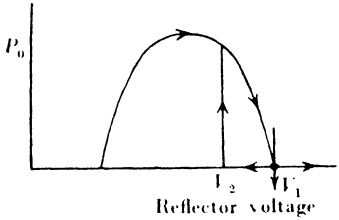

Fig. 9·1. Reflector voltage hysteresis.

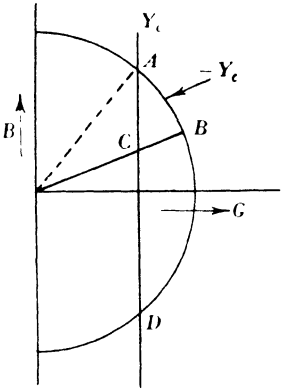

Fig. 9·2. Circle diagram of reflector operation.

When the reflector voltage is made more negative, oscillation persists to V_1, while when the direction of change is reversed, oscillation does not start again until V_2 is reached. Investigation of this phenomenon is best done graphically on a conductance-susceptance diagram. This is shown in fig. 9·2. The circuit admittance is a straight vertical line Y_c, and the locus of $-Y_e$, the negative of the electronic conductance, is a portion of a spiral. As the reflector voltage is altered $-Y_e$ rotates until it reaches A when oscillations start. When the reflector is made less negative so that $-Y_e$ reaches B, the amplitude of the oscillation builds up so that $-Y_e$, which is proportional to $J_1(\theta)/\theta$, decreases to C. Oscillations cease at D.

---

* Since this was written designs for millimetre wave reflex klystrons have been given by Lafferty (*J. Appl. Phys.* 17 (1946), 1061).

If $-Y_e$ has a violent bend as shown in fig. 9·3, the range of oscillation is different according to the direction of rotation of $-Y_e$. This observation was probably first made by Shepherd of the Bell Laboratories when developing the 723 A. tube.

The bend can be produced by a number of causes. For instance, if the electron optics of the reflector field are such that electrons can make multiple transits through the gap, $-Y_e$ will show kinks wherever the transits come into phase and out of phase with the desired single transit. Another cause of importance in gridless tubes is that the diameter of the beam at the tuning point is a function of the amplitude of the oscillation as well as of the focusing potentials. If this diameter increases too much the slow electrons, which are thrown to the outside of the bunch, are not focused back through the gap and G_e falls suddenly.

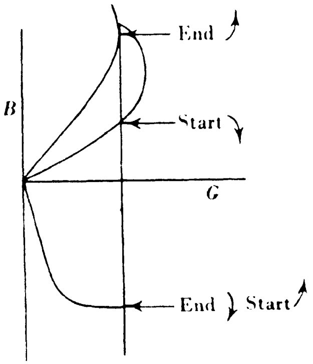

Fig. 9·3. Hysteresis occurs when the electron admittance curve is kinked.

Another type of hysteresis found in gridless high-power c.w. klystrons has been discussed by Beck. As one resonator is tuned a sudden burst of oscillation sets in and dies away immediately, but oscillation increases as the tuning is adjusted further until a region of instability is reached and the tube finally drops out of oscillation. The phenomenon is illustrated in fig. 9·4. The tuning has to be adjusted right back to the point at which the oscillations started before any oscillation is found. Investigation showed that the curved catcher field can reflect electrons so that they detune and load the buncher. As the main tuning is adjusted to overcome the detuning the reflected electrons come into phase with the input and cause regeneration and instability. When the regeneration is sufficient the input becomes so large that bunching takes place much too near to the buncher and the tube ceases to oscillate, leaving the resonators a long way apart in frequency. The effect depends on the dimensions of the tube and can be overcome by tilting the catcher gap.

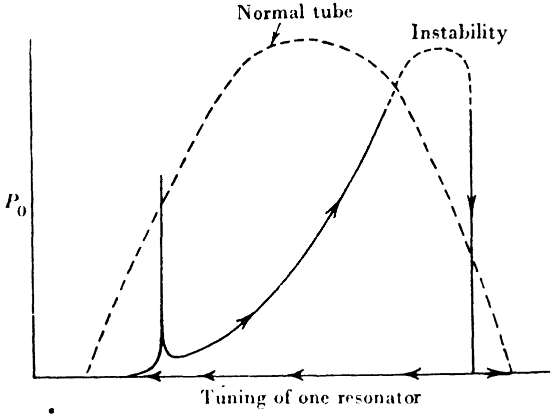

Fig. 9·4. Phenomena in tuning hysteresis.

9·3. Modulation problems

We have already seen that the power output from a klystron is by no means a linear function of the current. Amplitude modulation, of course, requires that the power output should be directly proportional to V_0, the grid voltage which controls the beam current. In fact, the grid can be designed to improve the overall linearity of the modulation characteristic, but it is usually found that not more than about 70 % modulation is tolerable if linearity is important. The modulation is accompanied by frequency modulation due to changes in the beam susceptance, and even with high Q resonators this effect can be quite large. It is therefore correct to say that, except for the crudest work, direct amplitude modulation should not be attempted. Various indirect schemes have been proposed, but the complications introduced are rather formidable.

Phase modulation is a possibility with klystron amplifiers, since the phase of the output voltage is such that it goes through its negative maximum when the bunch reaches the centre of the catcher gap. If the catcher voltage is increased so as to change the transit time from one mode to the next a phase change of 180° results, accompanied by a considerable change in amplitude. It is possible to use amplitude limiters in a phase-modulation system so that the defect can be overcome.

Much the best modulation technique is to use frequency modulation, using a reflex tube as modulator. The modulating signal is injected in series with the reflector, and as we have already said, frequency deviations of the order of ±1% are fairly readily obtained. The amplitude modulation can be reduced by arranging the succeeding amplifier so that it is over-excited at the middle of the range. Receiver limiters take care of the remaining change in level.

Chapter 10

THE DESIGN REQUIREMENTS, AND MANUFACTURE OF VELOCITY-MODULATION TUBE COMPONENTS

There are two broad classifications into which all V.M. tubes fall. These are:

(1) Tubes in which the resonator is partially outside the vacuum enclosure.

(2) Tubes in which the resonator is totally enclosed by the vacuum retaining walls.

Both types have a great deal to be said for them, so we now summarize the pros and cons.

(1) The main advantages of this class are that the construction is cheap and can be carried out without elaborate tooling. Tuning and coupling devices can be easily fitted and modifications can be introduced without much trouble, so that this type is very useful for experimental purposes.

The disadvantage is that the presence of dielectric in the resonators increases the circuit losses very much. If fundamental resonators are used it is impracticable to make tubes of this type operate on wave-lengths much less than 5 cm. This is overcome to some extent by using harmonic resonators with the glass sealed at a node of the electric field, thereby eliminating dielectric losses at one frequency and reducing them over a range of frequencies. By this device oscillations of much shorter wave-length can be generated. Harmonic resonators are not, however, an unalloyed blessing, and much research remains to be done on them.

(2) These tubes are very suitable for mass production because all the parts can be carefully tooled and assembled in jigs so that variations from the desired dimensions are minimized. The resonator losses are reduced to those caused by resistive losses in the walls and the losses of the coupling device.

The main advantage is also the major disadvantage, modifications are difficult and expensive to introduce. Tuning and coupling devices are difficult or impossible to modify. Care must also be taken to ensure that the resonator is in good thermal contact with the shell, or the rise in temperature may be great enough to annul the good effects of omitting the dielectric.

Broadly speaking, all English V.M. tubes have belonged to class (1) and most American tubes to class (2). Historically, this is due to the fact that the manufacture of all-metal receiver valves was a well-developed technique in the U.S.A. while no such valves had been made in this country, and essential machines, such as the heavy current ring welders required to seal the shell to the header, were not available. However, the English valve manufacturers brought considerable ingenuity to bear on the problems set to them by the large-scale production of copper-glass tubes and the principal difficulties were overcome. Unfortunately, it is not likely that copper-glass tubes represent more than an interim state of the art, and as the required wave-lengths decrease, the totally enclosed tube becomes more and more necessary. English practice is therefore developing in the direction of totally enclosed tubes in which the shell is of glass. Difficult problems are encountered in arranging vacuum-tight seals on the coupling device, but if these can be solved in production, this modification comprises the best features of both classes.

With this preliminary survey of the general problem in mind, we can proceed to the consideration of the design of the various elements of the complete tube.

10·1. Cathodes

10·1·1. *Oxide-coated cathodes*

Oxide-coated cathodes are far the most commonly encountered electron emissive device, and during the war they have been used in conditions which were held, not more than six or seven years ago, to be certain to destroy the cathode. For instance, 3 kV. was considered to represent the upper limit to the voltage which could be applied to a tube with an oxide cathode, but tubes have been used with up to 6 kV. for c.w. operation, and three or four times as much for pulse operation. In the same way, an emission of 200 mA./cm.^{2} was considered an absolute maximum, but to-day figures much in excess of this are common in c.w. tubes, and even more disparate results are obtained in pulse conditions. This last case is hardly a fair comparison because new phenomena appear when the pulse current from oxides is studied, so we shall say something more about this at a later date. The golden rule in setting limits on cathode conditions is to fix conditions which appear reasonable and then to run life tests on a number of tubes. If the life test is unsatisfactory either the processing technique must be modified or the conditions must be relaxed.

Patent literature on the subject of oxide cathodes reads rather like an alchemist's notebook, so it is worth while including some general remarks on the preparation of the coating and its activation in the tube. The coating consists of a mixture of barium and strontium carbonates, usually about 56 % $BaCO_3$ and 44 % $SrCO_3$ by weight to compensate for the preferential distillation of barium from the activated cathode. The carbonates are ball-milled into a fine suspension with a small percentage (1 %) of organic binder such as nitrocellulose and a mixture of organic solvents, usually amyl acetate with additions. The choice of solvent largely depends on the method of applying the coating to the base metal. V.M. tube cathodes are invariably sprayed, in which case the solvent must be chosen so that the coating does not become electrostatically charged in the nozzle of the spray gun, thereby clogging the jet, and the rate of evaporation of the solvent must be great enough to allow of a dry deposit being obtained on the cathode. A wet spray gives very even cathodes, but they are usually thick and tend to flake off in activation.

The thickness of the coating is not very important, for c.w. valves at any rate. Figures of between 5 and 15 mg./cm.^{2} are usual.

A considerable amount of work has been carried out on the effect of the base metal upon the activity of the cathode. Various types of nickel were used, usually containing a small percentage of manganese with a view to speeding the activation process. While it is probably true that these additions do make activation easier in certain circumstances, their use is to be deprecated because at the temperatures now used there is apt to be some distillation of the impurity giving rise to a conducting film on micas and other insulators. In our experience pure nickel is just as active in good vacuum conditions and is completely free from this trouble.

If poor activities are observed, they are far more likely to be due to lack of cleanliness in the preparation of the tube, or the use of injurious cleaning agents than to be caused by the particular cathode coating or base metal used. The most frequent causes of poor activity are grease and chlorides. Chlorides are very soluble and so may be removed by a final washing of the assembly in hot distilled water. Obviously hydrochloric acid should never be used as a cleaning agent unless the subsequent treatment of the parts is very thorough and even then it is better not to use it. Commercial bright dipping solutions and descaling agents contain HCl and are even more objectionable than the diluted acid.

The cathode bases are sprayed in a jig, which holds a reasonable number in such a way as to prevent unwanted surfaces receiving the coating. Test strips are used to determine the range at which the spray gun produces the desired degree of wetness and to determine the number of passes required to build up the correct thickness. After spraying, the bases are usually put in an air oven at between 100 and 200° C. to harden the coating so as to lessen the danger of damage in subsequent handling. When this has been done the bases can be stored until required. Care should be taken to prevent dirt and dust settling on the sprayed surface, and it should be remembered that the atmosphere may contain a perceptible amount of chlorides. For these reasons cathodes should not be stored too long and should be kept in a desiccator while awaiting assembly. Similarly, completed gun assemblies should be used as soon as possible. It is desirable to wash the gun immediately before assembling it into the tube. Boiling distilled water, of the highest degree of purity, is used for this purpose, and the gun is dried in an air furnace as before.

If all these precautions have been observed activation is extremely easy. After the tube has been baked, the heater voltage is fairly slowly increased to about 1100° C. At this temperature the dissociation of alkali earth carbonates into their oxides is rapid and complete. The CO_2 evolved in the process should be pumped away in about 1½–2 min., i.e. a h.f. leak tester should show no discharge after this time. If the gas does not clear, either the tube is leaky or dirty or the activation temperature was too low. In the last case a slight increase in heater voltage will produce more gas. Directly the CO_2 clears, the heater voltage should be reduced until the cathode temperature is about 900° C. The tube elements can then be outgassed by eddy-current heating or, in the undesirable cases where this is impossible, by electron bombardment. When outgassing is complete, voltages are applied to the electrodes and current flows immediately. The tube is usually run at an input well above its normal rating for several minutes before sealing off. It is desirable to keep the cathode temperature above the running figure of 750–850° C. during these operations so as to minimize the risk of 'poisoning' it. If much gas is evolved, the input should be reduced until it has been pumped away, so as to prevent positive-ion bombardment from destroying the cathode surface.

When it is clear that no more gas is being evolved, the voltages are removed and the tube is sealed off after firing the getter. Sometimes the getter, or a proportion of it, is only fired after the tube has been sealed off. Tubes manufactured in this way require no ageing or after-treatment of any sort. To be successful the method demands that the utmost care be taken to keep all the electrodes clean and free from grease. Since the life of a tube depends primarily on the extent to which the processing has removed gas and sources of gas, it is desirable to aim for complete cleanliness in spite of the fact that more elaborate activation schedules do not make such high demands in this respect. Moreover, the occurrence of failures in processing is a sure sign that some cleaning process is being improperly carried out.

In conclusion, we should say that rapid activation as described above is not suitable for all purposes. It is particularly unsuitable for hydrogen-filled valves for the following reason. If the pressure of CO_2 rises to a large value, in the presence of rather hot and clean metal surfaces a certain degree of dissociation into carbon and oxygen takes place, the carbon remaining as a dirty film on the surface facing the cathode. This is not objectionable, except from the point of view of appearance, in a V.M. tube, but in a hydrogen-filled valve it seems to increase the rate of disappearance of hydrogen by a large factor. To obtain reasonable lives in such conditions it is necessary to carry out the activation very slowly, limiting the partial pressure of CO_2 in the vacuum enclosure to values which are experimentally found to show little or no dissociation.

10·1·2. *Bombarded cathodes*

Technical improvements in metallurgy have enabled us to make use of another type of unipotential cathode in which the emitting surface consists of a disk of high melting-point metal such as molybdenum, or better, tantalum. This plate is maintained at a high temperature by electron bombardment from a subsidiary oxide-coated cathode, bombarding energies of several hundred volts being used. It is possible to use an ordinary coated heater in some circumstances, but the temperatures required to obtain the emission figures used in practice are so high that the heater, which must be 200–300° C. hotter than the cathode, would have a short life. The relatively high electrical conductivity of heater coating at such elevated temperatures is another factor which influences one against their use.

The major problem of design in bombarded cathode technique is to ensure that the temperature of the tantalum disk is even over the working surface. This means that the current from the bombarding source must be evenly distributed, and either that the cathode supports must be arranged to conduct as little heat as possible, or the emission must be taken from a relatively small area near the centre.

Bombarded cathodes can be used with the very highest voltages. They are considerably more complicated than a tungsten spiral but they have the considerable advantage that they can be applied in conventional electron guns. A minor advantage is that the heater supply is a fairly low current at a rather high voltage, which obviates any difficulties which might be experienced in designing the heater lead seals. It is likely that methods of enhancing the emission from tantalum will be discovered, in which case the technique may become widespread.

10·2. Heaters

Little need be said on this subject. Heaters used with oxide-coated cathodes are manufactured in exactly the same way as those used in receiving tubes, that is to say, tungsten or molybdenum tungsten alloy wire is wound upon soft iron mandrels which can be bent to any required shape and then annealed. The mandrel is then dissolved out with acid. The heater is next sprayed with a suspension of alkaline earth oxide in organic solvents, after which the coating is sintered at a high temperature (up to about 1700° C.) in a molybdenum tube furnace so as to obtain sufficient adhesion between the coating particles and allow one to handle it with moderate safety. The coating is usually alumina, often with a few per cent of beryllia added to reduce the electrical conductivity.

V.M. tube gun constructions usually allow one sufficient space for a heater of rather thick wire so that the heater life is not a problem. It is often important to design an astatic heater in order that magnetic effects shall not produce any modulation of the beam. Various types of bifilar and zigzag winding have been produced for this purpose, but it is still sometimes necessary to use d.c. heating power to eliminate the last traces of modulation from this source.

10·3. Gun electrodes

Gun electrodes for experimental tubes are easily made by wrapping nickel strip round a mandrel of the required diameter and spot-welding the ends together. In large-scale production and for accurate work they are made by drawing or pressing. Sometimes it is necessary to machine complicated shapes, but this is clearly very expensive.

J. R. Pierce has described electron guns which can be designed, to a fair degree of approximation, on paper. Such guns are rather elaborate, and it has been our practice to spend a good deal of time on electron optical design with a view to producing a gun which will give the required current in the simplest and most convenient way, using simple cylindrical shapes. Besides the fundamental requirement that the gun must produce a certain current at a specified voltage, it should fulfil other less obvious conditions. For instance, the full cathode surface should be utilized and the fields should be uniform over the cathode surface so that the beam density is also uniform. Again, although it is often possible to make use of badly aberrated beams, it is much better, from the point of view of uniformity of performance in the completed tubes, to make sure that the gun does not produce an aberrated beam. If the beam is non-uniform and the aberration large, small manufacturing variations in the spacings can produce first-order changes in the magnitude of the non-uniformities, although only second-order changes are produced in the total current. This may lead to faults which are rather difficult to diagnose, such as the appearance of oscillation hysteresis in certain members of a batch of apparently identical tubes.

One of the most difficult questions in modern gun design is how to obtain small accurately held spacings, and yet preserve the thermal insulation of the cathode. In some low-voltage tubes, the clearance between the cathode and the control grid is of the order of 0·005–0·010 in. Since the control grid is often at cathode potential it seems an attractive idea to space the cathode by means of metallic lugs. Unfortunately, such lugs conduct too much heat away, even when the area of contact is small and the lugs are made of a poorly conducting material such as nickel-iron. The difficulty has to be overcome by mounting the cathode on ceramic or mica disks which can be pressed home against metal collars, or on a metal cylinder sliding inside the grid. The cathode should be mounted as close to the insulator as possible so as to reduce the change in spacing due to thermal expansion of the supports. The supports themselves are often made of nickel-iron because of its low thermal conductivity and high mechanical strength. The mechanical design of the supports also has to be taken into account, in relation both to sudden shocks and maintained vibration.

Care must be taken that mica insulators do not become too hot either in processing or in running because mica decomposes above 400° C. and provides an annoying source of gas which is often difficult to track down. Ceramics have the disadvantage that conducting films seem to form more readily on them than on mica, but some successful designs have been worked out in which this fault is overcome by allowing the ceramic to run hot, only about a hundred degrees below the cathode temperature.

The design of the complete gun is governed to a large extent by the necessity of arranging matters so that the cathode can either be held in a jig while it is welded into position, or can be forced into the desired position after welding. Ideally, the jig used for these purposes should also ensure that the cathode is not tilted. Usually it is not certain that this condition is obeyed, and a second jig may be required to eliminate tilt.

Once the gun itself is completed, the centring with respect to the tunnel and the spacing between the positive electrode and the grid cylinder have to be considered. The positive electrode is usually the body of the resonator, but sometimes an auxiliary electrode is used. Let us first consider the centring problem. The severity of the requirements depends on the diameter of the tunnel, as the actual centring tolerance is the important variable. In the particular case of a valve with a 2 mm. diameter tunnel, in which the gun had been rather carefully designed to produce some 90%

of the theoretically possible current, a movement of 0·125 mm. reduced the current through the valve to about 80% of its central value. Tubes are in use with tunnels of less than 1 mm. diameter, in which case the centring must be correct to within 0·025 mm. It is possible to manufacture mica centring disks to the required accuracy, but special measures have to be adopted to obtain points to determine the location of the disk. In the totally enclosed type of tube it is usually fairly easy to arrange that the shell, or some auxiliary cylinder, is jig mounted in such a way as to be concentric with the tunnel, but in a metal-glass tube more difficulties present themselves.

A very ingenious solution to this problem has been found, which is usually called 'dimpling'. A typical example of the application of this process is to construct a mandrel, one end of which is turned down so as to be a sliding fit in the tunnel, the other end being 3–4 mm. less in diameter than the glass tube which has to be dimpled. The two ends of the mandrel must, of course, be concentric and truly round. The copper electrodes are sealed into the glass to form the body of the tube, which is then slipped over the mandrel. A small pointed gas flame is then moved over the glass surface in an axial line, so as to melt a line of glass, leaving the rest of the glass cool. When the heated part is molten, a tool is brought up which forces the molten glass down on to the mandrel, which is warmed sufficiently to prevent the glass from cracking. When the first dimple has been made, the tube and mandrel are indexed round by 90 or 120°, a second dimple is made, and so on. By this means it is possible to obtain a three- or four-point location for the centring disk which ensures that the disk is held concentrically with the tunnel. The dimple can be made long enough so that two micas, spaced by a distance great enough to eliminate any tilting of the whole gun, can be used. Moreover, it is possible to cut back a portion of the tool used to deform the glass so that the dimple has a step at the resonator end. The front mica can be accurately positioned longitudinally on the gun so that it serves to locate the gun in the axial direction when forced home against the step. A less used variant of dimpling is to tool the glass down to the mandrel diameter in a lathe.

Because of the thermal expansion of the mandrel and the contraction of the glass in cooling, it is rather difficult to obtain a predetermined radius for the circle defined by the dimples. The radius can either be corrected experimentally or the mica disks can be made to fit the dimples produced by tools of standard sizes.

All methods of longitudinal positioning are essentially the same as that described above, viz. the forcing of a locating member against a stop. No more need be said than to give the reminder that the usual commonsense engineering criteria, such as putting on stops after an assembly has been soldered together so as not to include uncontrolled soldered joints in the overall tolerances, must be obeyed.

10·4. Gap grids

Gap grids in V.M. tubes are always positive and therefore draw current from the beam and have to dissipate power. Gun grids are usually negative, but they are generally tubular structures with no wires extending across the beam. Some tubes have used positive wire grids spaced very close to the cathode so as to draw off current, but the design problem in this case is exactly that of the gap grid. If the axial extent of the grid is small, it is usually found that the current to the grid can be calculated from the space factor. The space factor is defined as the percentage of the tunnel area which is not occupied by the grid wires. For instance, if the wires occupy 40% of the tunnel area, the space factor is 60% and the grid is assumed to receive 40% of the electrons arriving at it. If the axial length of the grid is large, this estimate may be nowhere near the truth, particularly if the electron paths are much inclined to the axis in the grid region. In these circumstances one must rely on direct measurements of the grid interception, which are themselves somewhat difficult to interpret, because of secondary emission.

If a reasonable estimate of the current can be made and it is also assumed that the grid will run at a temperature low enough for the thermal radiation to be neglected, it is easily found that the grid should be made of good thermally conducting material, which in practice means copper. Silver has a rather high vapour pressure which limits its use. On the other hand, in those cases where the thermal radiation is large, the largest power dissipation is obtained by using high melting-point materials such as molybdenum, tungsten and their alloys. Since all dimensions of a tube diminish as the wave-length decreases, it is necessary to use thin grids in all tubes below about 5 cm. wave-length, and these grids rely on radiation cooling. High grid temperature, of course, increases the h.f. losses in the resonator, but this factor is outweighed by the gain in running current.

Various forms of grid have been used in the past, but at present wound grids are almost universal in reflex tubes. Mesh is not commonly used, although it has one or two theoretical advantages, particularly in regard to h.f. resistance. Tungsten mesh, however, usually introduces more loss in poor contacts at the corners of the mesh than is gained by the more nearly radial current flow. Copper mesh has been prepared by electroplating on blocks of bitumen resist which have had a mesh imprinted on them by photographic means. Such blocks can be plated and mechanically stripped several times, so their use is quite economical. While this copper mesh is very useful in high-frequency triodes it is much inferior to wound tungsten from the point of view of power dissipation. Wound grids are usually prepared on a base-plate of some sort. One common way of making grids is to punch a series of holes, equal in diameter to the tunnel, in a piece of molybdenum sheet. The sheet is then mounted in the chuck of a winding machine and wire is wound over both sides of the sheet, thin gold washers being placed round each hole under the wire. When the strip has been wound it is removed from the chuck and placed in a furnace containing an inert atmosphere, usually nitrogen. Gold runs freely under these conditions and each grid wire is firmly soldered into place. The gold is sometimes kept from flowing along the wires by painting Aquadag over the wires in the aperture. The grids are completed by punching out a small ring concentric with the original hole, so that a washer-shaped piece, with wires soldered to one side, is left. It is easy to mount such washers. Modifications of this idea can be used to apply grids to awkwardly shaped parts. Consider, for instance, the tunnel assembly shown in fig. 10·1. The nozzle is electroplated with gold or copper and the assemblies are mounted on a strip of molybdenum. The grid is wound round the strip and over the nozzle. The wound strip is furnaced as before, and the unwanted wire can be cut away.

With care in winding and the correct choice of base material, so that thermal stresses do not snap the wires, it is possible to use wires down to about 0·008 mm. diameter, though it is naturally a delicate and costly business handling such wires.

An interesting method of making grids for higher powered tubes has been worked out by W. J. Scott of the B.T.H. Laboratories and employed by the Sperry Co. The grids produced look like sections through a honeycomb, and have a good space factor as well as a reasonable conduction area. The process consists of taking a number of soft iron wires whose diameter is that of the holes required in the honeycomb, and plating them with the metal which is to be used for the grid. The iron wires are then tightly loaded into a rather soft outer tube, for instance, of soft iron, and the outer tube is placed in a swageing machine which forces the wires tightly together. The resulting rod is then cut into sections of the required thickness in a lathe and the iron dissolved out in acid. The honeycomb can be soldered either into a strengthening ring or straight into the tunnel.

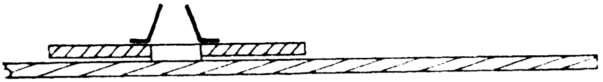

Fig. 10·1. Assembly for making grid on a tunnel.

It is somewhat difficult to give a criterion for judging the maximum spacing between wires which will still not allow the h.f. field to penetrate it to a significant extent. A very rough guide is that the spacing should be kept below 1% of the wave-length if the grid is to be called perfect. Grids with much larger spacings will, of course, materially reduce the losses at a gap, but their parameters are intermediate between those of a perfect grid and those of a gridless gap.

10·5. Resonators and resonator seals

In this case there are considerable differences between the techniques used in the construction of totally enclosed tubes and those in which the resonator is sealed through the walls.

Totally enclosed resonators are usually pressed or machined out of copper. It is common practice to construct the resonator in two parts, as indicated in fig. 10·2. The parts are silver plated and furnaced at 780° C. so that the copper-silver eutectic alloy is formed and the parts are firmly soldered together with a high-conductivity joint. At shorter wave-lengths the resonator dies are simply pressed into thick copper or the required shape is cut in with a special tool.

When resonators are to be made by sealing through glass, a pressing is used. The maximum thickness of copper which can be sealed through the wall is limited to about 0·015 in., but even at this figure considerable care has to be taken. Thicknesses between 0·006 and 0·010 in. are very easy to handle and are normally used. Spinnings were frequently used in early tubes, but they are considerably more variable in shape than pressings. If, however, the shape of the resonator is complicated and many pressing operations are needed to complete it, one often finds that the work can be reduced by making a preliminary spinning which is brought to the final shape by pressing. This technique often saves time and expense in experimental work.

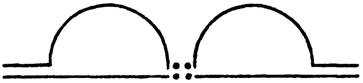

Fig. 10·2. Assembly of resonant cavity.

After the final pressing operation the coppers are cleaned and 'borated'. Borating is perhaps rather a bad name for the process, for what is actually done is to prepare a film of red copper oxide of a fairly definite thickness. The technique is to raise the copper to a barely perceptible dull red heat in a gas flame or air furnace and then to quench it in a saturated solution of borax in water. It is then replaced in the flame and heated until the borax melts. When the copper cools it has a rich crimson colour, which, if the cleaning has been adequate, is very even over the surface. Pressings prepared in this way are mounted on a central mandrel in a vertical sealing machine, spaced by pieces of glass tubing cut to the required length. A small hot gas flame is played on the copper bringing it nearly to its melting-point, and the glass is melted by conduction, an axial weight being used to press the parts together. When a reasonable amount of glass has been melted into the seal, the flame is moved to the next lower pressing and so on until all the seals have been completed, when the bulb is removed from the mandrel and annealed if necessary. The borating acts first as a flux which protects the copper oxide layer, and secondly as a means of controlling the thickness of the oxide layer. The oxide layer is very important because the mechanical strength of the seal depends upon the bond which is formed by the solution of copper oxide in glass. When cool the copper glass interface in the best seals should have the same crimson colour that the borated spinning had, although it is possible to get perfectly good seals which have been worked longer and at a higher temperature so that they show a yellow colour.

A production method of oxidizing is to raise the coppers to a specified temperature for a specified time in an atmosphere of carbon dioxide. It is said that seals made with such coppers stand up to extremes of damp heat better than borated ones, but the evidence is not conclusive.

Various mechanical devices have been used to ensure that the seals are made of the thickness required to bring the edges of the gap to the desired spacing. For instance, the coppers have been allowed to come together until the further motion was stopped by wires or tapes which could be shaken out of the completed bulb. Chemical pellets which would resist the high temperature but were highly soluble have also been used. In our experience, the best technique has been to rely on the operator to achieve something like the correct setting, and then to attach a resonator and tune the bulb to resonance with a standard frequency oscillator by mechanical deformation of the gap. This is easily done since the coppers are left dead soft after the sealing operation. The bulb need not be cleaned before presetting, as there is normally plenty of h.f. power available.

Since the permissible thickness of the coppers is rather small, they are flimsy, and contact to the main body of resonator is obtained by deforming the coppers so that they make a really intimate connexion with the body. This means that any form of clip-on resonator is out of the question, and forces one to provide the resonator as an integral part of the tube. This disadvantage was overcome at Bristol by the development of a similar seal using 50–50% nickel-iron alloy. This alloy has the same coefficient of expansion as Wembley L 1 glass, and therefore any thickness can be sealed through a glass tube. The alloy does not seal very well in its natural state, it is difficult to strike the correct degree of oxidization and the seals have a tendency to be very bubbly. Both these difficulties are overcome by plating the nickel-iron parts with

0·002–0·003 in. of copper. The plated parts are borated and sealed in exactly the same way as borated copper. The copper plate has a further advantage of reducing the surface resistivity to the value characteristic of copper, since the skin depth is far smaller than the plating thickness at the frequencies involved. A disk 1 mm. thick with a diameter of about 25 mm. is sufficiently rigid to allow one to plug the completed tube into strong spring contacts, and remove it again. In this type of seal it is not necessary that the glass tube should be of the same diameter on both sides of the disk, or even that there should be glass on both sides of the disk.

Although the nickel-iron seal is very useful, it is not so resistant to thermal shock as Kovar to hard glass seals, since the latter have a considerably lower average coefficient of expansion, the figures being approximately 50×10^{-7} per degree for Kovar as against 90×10^{-7} per degree for nickel-iron. We have used the plating and borating technique on Kovar with very good results, and it is to be expected that the use of this material will increase rapidly when British equivalents are freely available.

10·6. Reflectors

The problems of centring and spacing the reflector are exactly the same as those which we have already discussed in the section on electron guns. The only difference is that the insulation has to withstand a somewhat higher voltage, usually 1½–2 times as great. The insulation is a matter of some importance because the reflector is often supplied from a very high resistance potentiometer chain, so that the applied voltage will behave very oddly if the reflector takes current either from the beam or through the insulation.

The general principles of the electrical design have been dealt with in the chapter on reflex klystrons, where the design was considered with a view to optimizing the output efficiency. Apart from the question of obtaining the desired *R* value, there are more general conditions to be obeyed. First, the design must be such that the maximum current should be focused back through the tunnel. Secondly, the reflector field should only provide sufficient focusing to get the electrons back through the tunnel, since if the beam is confined too

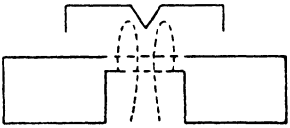

Fig. 10·3. Reflector designed to reduce multiple transits.

much to the centre of the tube, it may make several transits across the gap with resulting hysteresis in the oscillations. Another way of preventing multiple transits is shown in fig. 10·3. This method has been extensively employed by the Bell Telephone Laboratories.

10·7. Collectors

The principal function of the collector is to dissipate heat, but it is also required to be of a suitable shape so that secondary electrons emitted from it cannot penetrate into the interaction space. As in all power tubes, the type of cooling employed depends on the mean power dissipation. Radiation cooling is employed for low-power tubes, air-blast cooling at medium powers, and water cooling for high powers. Expressed quantitatively the approximate ranges of power are:

Radiation cooling	Up to 100 W.
Air-blast cooling	50 W. to 1 kW.
Water cooling	500 W. upwards.

10·7·1. *Radiation cooling*

There are two physical factors which limit the amount of heat which may be disposed of by radiation. First is the melting-point of the metal of which the collector is made and the second the size of the glass bulb surrounding the collector. In V.M. tube practice it is usual to find that the limit is the overheating of the bulb, and that it is not necessary to use the high melting-point metals, such as molybdenum and tantalum for collectors.* In these circumstances nickel and carbonized nickel are the preferred collector materials. Carbonized nickel will dissipate about 5 times as much power per unit area as bright nickel, but it requires to be handled and processed much more carefully. One must be careful not to overheat carbonized materials during the outgassing schedule, as there is a risk of removing the carbon, and it is slightly more difficult to attain a uniform standard of cathode activity when it is used. However, this last problem has, to a large extent, been overcome by the introduction of sheet carbonized on one side (used as the bulb side) only.

---

* It is possible to enlarge the bulb in the collector region, but the manufacturing complications introduced are rather formidable, and it is usually better to go over to air-blast cooling.

It is difficult to design a V.M. tube radiator theoretically, because the heat distribution is usually not at all uniform. The best that can be done is to take a cylindrical collector and to modify it by welding on cooling fins, until the desired result is obtained. The diameter of the cylinder should be small in comparison with its length, so that the probability of secondary electrons finding their way out is low. This desirable result is assisted by the fact that the beam is likely to be diverging quite rapidly by the time the end of the collector is reached.

The centring of the collector is unimportant. It may be held in place by mica disks or ceramic insulators and mounted on a stem or a single wire seal.

10·7·2. *Air blast and water cooling*

The mechanical and electrical design of air-blast and water-cooled collectors are very similar, and they need not be described separately. In this case, in addition to disposing of the required amount of heat, we have to include a vacuum-tight seal. The collector may be electrically connected to the resonator or it may be isolated by an insulator, involving two extra glass or ceramic to metal seals. In some constructions, particularly those using copper disk seals, it is easier to insulate the collector than to make it part of the resonator. From the experimental viewpoint it is extremely valuable to be able to measure the collector current separately, because it enables one to measure the gun efficiency and to observe the change in collector current as the valve goes into oscillation; but from the standpoint of operational convenience it is better to have the resonator and collector connected.

The collector should again be in the form of a long, narrow cylinder. The divergence of the beam can be used to reduce the concentration of current hitting the end of the tunnel, and thus to minimize localized overheating. It is now very important that the thermal conductivity of the collector material should be as high as possible, and that any soldered joints which may have to be made perpendicular to the direction of heat flow should not be made with soft solder which has a very poor thermal conductivity. Pure cadmium and silver solders are suitable, but care must be taken to ensure that no air pockets are left.

In fig. 10·4 we show a form of collector which has proved very useful in copper-glass seal klystrons. A rimmed cup *C* is drawn from nickel-iron or Kovar sheet, the draw being taken as deep as possible so as to maximize the distance between the heated area and the seal. A thick-walled cylinder *D* of some highly conducting material is next copper-brazed on to the cup at *B*, and if the beam is very concentrated it is an improvement to melt a considerable thickness of copper over the part of the surface of *C* which is bounded by *D*. The complete assembly is then copper-plated and borated before sealing to the glass tube. It is important to keep the face *A* flat, or else the seals will crack. A collector of this type can have either an air-blast cooler soldered on to it, or a water-jacket. A collector of this type in which the glass tube was 30 mm. diameter, *D* a nickel tube about 18 mm. diameter and 1 mm. thick, *C* a nickel-iron cup 1 mm. thick and about 7 mm. deep, dissipated 700 W. with a simple air-blast cooler made up from flat copper plates. The limitation was due to the overheating of *D* which could have been overcome by making it thicker or of a better thermal conductor.

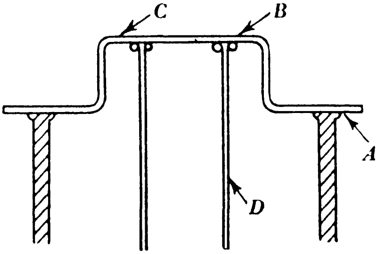

Fig. 10·4. High-power klystron collector.

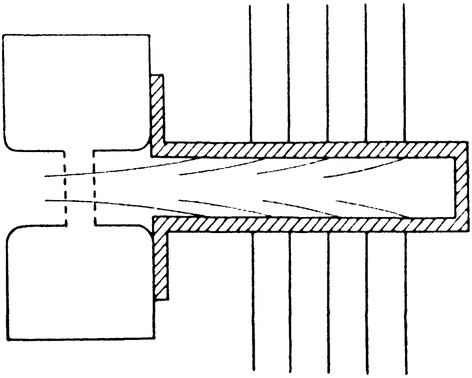

Fig. 10·5. Collector which is an integral part of the cavity structure.

Little needs to be said about collectors which are an integral part of the resonator. They are usually made from copper tube which is silver soldered to the resonator at one end. A cooler or water-jacket is easily attached to such a device. Fig. 10·5 shows the general idea of such an arrangement.

10·8. Tuning means

We have already said something about tuning in Chapter 2. It is impossible to give here a complete account of tuning methods which have been used with external circuit tubes, so we restrict ourselves to totally enclosed tubes.

Only two practical methods for tuning a totally enclosed tube are at present available. These are:

(1) The deformation of a flexible member from outside the vacuum enclosure.

(2) Thermal tuning, in which the deformation is accomplished by electrical means inside the vacuum.

In both cases the motion is used to vary the spacing between the grids.

10·8·1. *Deformation from outside the vacuum*

The principal difficulties to be overcome are mechanical failure of the flexion member, either by overstraining it or by fatigue, and secondly, the provision of a drive without backlash or drift. In general it is fair to say that valves with this type of tuning have a very limited life if they are tuned continuously over the whole range. Except for experimental purposes, such as use in a wave-guide test bench, this condition is not likely to be encountered, and therefore does not constitute a major objection to the method. Backlash can be completely eliminated, but only at the cost of mechanical complication of the tuner. A compromise is usually adopted, a reasonably fine mechanical tuner being used in conjunction with reflector tuning. A typical arrangement is shown in fig. 10·6.

10·8·2. *Thermal tuning*

Thermal tuners do not suffer from the mechanical difficulties encountered above, because the flexible member is not required to act as part of the vacuum retaining wall and can therefore be made very weak. Early thermal tuners sometimes used a directly heated element which could be controlled from outside the tube, for instance, a bimetallic strip or the expansion of a thin wire. Nowadays it is more usual to build in a separate triode valve, the anode current being used to heat the expansion member and the grid voltage being used as a control. The advantage is, of course, that the control circuit requires no power to operate it. Bimetallic strip is somewhat erratic in performance, and it is good practice to employ the differential expansion between two strips of different material of high and low thermal expansion. It is important that the rate of tuning should be high enough to satisfy the requirements imposed by A.F.C. systems, and this demands that thermal capacities and mechanical inertia should be minimized. It is usual to cover a ±6% tuning range in about 4 sec.

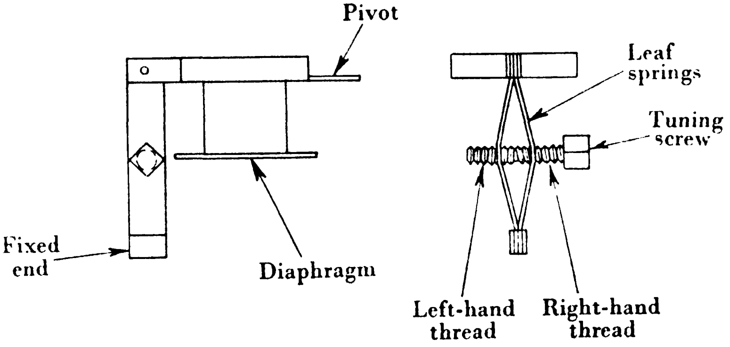

Fig. 10·6. A typical mechanical tuner (723 A/B tube).

10·9. Coupling in totally enclosed tubes

One of the main difficulties in the design of totally enclosed tubes is that of arranging the coupling, because one has to seal either a coaxial line or a wave guide out through the enclosure. It is clearly impossible to use a wave guide for the longer wavelengths because of its size. The size could be reduced by filling the guide with dielectric, but unfortunately most materials whose permittivity is high enough to effect a big enough reduction in size have at the same time large dielectric losses. Therefore a coaxial line is used, and using copper-plated Kovar or nickel-iron for the conductors the sealing difficulties can be overcome. As the wave-length diminishes it becomes possible to employ a wave guide, which is usually preferable from the circuit viewpoint, as it involves fewer impedance transformations with the attendant introduction of loss. The resonator can be coupled to the guide by means of a matching slot which can be adjusted by experiment. Slots are very reproducible in manufacture and introduce less loss than coupling loops.

10·10. Conclusion

In this chapter we have endeavoured to enumerate the principal considerations which must be remembered when designing a V.M. tube. It could not hope to be exhaustive, or to detail all the manufacturing techniques employed, but it was felt that the book would be incomplete without the information contained herein. A very useful historical survey of the development of V.M. tubes in the laboratories of the Société Française Radioélectrique, has been given by Warnecke;[*] this account very closely parallels the way in which development has taken place in this country[†] and in various American laboratories; and refers to most of the mechanical arrangements which have been attempted. Interested readers should refer to the original article.

---

[*] Warnecke, *Ann. Radioélect.* 1 (1945), 6.

[†] Broadway *et al.* *J. Inst. Elect. Engrs*, 93, pt IIIA, no. 5 (1946), 855.

Appendix 1

EXAMPLE OF THE DESIGN OF A HIGH-POWERED C.W. KLYSTRON

Data. A resonator of axial length 0·015 m., tunnel diam. 0·005 m., gap 0·001 has $Z_0 = 57\ k\Omega$ at $\lambda \div 0\cdot10$. The maximum voltage of operation is to be 2·2 kV. Electrostatic focusing has to be used and the maximum efficiency and power output are to be obtained.

Calculation of $\bar{\beta}^2$ and $2\bar{\gamma}/\bar{\beta}$. The distance travelled per cycle at 2·2 kV.:

$$S_0 = 1\cdot99 \times 10^{-3}\lambda V_0^{\frac{1}{2}}$$

$$= 9\cdot35 \times 10^{-3},$$

$$L = \frac{2\pi l}{S_0} = \frac{2\pi}{9\cdot35} = 0\cdot672,$$

$$R = \frac{2\pi r}{S_0} = \frac{2\pi \times 2\cdot5}{9\cdot35} = 1\cdot68.$$

Using figs. 3·7 and 3·8 we have

$$\bar{\beta}^2 = \frac{2J_0^2(\frac{1}{2}L)}{1 + f_1(R)} = \frac{1\cdot89}{3\cdot37} = 0\cdot56$$

$$2\frac{\bar{\gamma}}{\bar{\beta}} = \frac{LJ_1(\frac{1}{2}L)}{J_0(\frac{1}{2}L)} + [1 - F_1(R)] = 0\cdot12 + 0\cdot77$$

$$= 0\cdot89.$$

Calculation of P. The maximum current through the system is obtained when the resonators have one common wall. The tunnel length is then 0·03 m. Then

$$\hat{I}_0 = 38\cdot9 \times 10^{-6}\left(\frac{0\cdot005}{0\cdot030}\right)^2 \times (2200)^{\frac{3}{2}}$$

$$= 0\cdot111\ \text{A}.$$

Now
$$P = \frac{4V_0}{I_0 Z_0 \bar{\beta}^2} + 2\frac{\bar{\gamma}}{\bar{\beta}}$$

$$= \frac{4 \times 2\cdot2}{0\cdot111 \times 57 \times 0\cdot56} + 0\cdot89$$

$$= 2\cdot48 + 0\cdot89$$

$$= 3\cdot37.$$

The drift length. For mode 5 we have

$$S_5 = S_0 \times 1{\cdot}25$$
$$= 1{\cdot}17 \times 10^{-2}.$$

Similarly $\quad S_7 = 1{\cdot}64 \times 10^{-2}\ S_9 = 2{\cdot}10 \times 10^{-2}.$

From figs. 6·5, 6·6 and 6·7 we see at once that mode 9 gives the best efficiency, but remembering that the gaps should be in the middle third of the resonator if their length is to be a minimum, we see that the drift length should be $< 2 \times 10^{-2}$ m. Therefore either mode 7 must be used or the gap length and Z_0 determined for a resonator with the gap near one wall. In fact it turns out better to use mode 7 which, in addition, allows the catcher gap to be disposed so that spreading of the beam under dynamic conditions becomes unimportant.

Fig. 6·6 gives $\eta_7 = 15{\cdot}75\%$ at $P = 3{\cdot}37$.

The power input $\quad = 2200 \times 0{\cdot}111$

$= 244$ W.

Therefore P_0 $\quad = 244 \times 0{\cdot}158$

$= 38{\cdot}6$ W.

In mode 5 the efficiency would be 12·0%. Experimental valves have been made with these dimensions, and the efficiencies obtained are in good agreement with those calculated.

Sources of error. The main sources of error are: (i) errors in Z_0, (ii) neglect of deflexion loading.

Z_0 was measured by treating the resonator as a lumped constant circuit and varying L by varying the outside diameter. A plot of λ^2 against $\log_e(2b)$ should then be a straight line. C can then be calculated and if Q is measured at the working wave-length, Z_0 is obtained from $Z_0 = Q/\omega C$. In this method a good straight line is obtained but the value of C resulting therefrom is not in agreement with anything which might be defined as the lumped C of the circuit. However, estimates of Z_0 made in this way check with those made by injecting a measured amount of power into the resonator and measuring the resultant V.M. on the beam. The Q value can be very accurately measured but a rather simple method was used in our work and the result is probably in error to the extent of $\pm 5\%$. The variation of Z_0 with temperature has also been neglected, but this is not large. The Q was measured at 23° C. and the tubes ran at about 50° C.

Deflexion loss is impossible to estimate accurately. The beam loss is about 25 % of the total P in the above example. A similar amount of deflexion loss would reduce η_7 to about 10·5 %. To explain the measured efficiencies one would have to assume that the present theory underestimates the efficiency very considerably, which is impossible. It appears, therefore, that deflexion loss is small. This is largely confirmed by Feenberg's result although the differences of derivation make an exact comparison impossible.

Note. The method of converting lengths to transit angles used above is equivalent to the expressions given in the text but is better for computation.

Appendix 2

THE TRAVELLING WAVE TUBE

This tube was invented by Kompfner[*] in 1942 then working at Birmingham University. Some work was done on it there and later at Oxford, but although the tube showed promise it did not give a large gain in signal-noise ratio, which is the only point of interest as far as radar is concerned. Pierce[†] realized that the tube showed the way to very large band-width, and the Bell Telephone Laboratories have recently announced gains of 22 db. over a band-width of 800 Mc./sec.

The principle of the tube is to slow down an electromagnetic wave enough to obtain a phase velocity equal to that of electrons with energies 1–2 keV. This is done by winding a helix of wire and placing it coaxially in an outer metallic tube. This may be roughly thought of as a coaxial line wound into a helix which then has all common boundaries removed. The wave then makes only a small axial advance for each turn of the helix, and the closer the turns the slower the wave. Velocities of the order $c/10$–$c/15$ can be obtained by this means. Energy is fed from a matched wave-guide system into one end of the helix and the other end of the helix is matched into an output wave guide. An electron gun sends a beam along the axis of the device and, when the electron velocity is correct, the field and the beam interact continuously so that the input wave is amplified. It seems rather difficult to give a fully convincing physical picture of the interaction, but the phenomenon must be somewhat as follows. The electrons are, at entry, stationary with respect to the field if it is assumed that their velocity is exactly the same as the phase velocity of the wave. Consider a point in space where the field to the right is acting towards the gun, and to the left is acting towards the collector. Electrons in the half cycle to the right will be slowed down with respect to the unmodulated electrons at the zero field plane, and those to the left will be speeded up. Therefore, as the beam and field progress in space down the tube, a bunch will tend to form but this bunch will in turn induce a field in the helix. The induced field will act so as to slow the bunch down and will have a maximum value at the centre of the bunch. It will also be greater than the initial field. An amplified and phase-changed output should therefore be obtained. As we shall see, this is essentially what happens but the actual physical phenomena are considerably more complicated.

---

[*] Kompfner, *Proc. Inst. Radio Engrs, N.Y.*, 35 (1947), 124.

[†] Pierce and Field, *Proc. Inst. Radio Engrs, N.Y.*, 35 (1947), 108.

The inherently great band width of the tube is due to the fact that no high-*Q* circuits are involved, the band width of the helix itself extends from zero up to the frequency at which objectionable wave-guide modes are possible. The coupling devices can be made broad-band and can no doubt be improved upon. The amplification will fall off at low frequencies because the helix will then be short in terms of the wave-length; also the gain-band width product is a constant as in other amplifiers.

Several theories of the travelling-wave tube have now been given; Kompfner's original theory was based on the picture of bunching—action of bunch on helix—reaction of helix on beam and so on. The gain was deduced as an infinite, convergent series. Pierce[*] has given a very generalized theory but the simplest theory seems to be that of Bernier[†] which is repeated here. Let the axial field component $= E(z)e^{j\omega t}$. The charge density $= \rho_0 + \rho_1 e^{j\omega t}$, where ρ_1 is supposed to be $\ll \rho_0$. Similarly, the velocity $u = u_0 + u_1 e^{j\omega t}$. Then for the current density we have $\rho u = i_0 + i_1$. These quantities are related by the equation of motion and the condition of continuity:

$$\frac{du}{dt} = \frac{e}{m} E(z)\, e^{j\omega t}, \tag{1}$$

$$\frac{\partial(\rho u)}{\partial t} + \frac{\partial \rho}{\partial t} = 0, \tag{2}$$

also

$$\frac{d}{dt} = u_0 \frac{\partial}{\partial z} + \frac{\partial}{\partial t}.$$

Therefore

$$\frac{\partial u_1}{\partial z} u_0 + j\omega u_1 = \frac{e}{m} E(z). \tag{3}$$

---

[*] Pierce, 'Theory of the beam-type travelling-wave tube'. *Proc. Inst. Radio Engrs, N.Y.*, 35 (1947), 111.

[†] Bernier, 'Essai de theorie du tube électronique à propagation d'onde', *Ann. Radioélect.* 21 (1947), 87.

For small signals, neglecting cross products of a.c. quantities, we can write

$$i = \rho_0 u_1 + u_0 \rho_1.$$

From (2) we then have

$$\frac{\partial i}{\partial z} + j\omega\rho_1 = 0. \tag{4}$$

If we eliminate u_1 and ρ_1 we obtain an equation relating i and $E(z)$. Writing

$$\frac{\omega e \rho_0}{m u_0^2} = \frac{\omega}{u_0}\frac{i_0}{2V_0}, \quad i = f(z), \quad k_0 = \frac{\omega}{u_0} \quad \text{and} \quad Z_0 = \frac{V_0}{a i_0},$$

where a = cross-section of beam, this equation reads

$$\frac{d^2 i}{dz^2} + 2jk_0 \frac{di}{dz} - k_0^2 i = \frac{jk_0}{2aZ_0} E(z). \tag{5}$$

We next require an equation giving the field at any point in a matched line, which, instead of being excited at only one point, is being driven along its whole length by an as yet indeterminate distribution of sources. This problem bears the same relation to a singly excited line problem that a continuously loaded beam problem does to a point loaded beam. The result is

$$\frac{d^2 E}{dz^2} - \Gamma^2 E = -\Gamma A(z), \tag{6}$$

where Γ = propagation constant and $A(z)$ is the distribution function of the sources. The boundary conditions are

$$\left.\begin{aligned} E(0) &= E_0 + \frac{1}{2}\int_0^l A(z)\, e^{-\Gamma z}\, dz, \\ \left(\frac{dE}{dz}\right)_0 &= -\Gamma E_0 + \tfrac{1}{2}\Gamma \int_0^l A(z)\, e^{-\Gamma z}\, dz, \\ \text{whence} \qquad E(0) - \frac{1}{\Gamma}\left(\frac{dE}{dz}\right)_0 &= 2E_0. \end{aligned}\right\} \tag{7}$$

Next we put $A(z) = -k^2 Zai(z)$, which gives Z the dimensions of an impedance, the beam coupling impedance. Eqn. (6) then becomes

$$\frac{d^2 E}{dz^2} - \Gamma^2 E = \Gamma k^2 Zai(z), \tag{8}$$

and eqns. (8) and (5) describe the complete interaction of field and beam. It should be noted at this point that, in any given structure, there may be formidable mathematical difficulties in calculating Z. However, for the moment we assume that it is known. Eqns. (8) and (5) are simultaneous second-order equations whose solution is found to be*

$$i(z) = \sum_1^4 A_n e^{P_n z}, \quad E(z) = \sum_1^4 B_n e^{P_n z}, \tag{9}$$

where the P are the solutions of

$$\begin{vmatrix} (P+jk_0)^2, & \dfrac{jk_0}{2Z_0 a} \\ \Gamma k^2 Za, & P^2 - \Gamma^2 \end{vmatrix} = 0. \tag{10}$$

Also

$$A_n = \frac{P_n^2 - \Gamma^2}{\Gamma k^2 Za}. \tag{11}$$

Since (10) has terms of the order P^4 there are four possible propagation constants corresponding to four waves on the wire. The boundary conditions (7) allow us to relate their amplitudes to the amplitude of the input wave. A rather elaborate discussion shows that the four waves behave as follows:

(1) Wave of very small amplitude propagated to the left and attenuated. The attenuation is of the order of the cold attenuation of the helix.

(2) Initial amplitude $= \frac{1}{3}E_0$. Propagated to the right and attenuated the same amount as (1). Velocity slightly greater than that of the original wave.

(3) Initial amplitude $= \frac{1}{3}E_0$. Propagated to the right and strongly attenuated. Slightly slower than original wave.

(4) Initial amplitude $= \frac{1}{3}E_0$. Propagated to the right and strongly amplified. Slightly slower than original wave.

It is seen that all the amplification comes from the last wave, and that the first sets a limit to the maximum gain which can be obtained before self-oscillation occurs. If Z is supposed to be real and the electron velocity at entry is exactly equal to the initial phase velocity, the power gain

$$G_p = -9{\cdot}6 - \frac{8{\cdot}68}{m}\gamma l + 7{\cdot}52\, kl\left(\frac{Z}{4Z_0}\right)^{\frac{1}{3}}, \tag{12}$$

---

[*] Ince, *Ordinary Differential Equations*, Longmans, p. 144.

where $l =$ length of helix and m is a numerical factor $\div 3$. This should be compared with Pierce's asymptotic formula for low circuit loss ($\gamma \to 0$) high-gain tubes:

$$G_p = \tfrac{1}{9} \exp (2\pi 3^{\frac{1}{2}} CN)$$

$$C = \left(\frac{E(z)^2}{k^2 Wi} \frac{1}{8Z_0} \right)^{\frac{1}{3}}. \tag{13}$$

Here $N =$ length of helix in cycles, $E =$ peak axial field strength for input power Wi. Allowing for differences of notation the results are identical. The first term of (12) is found to increase slightly when there is a difference between electronic velocity and wave velocity, but is independent of l, i_0 and w.

Eqn. (12) shows that, for a given length l, there is a minimum d.c. current below which the tube will not amplify. This current obviously plays a similar role to that played by the starting current in a V.M. oscillator, in that the operation of the tube can be expressed in terms of it.

Pierce* gives the noise figure as $80F^2V_0C$ which means that the voltage and current should both be low for a small noise figure.

It is too early to attempt much in the way of an evaluation of the travelling wave tube. To counterbalance the enormous gain-band width product one must consider the unwieldy length and the rather low output power which this entails if very large magnetic fields are to be avoided. The noise figure is not yet good enough to make the tube of interest in radar but in systems such as television relays, where the signal can be maintained well above the noise level, the travelling-wave valve shows great promise.

* Pierce, *loc. cit.*

Tables

Table 2. *Length factors for gaps*

With grids				No grids	
L	$\bar{\beta}$	$\bar{\beta}^2$	$2\bar{\gamma}/\bar{\beta}$	$2J_0^2(\frac{1}{2}L)$	$\dfrac{LJ_1(\frac{1}{2}L)}{J_0(\frac{1}{2}L)}$
0	1	1	0	1	0
0·2	0·998	0·996	0·006	1·995	0·001
0·4	0·994	0·988	0·028	1·960	0·040
0·6	0·985	0·970	0·061	1·915	0·091
0·8	0·975	0·951	0·115	1·840	0·164
1·0	0·959	0·920	0·169	1·760	0·258
1·2	0·940	0·884	0·245	1·685	0·378
1·4	0·920	0·846	0·337	1·555	0·523
1·6	0·896	0·803	0·444	1·430	0·698
1·8	0·870	0·757	0·570	1·305	0·905
2·0	0·842	0·709	0·715	1·138	1·150
2·2	0·810	0·656	0·880	1·035	1·440
2·4	0·777	0·604	1·070	0·900	1·780
2·6	0·740	0·548	1·280	0·770	2·190
2·8	0·704	0·496	1·520	0·642	2·770
3·0	0·665	0·442	1·790	0·523	3·270

Table 3. *Radius factors for tubes without grids*

R	$1-F_1(R)$	$1+f_1(R)$	R	$1-F_1(R)$	$1+f_1(R)$
0·8	0·277	2·315	1·6	0·735	3·249
1·0	0·392	2·500	1·7	0·779	3·402
1·1	0·452	2·608	1·8	0·830	3·552
1·2	0·519	2·715	1·9	0·842	3·740
1·3	0·575	2·833	2·0	0·895	3·895
1·4	0·630	2·967	2·2	0·962	4·233
1·5	0·676	3·104			

Table 4. *Efficiency, etc., against P for mode 5*

P	S_5	α_1'	α_2'	$\hat{\eta}_0$ %	$\eta_0$min. %
0·828	7·857	0·463	2·796	79·2	26·0
1·16	7·8597	0·458	2·245	55·1	24·6
1·75	7·867	0·445	1·323	32·6	21·2
2·21	7·875	0·432	1·044	24·1	18·6
2·96	7·888	0·406	0·769	15·8	14·6
4·17	7·911	0·354	0·525	7·60	—
5·16	7·931	0·303	0·386	3·67	—
5·99	7·946	0·252	0·293	1·68	—
6·66	7·958	0·201	0·220	0·66	—
7·21	7·966	0·151	0·158	0·20	—
7·60	7·973	0·100	0·210	0·04	—

Table 5. *The same for mode 7*

P	S_7	α_1'	α_2'	$\hat{\eta}_0$ %	$\eta_0$min. %
1·16	10·997	0·331	1·999	56·6	30·8
1·63	11·089	0·327	1·603	39·3	27·7
2·45	11·005	0·318	0·946	24·4	22·2
3·09	11·010	0·309	0·748	17·9	17·9
4·14	11·020	0·290	0·550	11·3	—
5·82	11·038	0·254	0·376	5·46	—
7·19	11·051	0·217	0·277	2·65	—
8·35	11·062	0·181	0·210	1·21	—
9·29	11·071	0·145	0·158	0·48	—
10·06	11·077	0·108	0·087	0·15	—
10·59	11·082	0·072	0·073	0·03	—

Table 6. *Efficiency, etc., against P for mode 9*

P	S_9	α_1'	α_2'	$\hat{\eta}_0$ %	$\eta_0$min. %
1·49	14·131	0·258	1·556	43·98	31·7
2·09	14·133	0·255	1·111	30·6	27·2
3·15	14·138	0·248	0·737	18·9	18·9
3·97	14·142	0·240	0·582	13·98	—
5·32	14·149	0·226	0·428	8·81	—
7·47	14·162	0·198	0·293	4·26	—
9·23	14·173	0·169	0·216	2·07	—
10·72	14·182	0·141	0·164	0·94	—
11·94	14·189	0·113	0·123	0·38	—
12·91	14·193	0·085	0·089	0·12	—
13·61	14·197	0·056	0·057	0·02	—

Note. These tables are only calculated to slide-rule accuracy.

LIST OF SYMBOLS

Note. All formulae in this book are given in m.k.s. units.

B = susceptance.
C = capacitance.
$\mathbf{E}$ = electric field strength.
e = electronic charge.
F^2 = space-charge reduction factor.
G = conductance. Power gain.
$\mathbf{H}$ = magnetic field strength.
h = debunching parameter.
I_0 = d.c. current.
I = Bessel function of imaginary argument.
J_0, J_1, J_2 = Bessel functions of the first kind.
k = Boltzmann's constant.
L = normalized distance in gap. Transit angle in gap.
l = gap length.
M = mutual inductance.
m = electronic mass.
P = efficiency parameter.
Q = quality factor of resonator.
R = resistance, normalized radius.
r = tunnel radius.
S_0 = distance travelled per cycle by unmodulated electron.
T = temperature ° K.
u = electron velocity.
V_0 = d.c. voltage.
W = power.
X = reactance.
Y = admittance.
Z = impedance.
Z_0 = resonant impedance.
z = axial co-ordinate in cylindrical system.
α = depth of modulation.
β = V.M. coefficient.
γ = V.M. coefficient.
δ = phase angle.
ϵ_0 = permittivity of vacuum.
$\eta_{\text{conv.}}$ = conversion efficiency.
η_0 = output efficiency.
$\theta = \frac{1}{2}S\alpha\beta$, the bunching parameter.
λ = free space wave-length.
μ_0 = permeability of vacuum.
ρ = charge density.
σ = conductivity.
τ = transit time.
ϕ = transit angle.
ω = angular frequency.

BIBLIOGRAPHY

(*a*) *Textbooks*

HUXLEY. *Principles and Practice of Wave Guides.* Cambridge University Press.

M.I.T. RADAR SCHOOL. *Principles of Radar.* McGraw Hill Book Co.

RAMO and WHINNERY. *Fields and Waves in Modern Radio.* John Wiley and Sons.

SCHELKUNOFF. *Electro-magnetic Waves.* Van Nostrand.

SLATER. *Microwave Transmission.* McGraw Hill Book Co.

STRATTON. *Electromagnetic Theory.* McGraw Hill Book Co.

(*b*) *Some general papers not mentioned in the text*

CONDON, E. U. Principles of Micro-Wave Radio. *Rev. Mod. Phys.* 14 (1942), 341.

HAGSTRUM, H. Microwave generators. *Proc. Inst. Radio Engrs, N.Y.*, 35 (1947), 548.

SLATER, J. C. Microwave electronics. *Rev. Mod. Phys.* 18 (1946), 441.

INDEX

Acoustic resonators, 23
Amplification, power, 81 *et seq.*; signal, 92 *et seq.*
Amplifier, multi-resonator, 88; klystron, 81; travelling wave, 169
Applegate diagram, 11
Automatic frequency control, 116, 123

Beam, electrostatic focusing, 73–5; impedance, 51; magnetic focusing, 75–9
Beta factor, definition, 61; of gridded gap, 62; general gap, 65
Bessel functions, 48
Borating, 157

Capacitance of Posts, 32
Cathodes, 146 *et seq.*
Cavity resonators, 22 *et seq.*
Characteristic impedance, 33
Coaxial lines, 33–5
Collectors, 160 *et seq.*
Conversion efficiency, 48
Cooling, 160 *et seq.*
Copper loss, 35
Coupling devices, 37

Debunching theories, 83 *et seq.*
Depth of modulation, 47
Dimpling, 153
Drift tube, 10

Echo box, 41
Electron guns, 72–9; motion, 42–3
Equations, Maxwell's, 25, 42
Equivalence of cavity and circuit, 36–7
Equivalent circuit of klystron oscillator, 97

Feed-back oscillator, 13
Frequency, cavity resonance, 27 *et seq.*; multiplication, 95; reflector pulling, 123–5; stability, 126

Gain, klystron amplifier, 82; frequency multiplier, 96; multi-resonator, 91
Gamma factor, definition, 61; gridded gap, 62; general gap, 65
Graphical methods, 44
Grid construction, 154

Hahn-Metcalf tube, 19
Heil tube, 17
Hysteresis, oscillation, 141; tuning, 143

Impedance-beam, 51; circuit, 36; output, 109
Inductive output tube, 19

Klystron, amplifier, 80 *et seq.*; multi-resonator, 88; oscillator, 97; reflex, 110
Kovar, 159

Load matching, 109
Local oscillators, 2, 116

Magnetic focusing, 76
Maximum amplitude conditions, 103
Mixers, bunching, 132; velocity sorting, 129
Modes, cavity resonator, 28
Modulation methods, 143
Monotron, 133
Multireflexion tube, 130
Mutual inductance coupling, 97

Noise, in amplifiers, 92; in mixers, 129 *et seq.*; in travelling wave tube, 173

Oscillator, klystron, 97 *et seq.*; reflex, 116 *et seq.*; Heil tube, 111; multireflexion, 130
Output-coupling, efficiency, 53

Parameter, klystron, 105; reflex, 117
Perturbation, 38
Phase modulation, 144
Power-amplifier, klystron, 82
Power-output, oscillator, 108, 109, 110; Heil tube, 112, 113, 114; Samuel tube, 112, 113, 114; reflex, 118, 121

Q Quality factor, cavity resonator, 36

Radio frequency amplifier, 92; lines, 33
Reactance valve, 135
Rectangular cavity resonator, 27
Reflector, 159

Reflex klystron, 116 *et seq.*
Relaxation process, 39
Rieke diagram, 126

Samuel tube, 18
Seals, metals to glass, 156–9
Secondary emission, 16
Signal-to-noise ratio, 92
Skin depth, 35
Symbols, 176

Travelling wave tube, 167
Toroidal resonator, 29
Tuning methods, 37, 163

Velocity modulation process, first order approximation, 45; second order approximation, 55; general expression, 58

Wave-length, minimum attainable, 139

DATE OF ISSUE

This book must be returned within 3, 7, 14 days of its issue. A fine of ONE ANNA per day will be charged if the book is overdue.